Network Navigation With Scheduling: Error Evolution

Tianheng Wang, *Student Member, IEEE*, Yuan Shen, *Member, IEEE*, Andrea Conti, *Senior Member, IEEE*, and Moe Z. Win, *Fellow, IEEE*

***Abstract*— Network navigation is a promising paradigm for providing location awareness in wireless environments, where nodes estimate their locations based on sensor measurements and prior knowledge. In the presence of limited wireless resources, only a subset rather than all of the node pairs can perform inter-node measurements. The procedure of selecting node pairs at different times for inter-node measurements, referred to as network scheduling, affects the evolution of the localization errors. Thus, it is crucial to design efficient scheduling strategies for network navigation. This paper introduces *situation-aware scheduling* that exploits network states to select measurement pairs, and develops a framework to characterize the effects of scheduling strategies and of network settings on the error evolution. In particular, both sufficient and necessary conditions for the boundedness of the error evolution are provided. Furthermore, opportunistic and random situation-aware scheduling strategies are proposed, and bounds on the corresponding time-averaged network localization errors are derived. These strategies are shown to be optimal in terms of the error scaling with the number of agents. Finally, the reduction of the error scaling by increasing the number of simultaneous measurement pairs is quantified.**

***Index Terms*— Network navigation, scheduling strategies, fisher information, localization error evolution, error scaling.**

I. Introduction

NETWORK NAVIGATION is a promising paradigm for providing location-awareness [1]–[8], which is a key enabler for a myriad of applications including those in diverse areas such as autonomous vehicles [9], smart cities [10], logistics [11], public safety [12], distributed sensing [13], social networks [14], medical services [15], and environmental monitoring [16]. In GPS-challenged environments such as indoor and urban areas, network navigation enables location-awareness based on sensor measurements and prior knowledge [17]–[30]. Wireless networks with navigation capability, referred to as wireless navigation networks, consist of anchor nodes with known locations and agent nodes with unknown locations. The goal of navigation is to estimate the location of each agent as it moves through the network. In particular, the agents scatter in the network and are equipped with sensors for inter-node and intra-node measurements.[1] The location of each agent can then be estimated based on inter-node measurements (e.g., range) with neighboring nodes (anchors and agents), intra-node measurements (e.g., acceleration), and prior knowledge (e.g., mobility model) [31]–[41]. The applications enabled by location-awareness have motivated a wide range of research in localization and navigation networks [42]–[56].

In wireless navigation networks, typically only a subset of node pairs can simultaneously perform inter-node measurements due to limited wireless resources. Therefore, it is indispensable to design scheduling strategies for selecting *measurement pairs*,[2] i.e., node pairs for performing inter-node

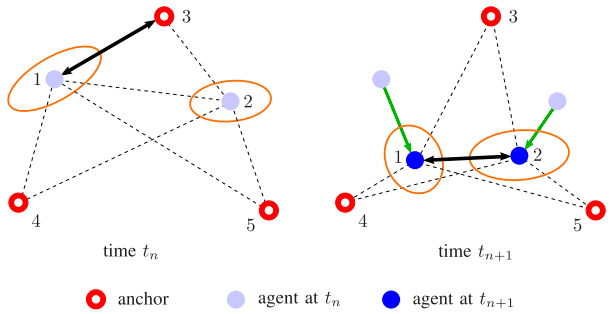

Fig. 1. Situation-aware scheduling for a two-agent navigation network: the localization error of an agent is represented by an ellipse with the major axis corresponding to the direction of the agent's largest localization error [4].

Manuscript received February 7, 2016; revised November 25, 2016; accepted February 20, 2017. Date of publication June 20, 2017; date of current version October 18, 2017. This work was supported in part by the Office of Naval Research under Grant N00014-16-1-2141 and Grant N00014-11-1-0397, in part by the Italian MIUR GRETA Project under Grant 2010WHY5PR, and in part by the Copernicus Fellowship. This paper was presented in part at the 2013 IEEE Global Communications Conference, at the 2014 IEEE International Conference on Communications, and at the 2015 IEEE International Conference on Communications.

T. Wang is with the Wireless Information and Network Sciences Laboratory, Massachusetts Institute of Technology, Cambridge, MA 02139 USA (e-mail: wangth@mit.edu).

Y. Shen was with the Wireless Information and Network Sciences Laboratory, Massachusetts Institute of Technology, Cambridge, MA 02139 USA. He is now with the Electronic Engineering Department, Tsinghua University, Beijing 100084, China (e-mail: shenyuan_ee@tsinghua.edu.cn).

A. Conti is with the Department of Engineering and CNIT, University of Ferrara, 44122 Ferrara, Italy (e-mail: a.conti@ieee.org). He is also visiting the University of Salamanca, Spain.

M. Z. Win is with the Laboratory for Information and Decision Systems, Massachusetts Institute of Technology, Cambridge, MA 02139 USA (e-mail: moewin@mit.edu).

Communicated by T. Javidi, Associate Editor for Communication Networks.

Color versions of one or more of the figures in this paper are available online at http://ieeexplore.ieee.org.

Digital Object Identifier 10.1109/TIT.2017.2717582

[1] Sensors for inter-node measurements can be wideband radios, infrared sensors, and acoustic sensors. Sensors for intra-node measurements can be accelerometers, gyroscopes, and magnetometers.

[2] Fig. 1 shows an example where only one measurement pair can be selected at a time due to limited wireless resources. At time t_n, the measurement pair $(1, 3)$ is selected since anchor 3 can efficiently help to reduce agent 1's localization error along the direction of its major axis. At time t_{n+1}, the two agents have moved to new positions, and the measurement pair $(1, 2)$ is selected since agent 1 can efficiently help to reduce agent 2's localization error along the direction of its major axis.

measurements. Scheduling strategies affect the localization errors as explained in the following. During the navigation process, the localization errors of the agents evolve in time with two competing tendencies: the errors are increased by the uncertainty in intra-node measurements and in prior knowledge, whereas the errors are reduced by the location information from inter-node measurements. Thus, the error evolution depends on the scheduling strategy through the selections of measurement pairs. A key requirement for the scheduling strategy is to maintain the *boundedness* of the error evolution, i.e., the localization errors should be kept bounded as the agents move. Furthermore, the error reductions provided by inter-node measurements depend on the *network states* consisting of the network topology, the agents' localization errors, and the measurement qualities [4], [44], [45]. These states can be exploited to select the measurement pairs that provide significant localization error reductions. However, such exploitation incurs additional communication overhead and computational complexity. In particular, network schedulers need to acquire the knowledge about network states and estimate the error reduction brought by each candidate measurement pair. Finally, efficient utilization of wireless resources calls for an understanding of the tradeoff between allocating the resources to a single measurement pair and sharing them among multiple measurement pairs.

The key questions related to the design of efficient scheduling strategies for network navigation are as follows:

1) How do scheduling strategies improve navigation accuracy in the presence of limited resources?
2) What gain can one expect from the exploitation of network states in scheduling strategies?
3) Can multi-agent resource sharing improve network navigation performance?

The answers to these questions rely on the analysis of the error evolution for different scheduling strategies and network settings.

The above questions have been addressed only partially in the existing literature. For example, the evolution of the error covariance matrix was analyzed for multi-robot navigation in [40] without constraints on the wireless resources for inter-node measurements. A distributed scheduling strategy exploiting the network states was proposed in [45] and the corresponding error evolution was analyzed without accounting for the correlation of agents' localization errors. The error evolution remains underinvestigated for other scheduling strategies such as those designed considering delay [53], overhead [54], and energy consumption [55], as well as those based on a game-theoretic approach [56]. Furthermore, results on the scheduling strategies for data networks [57]–[59] are not suited for navigation networks since the strategies for communication aim to improve throughput or delay while those for navigation aim to minimize localization error.

This paper introduces situation-aware scheduling for network navigation that exploits network states to select measurement pairs, and develops a framework to determine the error evolution for different scheduling strategies and network settings (e.g., agent trajectories, anchor deployments, measurement models, and multiple-access protocols). Both non-Bayesian and Bayesian estimations of agents' locations are considered.[3] The errors in these estimations, referred to as localization errors, can be characterized by the inverse of the Fisher information matrix (FIM), which provides a fundamental performance limit for parameter estimation [60]. Furthermore, to understand the performance gain provided by the exploitation of the network states, the error evolutions for the proposed opportunistic and random situation-aware scheduling strategies are compared, where the former selects measurement pairs based on the network states and the latter randomly selects measurement pairs. The key contributions of the paper are to:

- determine the recursive error evolution expression for different scheduling strategies and network settings;
- develop both sufficient and necessary conditions for the boundedness of the error evolution;
- derive upper bounds on the time-averaged network localization error (NLE) for the proposed opportunistic and random scheduling strategies;
- obtain universal lower bounds on the NLE and show that the proposed scheduling strategies achieve the optimal error scaling with the number of agents; and
- characterize the effect of resource sharing among multiple measurement pairs on the error evolution and show the reduction of error scaling via resource sharing.

The rest of the paper is organized as follows. Section II introduces the network settings and characterizes the error evolution. Section III provides conditions for the boundedness of the error evolution. Section IV proposes situation-aware scheduling strategies and provides their error upper bounds. Section V derives universal error lower bounds and the error scaling. Section VI extends the results to networks with multiple measurement pairs per time interval. Section VII specifies the results for a network with linear Gaussian measurement models and extends the results to 3-D networks. Section VIII shows numerical results for a case study. Finally, conclusions are given in Section IX.

Notation: A random variable and its realization are respectively represented in the form of x and x; a random vector and its realization are respectively represented in the form of $\mathbf{x}$ and $\boldsymbol{x}$; a random matrix and its realization are respectively represented in the form of $\mathbf{X}$ and $\boldsymbol{X}$; a random set and its realization are respectively represented in the form of X and $\mathcal{X}$; $\mathbb{R}_{\geq 0}$ denotes the set of nonnegative real numbers; $\mathbb{S}_{+}^{K}$ and $\mathbb{S}_{++}^{K}$ denote the sets of $K \times K$ symmetric positive semidefinite and positive definite matrices, respectively; $\emptyset$ denotes the empty set; $|\mathcal{X}|$ is the cardinality of a set $\mathcal{X}$; $\lceil \cdot \rceil$ denotes the smallest integer greater than or equal to its argument and $\lfloor \cdot \rfloor$ denotes the largest integer smaller than or equal to its argument; $\mathbb{P}\{\cdot\}$ denotes the probability of an event; $\mathbb{E}\{\cdot\}$ and $\mathbb{E}_{\mathsf{x}}\{\cdot\}$ denote the expectation with respect to all the randomness in the argument and the expectation with respect to $\mathbf{x}$, respectively; $\mathcal{N}(\boldsymbol{x}; \boldsymbol{\mu}, \boldsymbol{\Sigma})$ denotes the probability density function (PDF) of a random vector $\mathbf{x}$ following the Gaussian distribution with mean vector $\boldsymbol{\mu}$ and covariance matrix $\boldsymbol{\Sigma}$, evaluated at $\boldsymbol{x}$. The

[3] Agents' locations are modeled to be deterministic and random for non-Bayesian and Bayesian estimations, respectively.

relationships involving random quantities throughout the paper are all in the sense of "almost surely."

Vector $\mathbf{0}_K$ denotes the $K \times 1$ zero vector; matrices $\boldsymbol{O}_K$ and $\boldsymbol{I}_K$ denote the $K \times K$ zero and identity matrices, respectively; $\boldsymbol{x}^{(n_1:n_2)}$ denotes the concatenation of $\boldsymbol{x}^{(n_1)}, \boldsymbol{x}^{(n_1+1)}, \ldots, \boldsymbol{x}^{(n_2)}$ for $n_2 \geq n_1$; $\mathrm{diag}\{\boldsymbol{A}_1, \boldsymbol{A}_2, \ldots, \boldsymbol{A}_K\}$ is a block diagonal matrix with $\boldsymbol{A}_i$ being the ith block, $i = 1, 2, \ldots, K$; $\boldsymbol{A}^{\mathrm{T}}$ denotes the transpose of the matrix $\boldsymbol{A}$; $\mathrm{tr}\{\cdot\}$ denotes the trace of its argument; and $\otimes$ denotes the Kronecker product. The symmetric eigenvalue decomposition (SED) of a 2×2 real symmetric matrix $\boldsymbol{A}$ is expressed in the form of $\boldsymbol{A} = \sum_{l=1}^{2} \lambda_l(\boldsymbol{A}) \boldsymbol{u}(\psi_l(\boldsymbol{A})) \boldsymbol{u}^{\mathrm{T}}(\psi_l(\boldsymbol{A}))$, where $\lambda_1(\boldsymbol{A})$ and $\lambda_2(\boldsymbol{A})$ with $\lambda_1(\boldsymbol{A}) \geq \lambda_2(\boldsymbol{A})$ are the two eigenvalues of $\boldsymbol{A}$, $\boldsymbol{u}(\psi_1(\boldsymbol{A}))$ and $\boldsymbol{u}(\psi_2(\boldsymbol{A}))$ with $\psi_2(\boldsymbol{A}) = \psi_1(\boldsymbol{A}) + \pi/2$ are the corresponding eigenvectors, and $\boldsymbol{u}(\varphi) = \begin{bmatrix} \cos(\varphi) & \sin(\varphi) \end{bmatrix}^{\mathrm{T}}$. For matrices $\boldsymbol{A}$ and $\boldsymbol{B}$, $\boldsymbol{A} \succcurlyeq \boldsymbol{B}$ denotes that $\boldsymbol{A} - \boldsymbol{B}$ is positive semidefinite; for a sequence of matrices $\{\boldsymbol{A}_n\}$, $\lim_{n\to\infty} \boldsymbol{A}_n$ denotes element-wise limit. For sets $\mathcal{A}$ and $\mathcal{B}$ in $\mathbb{R}^d$, $\mathcal{A} + \mathcal{B}$ denotes the set $\{\boldsymbol{a} + \boldsymbol{b} : \boldsymbol{a} \in \mathcal{A}, \boldsymbol{b} \in \mathcal{B}\}$. For functions $g_1(\cdot)$ and $g_2(\cdot)$, $g_1(n) = \Theta(g_2(n))$ denotes that there exist c_{L}, c_{U}, and N such that $c_{\mathrm{L}} g_2(n) \leq g_1(n) \leq c_{\mathrm{U}} g_2(n)$ for all $n > N$.

The functions $f_{\mathsf{x}}(\boldsymbol{x}; \boldsymbol{\theta})$, $f_{\mathsf{x}}(\boldsymbol{x})$, and $f_{\mathsf{x}|\mathsf{y}}(\boldsymbol{x}|\boldsymbol{y})$ denote respectively the PDF of x parameterized by $\boldsymbol{\theta}$, the PDF of x, and the conditional PDF of x given y. For non-Bayesian estimation, define

$$\jmath_{\mathrm{bm}}\big(\boldsymbol{z}, a(\boldsymbol{\theta}_1, \boldsymbol{\theta}_2), \boldsymbol{\theta}_1\big) \triangleq -\frac{\partial^2 \ln f_{\mathsf{z}}\big(\boldsymbol{z}; a(\boldsymbol{\theta}_1, \boldsymbol{\theta}_2)\big)}{\partial \boldsymbol{\theta}_1 \partial \boldsymbol{\theta}_1^{\mathrm{T}}}$$

where $\boldsymbol{\theta}_1$ and $\boldsymbol{\theta}_2$ are deterministic unknown parameters, z is a random vector representing the measurement of $\boldsymbol{\theta}_1$ and $\boldsymbol{\theta}_2$, and a is a function of parameters. For Bayesian estimation, define

$$\jmath_{\mathrm{bm}}\big(\boldsymbol{z}, a(\boldsymbol{\theta}_1, \boldsymbol{\theta}_2), \boldsymbol{\theta}_1\big) \triangleq -\frac{\partial^2 \ln f_{\mathsf{z}|a(\boldsymbol{\theta}_1,\boldsymbol{\theta}_2)}\big(\boldsymbol{z} \,\big|\, a(\boldsymbol{\theta}_1, \boldsymbol{\theta}_2)\big)}{\partial \boldsymbol{\theta}_1 \partial \boldsymbol{\theta}_1^{\mathrm{T}}}$$

$$\jmath_{\mathrm{bp}}\big(b(\boldsymbol{\theta}_1), \boldsymbol{\theta}_2, \boldsymbol{\theta}_1\big) \triangleq -\frac{\partial^2 \ln f_{b(\boldsymbol{\theta}_1)|\boldsymbol{\theta}_2}\big(b(\boldsymbol{\theta}_1) \,\big|\, \boldsymbol{\theta}_2\big)}{\partial \boldsymbol{\theta}_1 \partial \boldsymbol{\theta}_1^{\mathrm{T}}}$$

where $\boldsymbol{\theta}_1$ and $\boldsymbol{\theta}_2$ are random unknown parameters, z is a random vector representing the measurement of $\boldsymbol{\theta}_1$ and $\boldsymbol{\theta}_2$, and a and b are functions of parameters. Whenever there is no ambiguity, the subscripts x and $\mathsf{x}|\mathsf{y}$ of f will be omitted. Finally, the notations of important quantities that are used throughout the paper are summarized in Table I.

TABLE I
NOTATIONS OF IMPORTANT QUANTITIES

Notation	Definition
$\mathcal{N}_{\mathrm{a}}$	Index set of agents with cardinality N_{a}
$\mathcal{N}_{\mathrm{b}}$	Index set of anchors with cardinality N_{b}
$\boldsymbol{p}_i^{(n)}$	Location of node i at t_n
$\boldsymbol{p}_{\mathrm{a}}^{(n)}$	Vector of agents' locations at t_n
$\boldsymbol{p}_{\mathrm{b}}^{(n)}$	Vector of anchors' locations at t_n
R	Communication range
L	Multiplexing factor
$\boldsymbol{z}_{ij}^{(n)}$	Vector of inter-node measurements between nodes i and j
$\boldsymbol{z}_{ii}^{(n)}$	Vector of intra-node measurements of agent i
(i_n, j_n)	Selected measurement pair in $[t_n, t_{n+1})$
$d_{ij}^{(n)}$	Distance between nodes i and j
$\varphi_{ij}^{(n)}$	Angle of the vector from node j to node i
$\varepsilon_{ij}^{(n)}$	Inter-node measurement error between nodes i and j
$\boldsymbol{J}^{(n)}$	FIM about agents' locations from t_1 to t_n
$\boldsymbol{E}_{i,j}^{(n)}$	An $n \times n$ matrix with all zeros except a 1 on entry (i, j)
$\boldsymbol{C}_{ij}^{(n)}$	FIM from inter-node measurements between nodes i and j
$\boldsymbol{D}^{(n)}$	FIM from intra-node measurements and prior knowledge
$\boldsymbol{Q}^{(n)}$	IFIM about agents' locations at t_n
$\boldsymbol{Q}_{ii}^{(n)}$	IFIM about agent i's location at t_n
$\boldsymbol{\Upsilon}_{ij}^{(n)}$	Error reduction matrix from inter-node measurements between nodes i and j
$\boldsymbol{\Delta}^{(n)}$	Error increase matrix
$\overline{\varepsilon}$	Upper bound on expected inter-node measurement error
$\overline{\delta}$	Upper bound on error increase
$\underline{\delta}$	Lower bound on error increase
q_N	Time-averaged NLE
$q_N^{\star}$	Time-averaged largest individual error
$\mathcal{N}_{\mathrm{b},i}^{(n)}$	Set of anchors within the communication range of agent i
$\mathcal{N}_{\mathrm{a},i}^{(n)}$	Set of agents within the communication range of agent i
μ_{b}	Anchor density
ζ_{b}	Probability that there exists at least one anchor within the communication range of an agent

II. MATHEMATICAL SETTING

This section presents the mathematical model for wireless navigation networks and the characterization of the error evolution.

A. Navigation Network

Consider a two-dimensional navigation network with a group of N_{a} mobile agents with index set $\mathcal{N}_{\mathrm{a}} = \{1, 2, \ldots, N_{\mathrm{a}}\}$ and N_{b} anchors with index set $\mathcal{N}_{\mathrm{b}} = \{N_{\mathrm{a}}+1, N_{\mathrm{a}}+2, \ldots, N_{\mathrm{a}}+N_{\mathrm{b}}\}$.[4] Let $\{t_n\}_{n\geq 1}$ be a sequence of time instants with $t_n < t_{n+1}$ for all $n \geq 1$. Furthermore, let the 2×1 vector $\boldsymbol{p}_i^{(n)}$ be the location of node i at t_n, $\boldsymbol{p}_{\mathrm{a}}^{(n)} = \begin{bmatrix} \boldsymbol{p}_1^{(n)\mathrm{T}} & \boldsymbol{p}_2^{(n)\mathrm{T}} & \cdots & \boldsymbol{p}_{N_{\mathrm{a}}}^{(n)\mathrm{T}} \end{bmatrix}^{\mathrm{T}}$, and $\boldsymbol{p}_{\mathrm{b}}^{(n)} = \begin{bmatrix} \boldsymbol{p}_{N_{\mathrm{a}}+1}^{(n)\mathrm{T}} & \boldsymbol{p}_{N_{\mathrm{a}}+2}^{(n)\mathrm{T}} & \cdots & \boldsymbol{p}_{N_{\mathrm{a}}+N_{\mathrm{b}}}^{(n)\mathrm{T}} \end{bmatrix}^{\mathrm{T}}$. Both non-Bayesian and Bayesian estimations [60] of agents' locations are considered. In the non-Bayesian case, the agents estimate their locations based only on the inter- and intra-node measurements, while in the Bayesian case, the agents estimate their locations based also on the prior knowledge about their movements. The measurements and the prior knowledge are introduced in the following.

1) Measurements: Two nodes can perform inter-node measurements only if they are within a communication range of R meters.[5] Let $\mathcal{N}_{\mathrm{a},i}^{(n)}$ and $\mathcal{N}_{\mathrm{b},i}^{(n)}$ be respectively the index sets of agents and anchors within R meters of agent i in the nth time interval $[t_n, t_{n+1})$. A limited number L of measurement pairs can be selected by a scheduling strategy in every time

[4]The paper mainly focuses on the 2-D case to provide insights. The extension to 3-D networks will be provided in Section VII-B.

[5]The communication range R is related to the received signal-to-noise ratio (SNR). For example, R is the maximum distance at which the expected received SNR is above a given threshold for successful inter-node measurements.

interval $[t_n, t_{n+1})$ due to limited wireless resources.[6] Each measurement pair consists of two agents or an agent and an anchor. Single measurement pair per interval ($L = 1$) is first considered as a basic case, and the extension to settings with multiple measurement pairs per interval ($L > 1$) will be provided in Section VI based on a transformation into the basic case. All the agents can perform intra-node measurements in every time interval. The inter- and intra-node measurements are described as follows.

- *Inter-node Measurements:* The inter-node measurements depend on nodes' locations via distances (e.g., range measurements). In particular, the vector of inter-node measurements $\mathbf{z}_{ij}^{(n)}$ between node i and node j in $[t_n, t_{n+1})$ follows the distributions $f\big(\boldsymbol{z}_{ij}^{(n)}; d_{ij}^{(n)}\big)$ and $f\big(\boldsymbol{z}_{ij}^{(n)} \big| d_{ij}^{(n)}\big)$ respectively in the non-Bayesian and Bayesian cases, where $d_{ij}^{(n)} = \big\|\boldsymbol{p}_i^{(n)} - \boldsymbol{p}_j^{(n)}\big\|$ is the Euclidean distance between node i and node j.
- *Intra-node Measurements:* The intra-node measurements depend on nodes' locations via displacements (e.g., acceleration measurements). In particular, the vector of intra-node measurements $\mathbf{z}_{ii}^{(n+1)}$ of agent i in $[t_n, t_{n+1})$ follows the distributions $f\big(\boldsymbol{z}_{ii}^{(n+1)}; \boldsymbol{p}_i^{(n+1)} - \boldsymbol{p}_i^{(n)}\big)$ and $f\big(\boldsymbol{z}_{ii}^{(n+1)} \big| \boldsymbol{p}_i^{(n+1)} - \boldsymbol{p}_i^{(n)}\big)$ respectively in the non-Bayesian and Bayesian cases.

All the measurements are considered to be independent, conditioned on agents' locations.

2) Prior Knowledge: The prior knowledge is given by the probability distribution of $\{\mathbf{p}_{\mathrm{a}}^{(n)}\}_{n\geq 1}$, which characterizes the knowledge about the movements of the agents. The prior knowledge is considered to satisfy the Markov property, i.e., the distribution of $\mathbf{p}_{\mathrm{a}}^{(1:n)}$ for $n \geq 1$ can be factorized as

$$f\big(\boldsymbol{p}_{\mathrm{a}}^{(1:n)}\big) = f\big(\boldsymbol{p}_{\mathrm{a}}^{(1)}\big) \prod_{k=2}^{n} f\big(\boldsymbol{p}_{\mathrm{a}}^{(k)} \big| \boldsymbol{p}_{\mathrm{a}}^{(k-1)}\big). \tag{1}$$

The PDF $f\big(\boldsymbol{p}_{\mathrm{a}}^{(k)} \big| \boldsymbol{p}_{\mathrm{a}}^{(k-1)}\big)$ is considered to depend on $\boldsymbol{p}_{\mathrm{a}}^{(k-1)}$ and $\boldsymbol{p}_{\mathrm{a}}^{(k)}$ via the displacement $\boldsymbol{p}_{\mathrm{a}}^{(k)} - \boldsymbol{p}_{\mathrm{a}}^{(k-1)}$.

B. Fisher Information Matrix

The localization errors are characterized based on the FIM, which has been extensively utilized for the performance analysis of estimation systems (e.g., [4], [23], [61]–[64]). The FIMs about agents' locations for the non-Bayesian and Bayesian cases are provided in the following. Let (i_n, j_n) be the measurement pair selected by a *scheduling strategy* in $[t_n, t_{n+1})$ and $\mathbf{z}^{(n)}$ be the concatenation of $\mathbf{z}_{i_n j_n}^{(n)}$ and $\{\mathbf{z}_{ii}^{(n+1)}\}_{i\in\mathcal{N}_{\mathrm{a}}}$. Let $\boldsymbol{J}^{(n)}$ be the $2N_{\mathrm{a}}n \times 2N_{\mathrm{a}}n$ FIM about agents' locations from t_1 to t_n.

For $n = 1$, the initial FIM $\boldsymbol{J}^{(1)}$ is described in the following.

- In the non-Bayesian case, $\boldsymbol{J}^{(1)}$ represents the contribution from the initial measurements $\mathbf{z}^{(0)}$ between the agents and some anchors, given by
$$\boldsymbol{J}^{(1)} = \mathbb{E}\Big\{\jmath_{\mathrm{bm}}\big(\mathbf{z}^{(0)}, \boldsymbol{p}_{\mathrm{a}}^{(1)}, \boldsymbol{p}_{\mathrm{a}}^{(1)}\big)\Big\}.$$
- In the Bayesian case, $\boldsymbol{J}^{(1)}$ represents the contribution from the initial measurements $\mathbf{z}^{(0)}$ and from the prior knowledge about $\mathbf{p}_{\mathrm{a}}^{(1)}$, given by
$$\boldsymbol{J}^{(1)} = \mathbb{E}\Big\{\jmath_{\mathrm{bm}}\big(\mathbf{z}^{(0)}, \mathbf{p}_{\mathrm{a}}^{(1)}, \mathbf{p}_{\mathrm{a}}^{(1)}\big)\Big\} + \mathbb{E}\Big\{\jmath_{\mathrm{bp}}\big(\mathbf{p}_{\mathrm{a}}^{(1)}, \emptyset, \mathbf{p}_{\mathrm{a}}^{(1)}\big)\Big\}.$$

The initial FIM $\boldsymbol{J}^{(1)}$ is considered to be invertible for both the non-Bayesian and Bayesian cases.

For $n \geq 2$, the FIM $\boldsymbol{J}^{(n)}$ about agents' locations from t_1 to t_n is given in the following proposition.

Proposition 1: The FIM $\boldsymbol{J}^{(n)}$ for $n \geq 2$ in both the non-Bayesian and Bayesian cases is given by

$$\boldsymbol{J}^{(n)} = \sum_{k=1}^{n} \boldsymbol{E}_{k,k}^{(n)} \otimes \boldsymbol{G}^{(k)} - \sum_{k=2}^{n} \big(\boldsymbol{E}_{k-1,k}^{(n)} + \boldsymbol{E}_{k,k-1}^{(n)}\big) \otimes \boldsymbol{D}^{(k)} \tag{2}$$

where $\boldsymbol{E}_{i,j}^{(n)}$ is an $n \times n$ matrix with all zeros except a 1 on the (i,j)th entry, and

$$\boldsymbol{G}^{(k)} = \begin{cases} \boldsymbol{J}^{(1)} + \boldsymbol{C}_{i_1 j_1}^{(1)} + \boldsymbol{D}^{(2)}, & k = 1 \\ \boldsymbol{D}^{(k)} + \boldsymbol{C}_{i_k j_k}^{(k)} + \boldsymbol{D}^{(k+1)}, & 2 \leq k \leq n-1 \\ \boldsymbol{D}^{(n)}, & k = n. \end{cases} \tag{3}$$

The matrix $\boldsymbol{C}_{ij}^{(k)}$ in (3) represents the contribution from the inter-node measurements between node i and node j in $[t_k, t_{k+1})$, given in the following.

- In the non-Bayesian case,
$$\boldsymbol{C}_{ij}^{(k)} = \boldsymbol{\Xi}_{ij}\big(\varepsilon_{ij}^{(k)}, \varphi_{ij}^{(k)}\big) \tag{4a}$$
$$\triangleq \frac{1}{\varepsilon_{ij}^{(k)}} \boldsymbol{A}_{ij} \boldsymbol{u}\big(\varphi_{ij}^{(k)}\big) \boldsymbol{u}^{\mathrm{T}}\big(\varphi_{ij}^{(k)}\big) \boldsymbol{A}_{ij}^{\mathrm{T}} \tag{4b}$$
where
$$\varepsilon_{ij}^{(k)} = \mathbb{E}\Big\{\jmath_{\mathrm{bm}}\big(\mathbf{z}_{ij}^{(k)}, d_{ij}^{(k)}, d_{ij}^{(k)}\big)\Big\}^{-1} \tag{5}$$
is the inverse of the Fisher information about $d_{ij}^{(k)}$ from $\mathbf{z}_{ij}^{(k)}$, $\varphi_{ij}^{(k)}$ is the angle of the vector from node j to node i at t_k, and
$$\boldsymbol{A}_{ij} = \begin{cases} \boldsymbol{e}_i \otimes \boldsymbol{I}_2, & i \in \mathcal{N}_{\mathrm{a}},\ j \in \mathcal{N}_{\mathrm{b}} \\ (\boldsymbol{e}_i - \boldsymbol{e}_j) \otimes \boldsymbol{I}_2, & i, j \in \mathcal{N}_{\mathrm{a}} \end{cases} \tag{6}$$
in which $\boldsymbol{e}_i$ is an $N_{\mathrm{a}} \times 1$ vector with all zeros except a 1 on the ith row.[7]
- In the Bayesian case,[8]
$$\boldsymbol{C}_{ij}^{(k)} = \mathbb{E}\Big\{\boldsymbol{\Xi}_{ij}\big(\boldsymbol{\varepsilon}_{ij}^{(k)}, \boldsymbol{\varphi}_{ij}^{(k)}\big)\Big\}. \tag{7}$$

The matrix $\boldsymbol{D}^{(k)}$ in (3) represents the contribution from the intra-node measurements in $[t_{k-1}, t_k)$ (and from the prior knowledge about $\mathbf{p}_{\mathrm{a}}^{(k-1:k)}$ for the Bayesian case), given by (74) and (75) respectively for the non-Bayesian and Bayesian cases.

Proof: See Appendix I-A. □

[6] The results of this paper apply to any wireless network with fixed total amount of communication resources. Note that a wireless network employing resource reuse over a large area can be subdivided into networks employing a fixed amount of resources over a small area (e.g., cells in a cellular network).

[7] A toy example of $\boldsymbol{C}_{ij}^{(k)}$ is provided in Appendix I-B.

[8] In the Bayesian case, $\boldsymbol{\varepsilon}_{ij}^{(k)}$ and $\boldsymbol{\varphi}_{ij}^{(k)}$ are random variables since they depend on agents' locations in $\mathbf{p}_{\mathrm{a}}^{(k)}$.

C. Error Evolution

Let $\boldsymbol{Q}^{(n)}$ be the inverse of the FIM (IFIM) about $\boldsymbol{p}_{\rm a}^{(n)}$ (non-Bayesian) and $\mathbf{p}_{\rm a}^{(n)}$ (Bayesian) from the measurements in $\mathbf{z}^{(1:n-1)}$ (and from the prior knowledge about $\mathbf{p}_{\rm a}^{(1:n)}$ for the Bayesian case). In particular, $\boldsymbol{Q}^{(n)}$ is given by the nth $2N_{\rm a}\times 2N_{\rm a}$ principal submatrix of $[\,\boldsymbol{J}^{(n)}]^{-1}$, and it provides a lower bound on the mean-squared estimation error of agents' locations at t_n according to the information inequality [4], [60]. The time evolution of the IFIM $\{\boldsymbol{Q}^{(n)}\}_{n\geq 1}$ is referred to as the *error evolution*, which is characterized in the following proposition.

Proposition 2: The error evolution $\{\boldsymbol{Q}^{(n)}\}_{n\geq 1}$ is given by

$$\boldsymbol{Q}^{(n+1)}=\boldsymbol{Q}^{(n)}-\boldsymbol{\Upsilon}_{i_nj_n}^{(n)}+\boldsymbol{\Delta}^{(n+1)} \tag{8}$$

where $\boldsymbol{Q}^{(1)}=[\,\boldsymbol{J}^{(1)}]^{-1}$, $\boldsymbol{\Delta}^{(n)}=[\,\boldsymbol{D}^{(n)}]^{-1}$, and

- in the non-Bayesian case,

$$\boldsymbol{\Upsilon}_{ij}^{(n)}=\frac{\boldsymbol{Q}^{(n)}\boldsymbol{A}_{ij}\boldsymbol{u}\big(\varphi_{ij}^{(n)}\big)\boldsymbol{u}^{\rm T}\big(\varphi_{ij}^{(n)}\big)\boldsymbol{A}_{ij}^{\rm T}\boldsymbol{Q}^{(n)}}{\varepsilon_{ij}^{(n)}+\boldsymbol{u}^{\rm T}\big(\varphi_{ij}^{(n)}\big)\boldsymbol{A}_{ij}^{\rm T}\boldsymbol{Q}^{(n)}\boldsymbol{A}_{ij}\boldsymbol{u}\big(\varphi_{ij}^{(n)}\big)} \tag{9}$$

- in the Bayesian case,

$$\boldsymbol{\Upsilon}_{ij}^{(n)}=\boldsymbol{Q}^{(n)}-\Big([\,\boldsymbol{Q}^{(n)}]^{-1}+\mathbb{E}\big\{\boldsymbol{\Xi}_{ij}(\upvarepsilon_{ij}^{(n)},\upvarphi_{ij}^{(n)})\big\}\Big)^{-1}. \tag{10}$$

Proof: See Appendix I-C. □

Remark 1: In (8), $\boldsymbol{\Upsilon}_{i_nj_n}^{(n)}\in\mathbb{S}_{+}^{2N_{\rm a}}$ is the *error reduction matrix* corresponding to the inter-node measurements between nodes i_n and j_n, and $\boldsymbol{\Delta}^{(n+1)}\in\mathbb{S}_{++}^{2N_{\rm a}}$ is the *error increase matrix* due to the uncertainty in the intra-node measurements (and in the prior knowledge for the Bayesian case). Thus, the total error reduction and increase in $[\,t_n,t_{n+1})$ are given by $\mathrm{tr}\{\boldsymbol{\Upsilon}_{i_nj_n}^{(n)}\}$ and $\mathrm{tr}\{\boldsymbol{\Delta}^{(n+1)}\}$, respectively. Higher accuracy of inter- and intra-node measurements corresponds to larger error reduction and smaller error increase, respectively.

According to (8)–(10), the error evolution depends on the scheduling strategy via the selected measurement pairs $\{(i_n,j_n)\}$, on the anchors' locations $\{\boldsymbol{p}_{\rm b}^{(n)}\}$, and on the measurement errors $\{\varepsilon_{i_nj_n}^{(n)}\}$ and $\{\boldsymbol{\Delta}^{(n)}\}$. In the non-Bayesian case, the error evolution depends also on the agents' locations $\{\boldsymbol{p}_{\rm a}^{(n)}\}$ as in (4a) and (74) since they are considered to be deterministic. In the Bayesian case, the error evolution does not depend on the agents' locations due to the expectation with respect to the prior knowledge as in (7), (70), and (75).

Following the nomenclature of data networks [58], $\boldsymbol{Q}^{(n)}$, $\boldsymbol{\Upsilon}_{i_nj_n}^{(n)}$, and $\boldsymbol{\Delta}^{(n+1)}$ in (8) can be viewed as the "queue length," "service," and "packet arrival" in $[\,t_n,t_{n+1})$, respectively. In contrast to queueing dynamics where the service rates are commonly independent of the queue lengths, the error reduction matrices in (9) and (10) depend on the IFIM $\boldsymbol{Q}^{(n)}$, the geometrical relationship of the measurement pair $\varphi_{i_nj_n}^{(n)}$ (for the non-Bayesian case), the measurement errors $\varepsilon_{i_nj_n}^{(n)}$, and the uncertainty in the prior knowledge (for the Bayesian case).

Finally, the recursive equation (8) can be used to characterize the error evolution for both synchronous and asynchronous networks. For synchronous networks, the clocks of all the nodes are synchronized and t_n is the start of the nth time interval, which is common to the entire network. For asynchronous networks, t_n is when the wireless channel is accessed (by a measurement pair) for the nth time.

Remark 2: Due to the unified structure of the error evolution in (8), the analysis in the rest of the paper holds for both the non-Bayesian and Bayesian cases. Thus, we will not emphasize non-Bayesian or Bayesian estimation unless otherwise necessary.

III. Boundedness of Error Evolution

This section provides both sufficient and necessary conditions for the boundedness of the error evolution, which is a primary requirement on the design of scheduling strategies for navigation networks. The results will later be used in Section IV to analyze the error evolution for the opportunistic and random situation-aware scheduling strategies.

A. Performance Metric for Network Navigation

The navigation performance in Section II-C is affected by the network topology (anchors' locations) and the selected measurement pairs (scheduling strategy). Thorough analysis of navigation networks requires the characterization of their performance over the ensemble of possible network topologies and measurement pairs. We consider anchors' locations following a spatial distribution in $\mathbb{R}^2$ and measurement pairs following a probability distribution defined by the scheduling strategy. Therefore, the error evolution becomes a random process $\{\mathbf{Q}^{(n)}\}_{n\geq 1}$.

The NLE at t_n is defined as $\mathrm{tr}\{\mathbf{Q}^{(n)}\}$, which is the total localization error of all the agents. Since we are interested in the localization accuracy over N time intervals, the following performance metrics are considered. Define the *time-averaged NLE* and the time-averaged largest individual error respectively as

$$q_N\triangleq\frac{1}{N}\sum_{n=1}^{N}\mathbb{E}\{\mathrm{tr}\{\mathbf{Q}^{(n)}\}\} \tag{11}$$

$$q_N^{\star}\triangleq\frac{1}{N}\sum_{n=1}^{N}\mathbb{E}\big\{\mathrm{tr}\{\mathbf{Q}_{\mathsf{i}_n^{\star}\mathsf{i}_n^{\star}}^{(n)}\}\big\}. \tag{12}$$

In (11) and (12), the expectation is with respect to the randomness in the network topology and in the scheduling strategy. In (12), $\mathbf{Q}_{ii}^{(n)}$ is the ith 2×2 principal submatrix of $\mathbf{Q}^{(n)}$, i.e., the IFIM about agent i's location at t_n, and

$$\mathsf{i}_n^{\star}\in\arg\max_{i\in\mathcal{N}_{\rm a}}\mathrm{tr}\{\mathbf{Q}_{ii}^{(n)}\}. \tag{13}$$

Note that the index $\mathsf{i}_n^{\star}$ of the agent with the largest localization error is time-variant.

Remark 3: For a navigation network in which agents perform inter-node measurements following a scheduling strategy, q_N in (11) characterizes the navigation performance averaged over the randomness in anchors' locations and the scheduling strategy. Furthermore, q_N can be used to characterize the

outage probability using the Markov's inequality as[9]

$$\mathbb{P}\Big\{\frac{1}{N}\sum_{n=1}^{N}\mathrm{tr}\{\mathbf{Q}^{(n)}\}\geq T\Big\}\leq\frac{q_N}{T}$$

for any positive threshold T, even though the exact outage probability is intractable to analyze due to the intricate structure of $\{\mathbf{Q}^{(n)}\}_{n\geq 1}$.

The following condition is considered.

Condition 1:

- There exists an $\overline{\varepsilon}<\infty$ such that

$$\mathbb{E}\big\{\varepsilon_{ij}^{(n)}\,\big|\,\varphi_{ij}^{(n)},\,\big|\,\mathsf{N}_{\mathrm{b},i}^{(n)}\big|=K,\,\mathbf{Q}^{(n)}\big\}\leq\overline{\varepsilon}\qquad(14)$$

  for all $K>0$, $i\in\mathcal{N}_{\mathrm{a}}$, $\mathsf{j}\in\mathsf{N}_{\mathrm{b},i}^{(n)}$, and $n\geq 1$.[10]
- There exists a $\overline{\delta}<\infty$ such that

$$\frac{1}{N}\sum_{n=1}^{N}\mathrm{tr}\{\boldsymbol{\Delta}^{(n+1)}\}\leq 2N_{\mathrm{a}}\overline{\delta},\quad\forall\,N\geq 1.\qquad(15)$$

- There exists a $\underline{\delta}>0$ such that

$$\boldsymbol{\Delta}^{(n)}\succcurlyeq\underline{\delta}\,\boldsymbol{I}_{2N_{\mathrm{a}}},\quad\forall\,n\geq 2.\qquad(16)$$

The inequality (14) requires that the expected inter-node measurement error between an agent and an anchor within the communication range is upper bounded. This is a mild condition that is satisfied by practical sensors for inter-node measurements [68]. The inequality (15) is implied by the following condition

$$\mathrm{tr}\{\boldsymbol{\Delta}^{(n)}\}\leq 2N_{\mathrm{a}}\overline{\delta},\quad\forall\,n\geq 2\qquad(17)$$

i.e., the total error increase is upper bounded. The inequality (17) is satisfied for agents with bounded velocities and for practical inertial measurement units (IMUs) with bounded intra-node measurement errors. The lower bound (16) on the error increase is reasonable since intra-node measurements and prior knowledge are always subject to uncertainty in practice.

B. Sufficient Condition for Boundedness

A sufficient condition for the boundedness of the error evolution is provided as follows.

Proposition 3: Consider an error evolution $\{\mathbf{Q}^{(n)}\}_{n\geq 1}$ satisfying (8) and Condition 1. For a function $\upsilon:\mathbb{S}_{+}^{2N_{\mathrm{a}}}\rightarrow\mathbb{R}_{\geq 0}$, if there exists a convex function $g:\mathbb{R}_{\geq 0}\rightarrow\mathbb{R}$ with $\lim_{x\rightarrow\infty}g(x)=\infty$ such that

$$\mathbb{E}\big\{\mathrm{tr}\{\boldsymbol{\Upsilon}_{\mathsf{i}_n\mathsf{j}_n}^{(n)}\}\,\big|\,\mathbf{Q}^{(n)}\big\}\geq g\big(\upsilon(\mathbf{Q}^{(n)})\big),\quad\forall\,n\geq 1\qquad(18)$$

then we have

$$\frac{1}{N}\sum_{n=1}^{N}\mathbb{E}\big\{\upsilon(\mathbf{Q}^{(n)})\big\}\leq B_N,\quad\forall\,N\geq 1\qquad(19)$$

where

$$B_N=\sup\Big\{x:g(x)\leq 2N_{\mathrm{a}}\overline{\delta}+\frac{1}{N}\,\mathbb{E}\big\{\mathrm{tr}\{\mathbf{Q}^{(1)}\}\big\}\Big\}\qquad(20)$$

is upper bounded and non-increasing with N.

Proof: See Appendix II-A. □

[9]The outage probability is a well known concept for performance evaluation of wireless communication systems (see, e.g., [65]–[67]). Here we evaluate the probability that the NLE rises above a given target.

[10]Since anchors' locations are drawn from a spatial distribution, the set $\mathsf{N}_{\mathrm{b},i}^{(n)}$ and the index j are random.

1) Interpretation of Proposition 3: Proposition 3 provides a general sufficient condition for the boundedness of an arbitrary function of the localization error. For example, if Proposition 3 holds for $\upsilon(\mathbf{Q}^{(n)})=\mathrm{tr}\{\mathbf{Q}^{(n)}\}$, then by (11), there exists a non-increasing sequence $\{B_N\}$ such that $q_N\leq B_N$ for all $N\geq 1$, which further implies $\limsup_{N\rightarrow\infty}q_N\leq B_1$. The latter inequality is akin to *strong stability* in data communication networks, which is defined as the boundedness of the time-averaged delay [59]. Moreover, if Proposition 3 holds for $\upsilon(\mathbf{Q}^{(n)})=\mathrm{tr}\{\mathbf{Q}_{\mathsf{i}_n^\star\mathsf{j}_n^\star}^{(n)}\}$, then by (12), there exists a non-increasing sequence $\{B_N^\star\}$ such that $q_N^\star\leq B_N^\star$ for all $N\geq 1$.

Proposition 3 can be used to derive upper bounds on the error evolution for different scheduling strategies. In particular, the expectation on the left-hand side of (18) is with respect to the randomness in the network topology and in the scheduling strategy. Given a scheduling strategy, if a lower bound on the expected error reduction in the form of (18) can be established, then an upper bound on the error evolution in the form of (20) can be obtained. An application of Proposition 3 on the localization error analysis will be demonstrated with details in Section IV-B. Furthermore, if in addition to convexity, $g(\cdot)$ in (18) is strictly increasing, then (20) can be written as

$$B_N=g^{-1}\Big(2N_{\mathrm{a}}\overline{\delta}+\frac{1}{N}\,\mathbb{E}\big\{\mathrm{tr}\{\mathbf{Q}^{(1)}\}\big\}\Big).\qquad(21)$$

An example of a convex and strictly increasing $g(\cdot)$ is $g(x)=ax^2/(x+b)$ with $a>0$ and $b\geq 0$. Lower bounds on the expected error reduction $\mathbb{E}\big\{\mathrm{tr}\{\boldsymbol{\Upsilon}_{\mathsf{i}_n\mathsf{j}_n}^{(n)}\}\,\big|\,\mathbf{Q}^{(n)}\big\}$ in this form of $g(\cdot)$ will be derived in the error analysis in Section IV-B.

Proposition 3 can also be used to compare the performance of different scheduling strategies. Consider scheduling strategies I and II. If there exist convex mappings $g_{\mathrm{I}}(\cdot)$ and $g_{\mathrm{II}}(\cdot)$ with $\lim_{x\rightarrow\infty}g_{\mathrm{I}}(x)=\infty$, $\lim_{x\rightarrow\infty}g_{\mathrm{II}}(x)=\infty$, and $g_{\mathrm{I}}(x)\geq g_{\mathrm{II}}(x)$ for all x such that

$$\mathbb{E}\big\{\mathrm{tr}\{\boldsymbol{\Upsilon}_{\mathsf{i}_n\mathsf{j}_n}^{(n)}\}\,\big|\,\mathbf{Q}^{(n)}\big\}\geq g_{\mathrm{I}}\big(\mathrm{tr}\{\mathbf{Q}^{(n)}\}\big),\quad\forall\,n\geq 1$$
$$\mathbb{E}\big\{\mathrm{tr}\{\boldsymbol{\Upsilon}_{\mathsf{i}_n\mathsf{j}_n}^{(n)}\}\,\big|\,\mathbf{Q}^{(n)}\big\}\geq g_{\mathrm{II}}\big(\mathrm{tr}\{\mathbf{Q}^{(n)}\}\big),\quad\forall\,n\geq 1$$

for scheduling strategies I and II, respectively, then according to (19) and (20) with $\upsilon(\mathbf{Q}^{(n)})=\mathrm{tr}\{\mathbf{Q}^{(n)}\}$, there exist $\{B_{\mathrm{I},N}\}$ and $\{B_{\mathrm{II},N}\}$ with $B_{\mathrm{I},N}\leq B_{\mathrm{II},N}$ for all $N\geq 1$ such that $q_N\leq B_{\mathrm{I},N}$ and $q_N\leq B_{\mathrm{II},N}$ for scheduling strategies I and II, respectively. Thus, scheduling strategies with larger error reductions lead to smaller upper bounds on the time-averaged NLE. Since exact time-averaged NLE for a scheduling strategy is often intractable to solve, the analytical comparison of the time-averaged NLEs (rather than their upper bounds) for different scheduling strategies remains an open problem.

2) Generalization of Proposition 3: The condition (18) in Proposition 3 is required to hold for every time interval. This requirement can be further relaxed for the boundedness of the time-averaged NLE. Considering $\upsilon(\mathbf{Q}^{(n)})=\mathrm{tr}\{\mathbf{Q}^{(n)}\}$, the following extension of Proposition 3 can be obtained.

Corollary 1: Consider an error evolution $\{\mathbf{Q}^{(n)}\}_{n\geq 1}$ satisfying (8), Condition 1, and (17). If there exist an $N_{\mathrm{r}}\geq 1$ and a convex function $g:\mathbb{R}_{\geq 0}\rightarrow\mathbb{R}$ with $\lim_{x\rightarrow\infty}g(x)=\infty$ such that

$$\mathbb{E}\big\{\mathrm{tr}\{\boldsymbol{\Upsilon}_{\mathsf{i}_n\mathsf{j}_n}^{(n)}\}\,\big|\,\mathbf{Q}^{(n)}\big\}\geq g\big(\mathrm{tr}\{\mathbf{Q}^{(n)}\}\big)\qquad(22)$$

for all $n = kN_{\rm r}$ with $k \geq 1$, then we have $q_N \leq B_N$ for all $N \geq 1$, where

$$B_N = \frac{N_{\rm r}-1}{N}\,\mathbb{E}\big\{\mathrm{tr}\{\mathbf{Q}^{(1)}\}\big\} + \frac{(N_{\rm r}-1)(N_{\rm r}-2)N_{\rm a}}{N}\,\overline{\delta} + \breve{B}_{K_N} + (N_{\rm r}-1)N_{\rm a}\overline{\delta} \quad (23)$$

is bounded from above and non-increasing with N, in which $K_N = \lfloor N/N_{\rm r} \rfloor$ and

$$\breve{B}_K = \sup\Big\{x : g(x) \leq 2N_{\rm r}N_{\rm a}\overline{\delta} + \frac{1}{K}\,\mathbb{E}\big\{\mathrm{tr}\{\mathbf{Q}^{(1)}\}\big\}\Big\}. \quad (24)$$

Proof: See Appendix II-B. □

In Corollary 1, the localization errors are effectively reduced in the sense of (22) every $N_{\rm r}$ steps, while the errors are not guaranteed to be reduced in the $(N_{\rm r}-1)$ intermediate steps. As a result, the upper bound (23) on the time-averaged NLE is an increasing function of $N_{\rm r}$.

Remark 4: In practical systems, it is often preferable to perform as few inter-node measurements as possible as long as a system requirement on the time-averaged NLE is satisfied. Such a strategy helps to reduce power consumption as well as interference to coexisting communication systems. In this case, the system designer can solve for $N_{\rm r}$ from (23) with B_N being the required time-averaged NLE. Then in order to meet the requirement on the time-averaged NLE, it is only necessary to perform inter-node measurements (that lead to effective error reduction in the sense of (22)) every $N_{\rm r}$ steps.

Finally, following the proof of Proposition 3, a result can be obtained on the boundedness of general matrix evolution.

Corollary 2: Consider a matrix evolution $\{\mathbf{Q}^{(n)}\}_{n\geq 1}$ on $\mathbb{S}^D_{++}$ with $D \geq 1$ following

$$\mathbf{Q}^{(n+1)} = \mathbf{Q}^{(n)} - \boldsymbol{\Upsilon}^{(n)} + \boldsymbol{\Delta}^{(n+1)} \quad (25)$$

where $\boldsymbol{\Delta}^{(n)}$ satisfies (15). If (18) holds with $\boldsymbol{\Upsilon}^{(n)}_{\mathrm{i}_n\mathrm{j}_n}$ being replaced by $\boldsymbol{\Upsilon}^{(n)}$, then $\{\mathbf{Q}^{(n)}\}_{n\geq 1}$ is bounded in the sense of (19) with $2N_{\rm a}$ being replaced by D in (20).

Remark 5: Corollary 2 can be used to analyze the boundedness of general matrix evolution in the form of (25). An example is the evolution of the error covariance in Kalman filters [69]–[73], where $\mathbf{Q}^{(n)}$ is the *a priori* estimate error covariance, $\boldsymbol{\Upsilon}^{(n)}$ is the difference between the a priori estimate and the a posteriori estimate error covariances, and $\boldsymbol{\Delta}^{(n+1)}$ is the covariance of the process noise at the nth step.

C. Necessary Conditions for Boundedness

If Proposition 3 holds for $\upsilon(\mathbf{Q}^{(n)}) = \mathrm{tr}\{\mathbf{Q}^{(n)}\}$, then (19) together with (11) implies $q_N \leq B_N$ for all $N \geq 1$. Since $\{B_N\}$ is non-increasing with N, we have $q_N \leq B_1$ for all $N \geq 1$. Such boundedness of q_N leads to the balance between the error increase and reduction as follows.

Proposition 4: For an error evolution $\{\mathbf{Q}^{(n)}\}_{n\geq 1}$ satisfying (8) and Condition 1, if there exist a $B < \infty$ and an $\delta \geq 0$ such that $q_N \leq B$ for all $N \geq 1$ and

$$\lim_{N\to\infty}\frac{1}{N}\sum_{n=1}^{N}\mathrm{tr}\{\boldsymbol{\Delta}^{(n+1)}\} = 2N_{\rm a}\delta \quad (26)$$

then

$$\lim_{N\to\infty}\frac{1}{N}\sum_{n=1}^{N}\mathbb{E}\big\{\,\mathrm{tr}\{\boldsymbol{\Upsilon}^{(n)}_{\mathrm{i}_n\mathrm{j}_n}\}\big\} = 2N_{\rm a}\delta. \quad (27)$$

Proof: See Appendix II-C. □

Equations (26) and (27) show that the asymptotic time-averaged total error increase and reduction are equal when the time-averaged NLE is bounded, which agrees with the intuition. Furthermore, a stronger condition on $\{\boldsymbol{\Delta}^{(n)}\}$ together with the boundedness of q_N leads to the following result.

Proposition 5: For an error evolution $\{\mathbf{Q}^{(n)}\}_{n\geq 1}$ satisfying (8) and Condition 1, if there exist a $B < \infty$ and an $\boldsymbol{\Delta} \in \mathbb{S}^{2N_{\rm a}}_{+}$ such that $q_N \leq B$ for all $N \geq 1$ and

$$\lim_{N\to\infty}\frac{1}{N}\sum_{n=1}^{N}\boldsymbol{\Delta}^{(n+1)} = \boldsymbol{\Delta} \quad (28)$$

then

$$\lim_{N\to\infty}\frac{1}{N}\sum_{n=1}^{N}\mathbb{E}\big\{\,\boldsymbol{\Upsilon}^{(n)}_{\mathrm{i}_n\mathrm{j}_n}\big\} = \boldsymbol{\Delta}. \quad (29)$$

Proof: See Appendix II-D. □

Equations (28) and (29) show that the asymptotic time-averaged error increase and reduction matrices are equal when the time-averaged NLE is bounded.

Following the proof of Proposition 4, a sufficient condition on the unboundedness of the time-averaged NLE can be obtained in the following.

Corollary 3: For an error evolution $\{\mathbf{Q}^{(n)}\}_{n\geq 1}$ satisfying (8) and Condition 1, if

$$\liminf_{N\to\infty}\frac{1}{N}\sum_{n=1}^{N}\mathbb{E}\{\mathrm{tr}\{\boldsymbol{\Upsilon}^{(n)}_{\mathrm{i}_n\mathrm{j}_n}\}\} < \liminf_{N\to\infty}\frac{1}{N}\sum_{n=1}^{N}\mathrm{tr}\{\boldsymbol{\Delta}^{(n+1)}\} \quad (30)$$

then there does not exist a $B < \infty$ such that $q_N \leq B$ for all $N \geq 1$.

Proof: See Appendix II-E. □

Corollary 3 agrees with intuition: if the asymptotic time-averaged error reduction is not large enough to compensate for the asymptotic time-averaged error increase as in the inequality (30), then the boundedness of the time-averaged NLE is not guaranteed.

IV. Scheduling Strategies and Error Analysis

This section presents the opportunistic and random situation-aware scheduling strategies for network navigation. Then the upper bounds on the corresponding time-averaged NLEs are quantified by applying the sufficient condition for boundedness in Proposition 3. The results provide an example of how Proposition 3 is applied for error analysis.

A. Situation-Aware Scheduling Strategies

The problem of finding the optimal scheduling strategies that minimize the expected NLE $\mathbb{E}\{\mathrm{tr}\{\mathbf{Q}^{(N)}\}\}$ at t_N or the time-averaged NLE q_N over the first N time intervals can be formulated under the framework of dynamic programming [74]. However, the corresponding optimal scheduling

strategies are often intractable to characterize or implement due to the nonlinearity of the error evolution and its intricate dependency on the scheduling strategy, network topology, and measurement errors. Furthermore, the focus of this paper is to understand the effects of measurement pair selection rather than collision control on the error evolution. Thus, we consider two scheduling strategies that avoid packet collisions although the application of the results in Section III is not limited to these strategies. Let $\mathcal{M}_n$ be the set of candidate measurement pairs in $[t_n, t_{n+1})$. The scheduling policies of the two strategies in $[t_n, t_{n+1})$ are introduced in the following.

1) Opportunistic Scheduling Strategy: The strategy selects a measurement pair providing the largest error reduction, i.e.,[11]

$$(\mathsf{i}_n, \mathsf{j}_n) \in \arg\max_{(i,j)\in\mathcal{M}_n} \mathrm{tr}\{\boldsymbol{\Upsilon}_{ij}^{(n)}\}. \tag{31}$$

If multiple measurement pairs can provide the largest error reduction, then the strategy uniformly selects one of them at random.

2) Random Scheduling Strategy: The strategy first uniformly selects an agent i_n at random, i.e., $\mathbb{P}\{\mathsf{i}_n = i\} = 1/N_{\mathrm{a}}$ for all $i \in \mathcal{N}_{\mathrm{a}}$. If there exist anchors within the communication range of agent i_n, i.e., $\mathsf{N}_{\mathrm{b},\mathsf{i}_n}^{(n)} \neq \emptyset$, then the strategy uniformly selects a j_n from $\mathsf{N}_{\mathrm{b},\mathsf{i}_n}^{(n)}$ at random; otherwise, if there exist agents within the communication range of agent i_n, i.e., $\mathsf{N}_{\mathrm{a},\mathsf{i}_n}^{(n)} \neq \emptyset$, then the strategy uniformly selects a j_n from $\mathsf{N}_{\mathrm{a},\mathsf{i}_n}^{(n)}$ at random. If both $\mathsf{N}_{\mathrm{b},\mathsf{i}_n}^{(n)} = \emptyset$ and $\mathsf{N}_{\mathrm{a},\mathsf{i}_n}^{(n)} = \emptyset$, then no pair is selected.

Remark 6: The opportunistic scheduling strategy is the one-step optimal strategy. It requires calculating $\mathrm{tr}\{\boldsymbol{\Upsilon}_{ij}^{(n)}\}$ for all measurement pairs (i, j). The computational complexity of calculating $\mathrm{tr}\{\boldsymbol{\Upsilon}_{ij}^{(n)}\}$ for one pair (i, j) based on (9) is $O(N_{\mathrm{a}})$, and hence the overall complexity of the opportunistic scheduling strategy is $O(N_{\mathrm{a}}^3)$.[12] Furthermore, since the network scheduler needs to gather information about the angles for all measurement pairs, the communication overhead of the opportunistic scheduling strategy is $O(N_{\mathrm{a}}^2)$.[13] For practical implementation, the exact knowledge of $\mathbf{Q}^{(n)}$ and $\{\varphi_{ij}^{(n)}\}$ is unavailable, and the scheduler should select measurement pairs based on their estimates $\widehat{\mathbf{Q}}^{(n)}$ and $\{\widehat{\varphi}_{ij}^{(n)}\}$. An example of a distributed implementation is provided in [45]. In contrast, the random scheduling strategy does not incur any communication overhead or computational complexity. It does not use the knowledge of the network states, except that each agent only needs to know which nodes are within its communication range. Thus, the random scheduling strategy is easier for distributed implementation.

B. Localization Error Analysis

The error evolution for the opportunistic and random situation-aware scheduling strategies is analyzed by applying the sufficient conditions for boundedness provided in Section III-B. Let $\mathcal{A} \subset \mathbb{R}^2$ be the region within which the agents move and $\mathcal{B} \subset \mathbb{R}^2$ be a circle centered at the origin with the radius being the communication range R. Note that agents can only perform inter-node measurements with the nodes in the region $\mathcal{A} + \mathcal{B}$. The anchors are considered to be static, i.e., $\mathbf{p}_{\mathrm{b}}^{(n)} = \mathbf{p}_{\mathrm{b}}^{(1)}$ for all $n \geq 1$. The spatial distribution of the anchors' locations in $\mathbf{p}_{\mathrm{b}}^{(1)}$ is modeled by a homogeneous Poisson point process (PPP) restricted to $\mathcal{A}+\mathcal{B}$ with density μ_{b} (unit: nodes/m^2) [75], [76].[14] The samples of the homogeneous PPP characterize different network topology, and the error evolution is analyzed in the average sense with respect to the randomness in the anchors' locations and in the scheduling strategy.

By applying the sufficient condition for boundedness in Proposition 3, we obtain the following result on the error evolution for the opportunistic and random scheduling strategies. Recall that $\overline{\varepsilon}$ and $\overline{\delta}$ are given in (14) and (15), respectively.

Proposition 6: Consider that the anchors' locations follow the homogeneous PPP restricted to $\mathcal{A} + \mathcal{B}$ with density μ_{b}. The error evolution $\{\mathbf{Q}^{(n)}\}_{n\geq 1}$ satisfying (8) and Condition 1 is bounded for the opportunistic and random scheduling strategies in the following sense,

$$q_N \leq \frac{N_{\mathrm{a}}}{\zeta_{\mathrm{b}}}\Big(\rho_N + \sqrt{\rho_N^2 + 4\zeta_{\mathrm{b}}\,\overline{\varepsilon}\rho_N}\Big), \quad \forall\, N \geq 1 \tag{32}$$

where ζ_{b} is the probability that there exists at least one anchor within the communication range of an agent, given by

$$\zeta_{\mathrm{b}} = 1 - e^{-\pi R^2 \mu_{\mathrm{b}}} \tag{33}$$

and

$$\rho_N = 2N_{\mathrm{a}}\overline{\delta} + \frac{1}{N}\,\mathbb{E}\big\{\mathrm{tr}\{\mathbf{Q}^{(1)}\}\big\}. \tag{34}$$

Furthermore, for the opportunistic scheduling strategy,

$$q_N^{\star} \leq \frac{1}{\zeta_{\mathrm{b}}}\Big(\rho_N + \sqrt{\rho_N^2 + 4\zeta_{\mathrm{b}}\,\overline{\varepsilon}\rho_N}\Big), \quad \forall\, N \geq 1. \tag{35}$$

Proof: See Appendix III. □

The upper bounds in (32) and (35) depend on the measurement errors through $\overline{\varepsilon}$ and $\overline{\delta}$ as well as on the anchor deployment (network infrastructure) through μ_{b}. In particular, these bounds are increasing functions of $\overline{\varepsilon}$ and $\overline{\delta}$, which respectively characterize the inter- and intra-node measurement errors as

[11] The opportunistic scheduling strategy is similar to the max-weight scheduling strategy in data communication networks, which selects a link with the largest queue length for transmission [57].

[12] From (9), the error reduction between nodes i and j is given by

$$\mathrm{tr}\{\boldsymbol{\Upsilon}_{ij}^{(n)}\} = \frac{\boldsymbol{u}^{\mathrm{T}}(\varphi_{ij}^{(n)})\,\boldsymbol{A}_{ij}^{\mathrm{T}}\mathbf{Q}^{(n)}\mathbf{Q}^{(n)}\boldsymbol{A}_{ij}\boldsymbol{u}(\varphi_{ij}^{(n)})}{\varepsilon_{ij}^{(n)} + \boldsymbol{u}^{\mathrm{T}}(\varphi_{ij}^{(n)})\,\boldsymbol{A}_{ij}^{\mathrm{T}}\mathbf{Q}^{(n)}\boldsymbol{A}_{ij}\boldsymbol{u}(\varphi_{ij}^{(n)})}$$

where $\mathbf{Q}^{(n)}\boldsymbol{A}_{ij}$ and $\boldsymbol{A}_{ij}^{\mathrm{T}}\mathbf{Q}^{(n)}\boldsymbol{A}_{ij}$ can be calculated using lookup tables by exploiting the structure of $\boldsymbol{A}_{ij}$ in (6). Then the complexity of calculating $\mathrm{tr}\{\boldsymbol{\Upsilon}_{ij}^{(n)}\}$ is the same as that of multiplying two $N_{\mathrm{a}} \times 1$ vectors, i.e., $O(N_{\mathrm{a}})$.

[13] To reduce communication overhead and computational complexity in a distributed network, an agent may select the best neighboring anchors and randomly select neighboring agents for inter-node measurements. In practice, it is often preferable for an agent to select neighboring anchors with known locations than neighboring agents whose knowledge of locations is subject to uncertainty.

[14] The PPP provides a probability model that characterizes the scattering of points on a plane, and such a model has been extensively used to characterize random network topologies in existing literature (e.g., [77]–[81]). The density μ_{b} is the expected number of anchors in a region of 1 m^2; small or large μ_{b} corresponds to the network infrastructure with sparsely or densely deployed anchors, respectively.

in (14) and (15). On the other hand, (32) and (35) are decreasing function of ζ_{b}.

Remark 7: The bound in (32) implies that for both the opportunistic and random scheduling strategies,

$$\limsup_{N\to\infty} q_N \le \frac{2N_{\mathrm{a}}}{\zeta_{\mathrm{b}}}\Big(N_{\mathrm{a}}\overline{\delta}+\sqrt{(N_{\mathrm{a}}\overline{\delta})^2+2\zeta_{\mathrm{b}}\,\overline{\varepsilon}N_{\mathrm{a}}\overline{\delta}}\Big) \quad (36)$$

where the upper bound is $\Theta(N_{\mathrm{a}}^2)$. In two special cases with perfect inter-node measurements ($\overline{\varepsilon}=0$) and perfect intra-node measurements ($\overline{\delta}=0$), the upper bound in (36) is given respectively by $4N_{\mathrm{a}}^2\overline{\delta}/\zeta_{\mathrm{b}}$ and 0. This result implies that the upper bound in (36) is dominated by intra-node measurement error $\overline{\delta}$. Therefore, the time-averaged NLE can be effectively reduced by using high-accuracy sensors for intra-node measurements.

As a special case, we have $\boldsymbol{\Delta}^{(n)}=\boldsymbol{O}_{2N_{\mathrm{a}}}$ and $\overline{\delta}=0$ for static networks where agents do not move. Then from (32), (34), and (11), the time-averaged NLE is upper bounded by

$$q_N \le \frac{N_{\mathrm{a}}}{\zeta_{\mathrm{b}}}\left(\frac{q_1}{N}+\sqrt{\frac{q_1^2}{N^2}+4\zeta_{\mathrm{b}}\,\overline{\varepsilon}\frac{q_1}{N}}\right),\quad \forall\, N\ge 1 \quad (37)$$

which implies $\limsup_{N\to\infty} q_N = 0$. This agrees with the intuition since there is no error increase in static networks and hence agents' localization errors monotonically decrease from inter-node measurements. Furthermore, as N goes to infinity, the upper bound in (37) decreases to zero as fast as

$$\widetilde{q}_N \triangleq \frac{N_{\mathrm{a}}}{\zeta_{\mathrm{b}}}\sqrt{4\zeta_{\mathrm{b}}\,\overline{\varepsilon}\frac{q_1}{N}}$$

and thus the time-averaged NLE q_N decreases to zero at least as fast as $\widetilde{q}_N$.

The sufficient condition for boundedness in Proposition 3 can be applied to analyze the time-averaged NLE for all scheduling strategies. Proposition 6 provides a concrete example of such analysis for the opportunistic and random scheduling strategies. For distributed scheduling strategies, in which agents make decisions on when and with whom to perform inter-node measurements based on local knowledge of the network states, collisions may happen. The corresponding error evolutions can be analyzed using Proposition 3 by accounting for failures of inter-node measurements, e.g., due to collisions, in the calculation of the expected error reduction in (18).

C. Extension to Other Anchor Spatial Distributions

The performance analysis in the previous section can be extended to other spatial distributions of anchors' locations besides homogeneous PPP. Let $\psi_i^{(n)}\in[0,2\pi)$ be an angle such that $\boldsymbol{u}(\psi_i^{(n)})$ is the eigenvector of $\mathbf{Q}_{ii}^{(n)}$ corresponding to the largest eigenvalue, i.e., the localization error of agent i is the largest along the direction of $\boldsymbol{u}(\psi_i^{(n)})$. Suppose that there is a positive probability that $\boldsymbol{u}(\psi_{\mathsf{i}_n^\star}^{(n)})$ is not orthogonal to $\boldsymbol{u}(\varphi_{\mathsf{i}_n^\star\mathsf{j}}^{(n)})$ for some anchor $\mathsf{j}\in\mathsf{N}_{\mathrm{b},\mathsf{i}_n^\star}^{(n)}$, i.e., there exist an $\alpha\in[0,\pi/2)$ and a $\zeta_\alpha>0$ such that for every $n\ge 1$, there exists a $\mathsf{j}\in\mathsf{N}_{\mathrm{b},\mathsf{i}_n^\star}^{(n)}$ satisfying

$$\mathbb{P}\big\{\big|\boldsymbol{u}^{\mathrm{T}}(\psi_{\mathsf{i}_n^\star}^{(n)})\boldsymbol{u}(\varphi_{\mathsf{i}_n^\star\mathsf{j}}^{(n)})\big|\ge\cos(\alpha)\big\}\ge\zeta_\alpha. \quad (38)$$

Then the localization error of agent $\mathsf{i}_n^\star$ can be effectively reduced by performing inter-node measurements with anchor j.[15] In particular, following derivations similar to those in Appendix III, we can show that

$$\mathbb{E}\big\{\mathrm{tr}\{\boldsymbol{\Upsilon}_{\mathsf{i}_n\mathsf{j}_n}^{(n)}\}\big|\,\mathbf{Q}^{(n)}\big\}\ge\frac{\zeta_\alpha\cos^2(\alpha)\big(\mathrm{tr}\{\mathbf{Q}_{\mathsf{i}_n^\star\mathsf{i}_n^\star}^{(n)}\}\big)^2}{2\big(\mathrm{tr}\{\mathbf{Q}_{\mathsf{i}_n^\star\mathsf{i}_n^\star}^{(n)}\}+2\overline{\varepsilon}\big)},\ \forall\, N\ge 1 \quad (39)$$

for the opportunistic scheduling strategy and

$$\mathbb{E}\big\{\mathrm{tr}\{\boldsymbol{\Upsilon}_{\mathsf{i}_n\mathsf{j}_n}^{(n)}\}\big|\,\mathbf{Q}^{(n)}\big\}\ge\frac{\zeta_\alpha\cos^2(\alpha)\big(\mathrm{tr}\{\mathbf{Q}_{\mathsf{i}_n^\star\mathsf{i}_n^\star}^{(n)}\}\big)^2}{2N_{\mathrm{a}}\big(\mathrm{tr}\{\mathbf{Q}_{\mathsf{i}_n^\star\mathsf{i}_n^\star}^{(n)}\}+2\overline{\varepsilon}\big)},\ \forall\, N\ge 1 \quad (40)$$

for the random scheduling strategy. By Proposition 3, (39) and (40) lead to upper bounds on the time-averaged NLE. Therefore, under all anchor spatial distributions satisfying (38), the time-averaged NLE is bounded for the opportunistic and random scheduling strategies.

Two examples of anchor spatial distributions satisfying (38) are provided here: 1) if the anchors' locations follow a homogeneous PPP with density μ_{b}, then (38) is satisfied with $\alpha\in[0,\pi/2)$ and $\zeta_\alpha=\frac{2\alpha}{\pi}\zeta_{\mathrm{b}}$ with ζ_{b} being given by (33); 2) if the anchors are deterministically placed on a grid with $R/\sqrt{2}$ spacing, then (38) is satisfied with $\alpha=\pi/4$ and $\zeta_\alpha=1$.

V. Error Lower Bound and Optimal Error Scaling

This section derives a universal lower bound on the NLE for *all* scheduling strategies and shows the optimality of the proposed situation-aware scheduling strategies in terms of error scaling with the number of agents.

A. Universal Lower Bound on NLE

The following lemma introduces the monotonicity property of the error evolution (8), which will be used to derive the lower bound on the NLE. Recall that $\underline{\delta}$ is given in (16). A universal lower bound on the NLE is provided in the following.

Proposition 7 (Universal Lower Bound): For given anchors' locations and selected measurement pairs, the error evolution satisfying (8) and (16) is lower bounded as

$$\mathrm{tr}\{\boldsymbol{Q}^{(n)}\}\ge\Big(\frac{N_{\mathrm{a}}^2}{2}+N_{\mathrm{a}}\Big)\underline{\delta}\,,\quad \forall\, n\ge\Big\lceil\frac{N_{\mathrm{a}}}{2}\Big\rceil+1. \quad (41)$$

Proof: See Appendix IV. □

Proposition 7 together with (11) implies that

$$\liminf_{N\to\infty} q_N\ge\Big(\frac{N_{\mathrm{a}}^2}{2}+N_{\mathrm{a}}\Big)\underline{\delta} \quad (42)$$

for all scheduling strategies. The lower bound (42) on the asymptotic time-averaged NLE is $\Theta(N_{\mathrm{a}}^2)$.

[15] If $\boldsymbol{u}(\varphi_{\mathsf{i}_n^\star\mathsf{j}}^{(n)})$ is parallel to $\boldsymbol{u}(\psi_{\mathsf{i}_n^\star}^{(n)})$, i.e., $\big|\boldsymbol{u}^{\mathrm{T}}(\varphi_{\mathsf{i}_n^\star\mathsf{j}}^{(n)})\boldsymbol{u}(\psi_{\mathsf{i}_n^\star}^{(n)})\big|=1$, then the localization error of agent $\mathsf{i}_n^\star$ along $\boldsymbol{u}(\psi_{\mathsf{i}_n^\star}^{(n)})$ can be mostly reduced from the inter-node measurements between agent $\mathsf{i}_n^\star$ and anchor j. An example is given in Fig. 1 with $\mathsf{i}_n^\star=1$ and $\mathsf{j}=3$.

B. Optimal Error Scaling with Number of Agents

Since both the upper bound (36) and lower bound (42) on the asymptotic time-averaged NLE scale quadratically with the number of agents $N_{\rm a}$, the following result holds.

Proposition 8 (Optimal Error Scaling): The *optimal scaling* of the asymptotic time-averaged NLE with the number of agents $N_{\rm a}$ is $\Theta(N_{\rm a}^2)$.

The scaling $\Theta(N_{\rm a}^2)$ is optimal since it is the smallest achievable scaling. Proposition 8 shows that, with one measurement pair per time interval, the time-averaged NLE tends to increase quadratically with the number of agents. The intuition for the scaling $\Theta(N_{\rm a}^2)$ can be explained as follows. On the one hand, the total error increase in every time interval is at least $N_{\rm a}\underline{\delta}$ due to (16). On the other hand, since one measurement pair is selected in every time interval, the error reduction per interval is roughly proportional to $\mathrm{tr}\{\mathbf{Q}^{(n)}\}/N_{\rm a}$ (see (116c) for example). Since the boundedness of the error evolution implies the balance between the time-averaged error increase and reduction (see (26) and (27)), the NLE is roughly proportional to $N_{\rm a}^2$.

Remark 8: Unlike data networks where scheduling strategies must exploit the network states to achieve the optimal delay scaling with the number of users [59],[16] in navigation networks, the random scheduling strategy without the exploitation of the network states still achieves the optimal error scaling with the number of agents. Thus, the random scheduling strategy can be employed in scenarios where the opportunistic scheduling strategy would be infeasible due to the overhead and complexity. Nevertheless, the opportunistic scheduling strategy can improve the performance over the random scheduling strategy in the time-averaged NLE, as will be shown in Section VIII.

VI. Multiple Measurement Pairs

This section extends the analysis of error evolution to networks with multiple measurement pairs per time interval. In particular, the total wireless resources per time interval are divided into L orthogonal resource blocks (RBs) (e.g., time slots and subbands), each of which can be used by a pair of nodes for inter-node measurements. Moreover, a node is allowed to use multiple RBs to perform inter-node measurements with other nodes in a time interval.[17] The parameter L is referred to as the *multiplexing factor*.

A. Error Evolution and Transformation

Following derivations similar to those in the proof of Proposition 2, the error evolution $\{\boldsymbol{Q}^{(n)}\}$ with L measurement pairs per time interval is given by

$$\boldsymbol{Q}^{(n+1)} = \left(\left[\boldsymbol{Q}^{(n)}\right]^{-1} + \sum_{l=1}^{L} \boldsymbol{C}^{(n)}_{\mathsf{i}_{n,l}\mathsf{j}_{n,l}}\right)^{-1} + \boldsymbol{\Delta}^{(n+1)} \quad (43)$$

[16]In data networks, the network states include the queue lengths and channel conditions, and the delay scaling refers to the scaling of the asymptotic time-averaged delay.

[17]Consider the navigation network with two agents and three anchors in Fig. 1. Suppose that the resources are divided into $L = 2$ RBs. The two selected measurement pairs in a time interval can be $\{(1,3),(2,5)\}$, $\{(1,3),(1,4)\}$, $\{(1,2),(1,2)\}$, and so on. That is, a node can use multiple RBs to perform inter-node measurements with others.

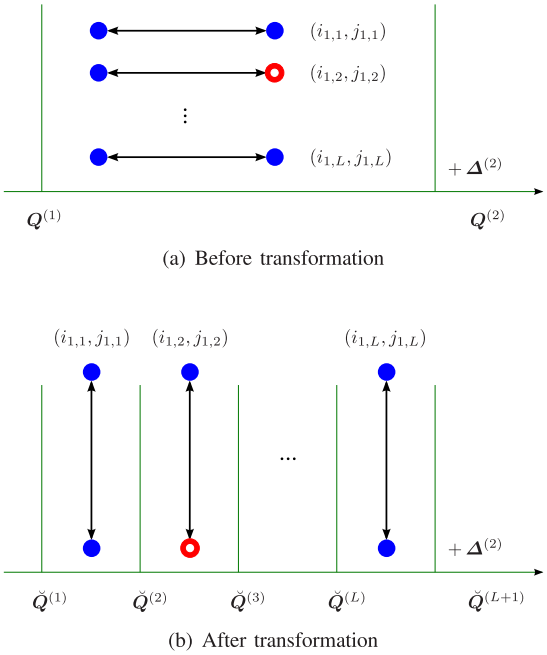

Fig. 2. Illustration of transformation: the error evolution with L measurement pairs per time interval is transformed into a form with one measurement pair per (smaller) time interval by incorporating the FIMs from inter-node measurements one by one in the error evolution. (a) Before transformation. (b) After transformation.

where $\boldsymbol{Q}^{(1)} = [\boldsymbol{J}^{(1)}]^{-1}$, i.e., the inverse of the initial FIM, $\{(i_{n,l}, j_{n,l})\}_{l=1}^{L}$ are the L measurement pairs selected in $[t_n, t_{n+1})$, and the FIM $\boldsymbol{C}^{(n)}_{ij}$ is given by (4a) and (7) for the non-Bayesian and Bayesian cases, respectively. The recursive equation (43) can be further transformed into a form similar to (8). The idea is to incorporate the L FIMs $\{\boldsymbol{C}^{(n)}_{i_{n,l}j_{n,l}}\}_{l=1}^{L}$ in (43) one by one in the error evolution as illustrated in Fig. 2.

Proposition 9: For integer $m \geq 1$, $n = \lfloor m/L \rfloor + 1$, and $l = m-(n-1)L$, let $(i_m, j_m) = (i_{n,l}, j_{n,l})$, $\breve{\varphi}^{(m)}_{i_m j_m} = \varphi^{(n)}_{i_{n,l}j_{n,l}}$, and $\breve{\varepsilon}^{(m)}_{i_m j_m} = \varepsilon^{(n)}_{i_{n,l}j_{n,l}}$. If $\{\breve{\boldsymbol{Q}}^{(m)}\}_{m\geq 1}$ is a matrix evolution satisfying

$$\breve{\boldsymbol{Q}}^{(m+1)} = \breve{\boldsymbol{Q}}^{(m)} - \breve{\boldsymbol{\Upsilon}}^{(m)}_{i_m j_m} + \breve{\boldsymbol{\Delta}}^{(m+1)} \quad (44)$$

where $\breve{\boldsymbol{Q}}^{(1)} = \boldsymbol{Q}^{(1)}$,

$$\breve{\boldsymbol{\Delta}}^{(m+1)} = \begin{cases} \boldsymbol{\Delta}^{(m/L+1)}, & \text{if } m = kL,\ k \geq 1 \\ \boldsymbol{O}_{2N_{\rm a}}, & \text{otherwise} \end{cases} \quad (45)$$

and

- in the non-Bayesian case,

$$\breve{\boldsymbol{\Upsilon}}^{(m)}_{ij} = \frac{\breve{\boldsymbol{Q}}^{(m)} \boldsymbol{A}_{ij} \boldsymbol{u}\big(\breve{\varphi}^{(m)}_{ij}\big) \boldsymbol{u}^{\mathrm{T}}\big(\breve{\varphi}^{(m)}_{ij}\big) \boldsymbol{A}_{ij}^{\mathrm{T}} \breve{\boldsymbol{Q}}^{(m)}}{\breve{\varepsilon}^{(m)}_{ij} + \boldsymbol{u}^{\mathrm{T}}\big(\breve{\varphi}^{(m)}_{ij}\big) \boldsymbol{A}_{ij}^{\mathrm{T}} \breve{\boldsymbol{Q}}^{(m)} \boldsymbol{A}_{ij} \boldsymbol{u}\big(\breve{\varphi}^{(m)}_{ij}\big)} \quad (46)$$

- in the Bayesian case

$$\breve{\boldsymbol{\Upsilon}}^{(m)}_{ij} = \breve{\boldsymbol{Q}}^{(m)} - \left(\left[\breve{\boldsymbol{Q}}^{(m)}\right]^{-1} + \mathbb{E}\big\{\boldsymbol{\Xi}_{ij}\big(\breve{\varepsilon}^{(m)}_{ij}, \breve{\varphi}^{(m)}_{ij}\big)\big\}\right)^{-1} \quad (47)$$

then $\breve{\boldsymbol{Q}}^{(m)} = \boldsymbol{Q}^{(n)}$ for $m = (n-1)L+1$ and $n \geq 1$.

Proof: See Appendix V-A. □

Note that in the reformulated error evolution $\{\breve{\boldsymbol{Q}}^{(m)}\}_{m\geq 1}$, the index m is used instead of n since the latter has been used as the index in the original error evolution (43).

B. Error Analysis

With anchors' locations drawn from a spatial distribution and measurement pairs generated from a scheduling strategy, the reformulated error evolution becomes a random process $\{\breve{\mathbf{Q}}^{(m)}\}_{m\geq 1}$. Similar to Condition 1, the following condition is considered.

Condition 2:

- There exists an $\overline{\varepsilon}_L < \infty$ such that

$$\mathbb{E}\big\{\breve{\varepsilon}_{\mathsf{ij}}^{(m)} \,\big|\, \breve{\varphi}_{\mathsf{ij}}^{(m)},\, \big|\mathsf{N}_{\mathrm{b},i}^{(m)}\big| = K,\, \breve{\mathbf{Q}}^{(m)}\big\} \leq \overline{\varepsilon}_L \qquad (48)$$

  for all $K > 0$, $i \in \mathcal{N}_{\mathrm{a}}$, $\mathsf{j} \in \mathsf{N}_{\mathrm{b},i}^{(m)}$, and $m \geq 1$.
- There exists a $\overline{\delta} < \infty$ such that

$$\frac{1}{K}\sum_{k=1}^{K} \mathrm{tr}\{\breve{\boldsymbol{\Delta}}^{(kL+1)}\} \leq 2N_{\mathrm{a}}\overline{\delta}, \quad \forall\, K \geq 1. \qquad (49)$$

- There exists a $\underline{\delta} > 0$ such that

$$\breve{\boldsymbol{\Delta}}^{(kL+1)} \succcurlyeq \underline{\delta}\, \boldsymbol{I}_{2N_{\mathrm{a}}}, \quad \forall\, k \geq 1. \qquad (50)$$

Inequalities (49) and (50) are similar to (15) and (16), respectively. Since $\breve{\boldsymbol{\Delta}}^{(m+1)} = \boldsymbol{O}_{2N_{\mathrm{a}}}$ for $m \neq kL$ with $k \geq 1$, (49) and (50) are imposed only on $\breve{\boldsymbol{\Delta}}^{(m+1)}$ for $m = kL$ with $k \geq 1$. Similar to Proposition 3, we have the following result on the boundedness of $\{\breve{\mathbf{Q}}^{(m)}\}_{m\geq 1}$.

Proposition 10: Consider an error evolution $\{\breve{\mathbf{Q}}^{(m)}\}_{m\geq 1}$ satisfying (44) and Condition 2. For a function $h : \mathbb{S}_{+}^{2N_{\mathrm{a}}} \to \mathbb{R}_{\geq 0}$, if there exists a convex function $g : \mathbb{R}_{\geq 0} \to \mathbb{R}$ with $\lim_{x\to\infty} g(x) = \infty$ such that

$$\mathbb{E}\big\{\mathrm{tr}\{\breve{\boldsymbol{\Upsilon}}_{\mathsf{i}_m\mathsf{j}_m}^{(m)}\} \,\big|\, \breve{\mathbf{Q}}^{(m)}\big\} \geq g\big(\upsilon(\breve{\mathbf{Q}}^{(m)})\big), \quad \forall\, m \geq 1$$

then we have

$$\frac{1}{M}\sum_{m=1}^{M} \mathbb{E}\big\{\upsilon(\breve{\mathbf{Q}}^{(m)})\big\} \leq \breve{B}_M, \quad \forall\, M \geq 1$$

where

$$\breve{B}_M = \sup\Big\{x : g(x) \leq \frac{2N_{\mathrm{a}}\overline{\delta}}{L} + \frac{1}{M}\,\mathbb{E}\big\{\mathrm{tr}\{\breve{\mathbf{Q}}^{(1)}\}\big\}\Big\} \qquad (51)$$

is bounded from above and non-increasing with M.

Proof: The proof follows derivations similar to those in Appendix II-A. In particular, (85) becomes

$$\begin{aligned} g(\upsilon_M) &\leq \frac{1}{M}\Big\lfloor\frac{M}{L}\Big\rfloor \cdot 2N_{\mathrm{a}}\overline{\delta} + \frac{1}{M}\,\mathbb{E}\big\{\mathrm{tr}\{\breve{\mathbf{Q}}^{(1)}\}\big\} \\ &\leq \frac{2N_{\mathrm{a}}\overline{\delta}}{L} + \frac{1}{M}\,\mathbb{E}\big\{\mathrm{tr}\{\breve{\mathbf{Q}}^{(1)}\}\big\} \end{aligned}$$

which leads to (51). □

The error evolution $\{\breve{\mathbf{Q}}^{(m)}\}_{m\geq 1}$ for the opportunistic and random situation-aware scheduling strategies can be analyzed using Proposition 10. The scheduling policies for these strategies are applied for every index m in $\{\breve{\mathbf{Q}}^{(m)}\}_{m\geq 1}$, i.e., the policies are applied for every RB. Define

$$\begin{aligned} \breve{q}_M &\triangleq \frac{1}{M}\sum_{m=1}^{M} \mathbb{E}\big\{\mathrm{tr}\{\breve{\mathbf{Q}}^{(m)}\}\big\} \\ \breve{q}_M^{\star} &\triangleq \frac{1}{M}\sum_{m=1}^{M} \mathbb{E}\big\{\mathrm{tr}\{\breve{\mathbf{Q}}_{\mathsf{i}_m^{\star}\mathsf{i}_m^{\star}}^{(m)}\}\big\} \end{aligned} \qquad (52)$$

where $\breve{\mathbf{Q}}_{ii}^{(m)}$ is the ith 2×2 principal submatrix of $\breve{\mathbf{Q}}^{(m)}$ and $\mathsf{i}_m^{\star} \in \arg\max_{i\in\mathcal{N}_{\mathrm{a}}} \mathrm{tr}\{\breve{\mathbf{Q}}_{ii}^{(m)}\}$. The following result holds.

Proposition 11: Consider that the anchors' locations follow a homogeneous PPP restricted to $\mathcal{A}+\mathcal{B}$ with density μ_{b}. The error evolution $\{\breve{\mathbf{Q}}^{(m)}\}_{m\geq 1}$ satisfying (44) and Condition 2 is bounded for the opportunistic and random scheduling strategies in the following sense,

$$\breve{q}_M \leq \frac{N_{\mathrm{a}}}{\zeta_{\mathrm{b}}}\Big(\rho_{M,L} + \sqrt{\rho_{M,L}^2 + 4\zeta_{\mathrm{b}}\,\overline{\varepsilon}_L\rho_{M,L}}\Big), \quad \forall M \geq 1 \qquad (53)$$

where ζ_{b} is given by (33) and

$$\rho_{M,L} = \frac{2N_{\mathrm{a}}\overline{\delta}}{L} + \frac{1}{M}\,\mathbb{E}\big\{\mathrm{tr}\{\breve{\mathbf{Q}}^{(1)}\}\big\}.$$

Furthermore, for the opportunistic scheduling strategy,

$$\breve{q}_M^{\star} \leq \frac{1}{\zeta_{\mathrm{b}}}\Big(\rho_{M,L} + \sqrt{\rho_{M,L}^2 + 4\zeta_{\mathrm{b}}\,\overline{\varepsilon}_L\rho_{M,L}}\Big), \quad \forall M \geq 1. \qquad (54)$$

Proof: See Appendix V-B. □

The bounds in (53) and (54) are in the same form of those in (32) and (35) with an additional parameter L. From (53), we have

$$\limsup_{M\to\infty}\, \breve{q}_M \leq \frac{2N_{\mathrm{a}}}{\zeta_{\mathrm{b}}}\left(\frac{N_{\mathrm{a}}\overline{\delta}}{L} + \sqrt{\frac{(N_{\mathrm{a}}\overline{\delta})^2}{L^2} + 2\zeta_{\mathrm{b}}\,\overline{\varepsilon}_L\frac{N_{\mathrm{a}}\overline{\delta}}{L}}\right) \qquad (55)$$

where the upper bound is $\Theta(N_{\mathrm{a}}^2)$ for fixed L.

C. Error Lower Bound and Optimal Error Scaling

Using arguments similar to those in Appendix IV, a universal lower bound on the NLE is given as follows.

Proposition 12: For given anchors' locations and selected measurement pairs, there exists an M_L such that the error evolution satisfying (44) and (50) is lower bounded as

$$\frac{1}{M}\sum_{m=1}^{M} \mathrm{tr}\{\breve{\boldsymbol{Q}}^{(m)}\} \geq \Big\lfloor\frac{M-M_L}{L}\Big\rfloor\frac{(N_{\mathrm{a}}^2 - 2N_{\mathrm{a}} - 1)}{2M}\underline{\delta} \qquad (56)$$

for all $M \geq M_L$ and all scheduling strategies.

Proof: See Appendix V-C. □

Proposition 12 together with (52) implies that

$$\liminf_{M\to\infty}\, \breve{q}_M \geq \frac{N_{\mathrm{a}}^2 - 2N_{\mathrm{a}} - 1}{2L}\underline{\delta}. \qquad (57)$$

With L being fixed, both the upper bound (55) and lower bound (57) on the asymptotic time-averaged NLE scale quadratically with the number of agents N_{a}. Therefore, the *optimal scaling* of the asymptotic time-averaged NLE with respect to N_{a} is $\Theta(N_{\mathrm{a}}^2)$, i.e., the quadratic error scaling holds for any fixed multiplexing factor.

D. Effect of Resource Sharing

In this part, the question of whether allocating the wireless resources to a single measurement pair (i.e., $L = 1$) or sharing them among multiple measurement pairs (i.e., $L > 1$) is answered. Consider that multiple pairs of nodes can perform inter-node measurements in a time interval via time division multiple access (TDMA) or frequency division multiple access (FDMA).

- TDMA: A time interval is divided into L time slots.
- FDMA: The frequency band in a time interval is divided into L subbands.

Here an RB corresponds to a time slot or subband in TDMA or FDMA, respectively.

Suppose that the lth time slot or subband is allocated to the measurement pair (i, j) in $[\,t_n, t_{n+1})$ for TDMA or FDMA, respectively. The inter-node measurement error $\varepsilon_{ij}^{(n)}$ between nodes i and j satisfies

$$\varepsilon_{ij}^{(n)} \propto \frac{1}{\beta_l^2\, \mathsf{SNR}_{ij,l}^{(n)}} \tag{58}$$

where

$$\beta_l = \left[\frac{\int_{-\infty}^{\infty} f^2 |S_l(f)|^2 df}{\int_{-\infty}^{\infty} |S_l(f)|^2 df}\right]^{1/2} \tag{59}$$

is the effective bandwidth of the signal with $S_l(f)$ being the spectrum, and $\mathsf{SNR}_{ij,l}^{(n)}$ is the received SNR [23], [60].

Consider that the total amount of wireless resources (duration or bandwidth) in a time interval is *fixed*. Then the relationship between the multiplexing factor and the inter-node measurement error is given as follows.

- TDMA: The received SNR can be increased by repeatedly sending the signal for inter-node measurements. In particular, consider that $\mathsf{SNR}_{ij,l}^{(n)}$ increases linearly with the number of signal repetitions that is proportional to the duration of a time slot. Also, the total duration of a time interval is equally divided into L time slots. Then the duration of a time slot is proportional to $1/L$. As a result, $\mathsf{SNR}_{ij,l}^{(n)}$ is proportional to $1/L$, which together with (58) implies that $\varepsilon_{ij}^{(n)}$ is proportional to L.
- FDMA: Consider that the shape of $S_l(f)$ is a rectangle with the width being the bandwidth of the lth subband.[18] Then with the total bandwidth being fixed, $\sum_{l=1}^{L} \beta_l^2$ is constant by (59). Consider that the bandwidth is divided in such a way that β_l^2's are equal. Then β_l^2 is proportional to $1/L$, which together with (58) implies that $\varepsilon_{ij}^{(n)}$ is proportional to L.

Recall that $\overline{\varepsilon}$ in (14) and $\overline{\varepsilon}_L$ in (48) are upper bounds on the expected inter-node measurement error for one and L measurement pairs per time interval, respectively. Following the above arguments, we have $\overline{\varepsilon}_L = L\overline{\varepsilon}$. Then the upper bound in (55) can be written as

$$\limsup_{M\to\infty} \breve{q}_M \le \frac{2N_{\mathrm{a}}}{\zeta_{\mathrm{b}}}\left(\frac{N_{\mathrm{a}}\overline{\delta}}{L} + \sqrt{\frac{(N_{\mathrm{a}}\overline{\delta})^2}{L^2} + 2\zeta_{\mathrm{b}}\,\overline{\varepsilon} N_{\mathrm{a}}\overline{\delta}}\right). \tag{60}$$

[18]Here a sinc function is considered as the baseband waveform for analytical tractability. In practice, the waveform should be time-limited (e.g., a truncated sinc function).

Note that both the upper bound (60) and lower bound (57) on the asymptotic time-averaged NLE decrease with the multiplexing factor L. Furthermore, the error scaling with the number of agents N_{a} can be reduced by increasing the multiplexing factor L with N_{a}. For example, by choosing $L = N_{\mathrm{a}}$, the inequalities (60) and (57) become

$$\limsup_{N\to\infty} \breve{q}_N \le \frac{2N_{\mathrm{a}}}{\zeta_{\mathrm{b}}}\left(\overline{\delta} + \sqrt{\overline{\delta}^2 + 2\zeta_{\mathrm{b}}\,\overline{\varepsilon} N_{\mathrm{a}}\overline{\delta}}\right) \tag{61}$$

$$\liminf_{N\to\infty} \breve{q}_N \ge \left(\frac{N_{\mathrm{a}}}{2} - 1 - \frac{1}{2N_{\mathrm{a}}}\right)\underline{\delta} \tag{62}$$

where the scalings of the upper bound in (61) and lower bound in (62) with respect to N_{a} are $\Theta(N_{\mathrm{a}}\sqrt{N_{\mathrm{a}}})$ and $\Theta(N_{\mathrm{a}})$, respectively. In particular, the scaling $\Theta(N_{\mathrm{a}}\sqrt{N_{\mathrm{a}}})$ of the upper bound results from the term $2\zeta_{\mathrm{b}}\,\overline{\varepsilon} N_{\mathrm{a}}\overline{\delta}$ inside the square root in (61); while the scaling $\Theta(N_{\mathrm{a}})$ of the lower bound is due to the zero measurement error in the reference evolution (introduced to derive the lower bound (57)) in Appendix V-C. Thus, the error scaling is at most $\Theta(N_{\mathrm{a}}\sqrt{N_{\mathrm{a}}})$ for $L = N_{\mathrm{a}}$. For comparison, the optimal error scaling with fixed L is $\Theta(N_{\mathrm{a}}^2)$ as shown in Section VI-C.

Remark 9: Intuitively, more flexibility in allocation of resources (time slots or subbands) offered by increasing the multiplexing factor L leads to a performance improvement. Note that the error evolution for $L = 1$ is a special case of that for $L > 1$ with all the time slots or subbands being allocated to a single measurement pair. Thus, the performance with $L > 1$ is no worse than that with $L = 1$.

VII. Discussions

In the following, the results from the analytical framework are specified for a concrete example, and the extension of the results to 3-D navigation networks is introduced.

A. Case Study

To obtain insights from the analysis in Sections II–VI, consider a navigation network as in Section II-A with the following measurement models.

- The inter-node measurement $\mathsf{z}_{ij}^{(n)}$ between nodes i and j in $[\,t_n, t_{n+1})$ is a range measurement, given by
$$\mathsf{z}_{ij}^{(n)} = d_{ij}^{(n)} + \mathsf{w}_{ij}^{(n)} \tag{63}$$
where $d_{ij}^{(n)} = \left\|\boldsymbol{p}_i^{(n)} - \boldsymbol{p}_j^{(n)}\right\|$ and $\mathsf{w}_{ij}^{(n)} \sim \mathcal{N}(0, \varepsilon)$.
- The intra-node measurement $\mathbf{z}_{ii}^{(n+1)}$ of agent i in $[\,t_n, t_{n+1})$ is a displacement measurement, given by
$$\mathbf{z}_{ii}^{(n+1)} = \boldsymbol{p}_i^{(n+1)} - \boldsymbol{p}_i^{(n)} + \mathbf{w}_{ii}^{(n+1)} \tag{64}$$
where $\mathbf{w}_{ii}^{(n+1)} \sim \mathcal{N}(\mathbf{0}_2, \delta_i \boldsymbol{I}_2)$.

The results for the non-Bayesian case with one measurement pair per time interval are considered as an example.

1) Error Evolution: For the inter-node measurement model in (63), we have

$$f\big(z_{ij}^{(n)} \big|\, d_{ij}^{(n)}\big) = \mathcal{N}\big(z_{ij}^{(n)};\, d_{ij}^{(n)},\, \varepsilon\big).$$

By substituting the above PDF into (73) and (5), the matrix $\boldsymbol{C}_{ij}^{(n)}$ is given by (4b) with $\varepsilon_{ij}^{(n)} = \varepsilon$. For the intra-node measurement model in (64), we obtain

$$f\big(\boldsymbol{z}_{ii}^{(n)} \,\big|\, \boldsymbol{p}_i^{(n)} - \boldsymbol{p}_i^{(n-1)}\big) = \mathcal{N}\big(\boldsymbol{z}_{ii}^{(n)};\, \boldsymbol{p}_i^{(n)} - \boldsymbol{p}_i^{(n-1)},\, \delta_i \boldsymbol{I}_2\big).$$

By substituting the above PDF into (74), we obtain $\boldsymbol{D}^{(n)} = \boldsymbol{\Delta}^{-1}$ with

$$\boldsymbol{\Delta} = \mathrm{diag}\big\{\delta_1 \boldsymbol{I}_2,\, \delta_2 \boldsymbol{I}_2,\, \ldots,\, \delta_{N_\mathrm{a}} \boldsymbol{I}_2\big\}.$$

Then following the derivations in Section II-C, the error evolution is given by (8) with $\varepsilon_{ij}^{(n)} = \varepsilon$ and $\boldsymbol{\Delta}^{(n)} = \boldsymbol{\Delta}$. Therefore, for measurement models (63) and (64), the inter-node measurement error and error increase are equal to the error covariances.

2) Error Analysis: The inequalities (14), (15), and (16) are satisfied with $\overline{\varepsilon} = \varepsilon$, $\overline{\delta} = \sum_{i=1}^{N_\mathrm{a}} \delta_i / N_\mathrm{a}$, and $\underline{\delta} = \min\{\delta_i\}_{i=1}^{N_\mathrm{a}}$. Then the time-averaged NLE for the opportunistic and random scheduling strategies is upper bounded by (32), and the time-averaged largest individual error for the opportunistic scheduling strategy is upper bounded by (35), with $\overline{\varepsilon} = \varepsilon$ and $\overline{\delta} = \sum_{i=1}^{N_\mathrm{a}} \delta_i / N_\mathrm{a}$. Furthermore, the universal lower bound (41) holds with $\underline{\delta} = \min\{\delta_i\}_{i=1}^{N_\mathrm{a}}$. Therefore, the optimal error scaling is $\Theta(N_\mathrm{a}^2)$, which can be achieved by both the opportunistic and random situation-aware scheduling strategies.

B. Extension to 3-D Networks

We now extend the analysis in Sections II–VI to 3-D networks.

1) Error Evolution: Similar to the derivation of (4a), by first taking the second derivative of f in (73) with respect to $d_{ij}^{(k)}$ and then taking the derivative of $d_{ij}^{(k)}$ with respect to $\boldsymbol{p}_\mathrm{a}^{(k)}$, the matrix $\boldsymbol{C}_{ij}^{(n)}$ for 3-D networks can be expressed in the form of (4b) with $\boldsymbol{u}\big(\varphi_{ij}^{(n)}\big)$ being replaced by

$$\boldsymbol{u}_{ij}^{(n)} = \frac{1}{d_{ij}^{(n)}}\big(\boldsymbol{p}_i^{(n)} - \boldsymbol{p}_j^{(n)}\big)$$

i.e., the unit direction vector from node j to node i. Following the derivations in Sections II-B and II-C, the error evolution for 3-D networks is given by (8) with $\boldsymbol{u}\big(\varphi_{ij}^{(n)}\big)$ being replaced by $\boldsymbol{u}_{ij}^{(n)}$.

2) Sufficient Condition for Boundedness: For 3-D networks, the inequality (15) is replaced by

$$\frac{1}{N}\sum_{n=1}^{N} \mathrm{tr}\{\boldsymbol{\Delta}^{(n+1)}\} \le 3N_\mathrm{a}\overline{\delta}, \quad \forall\, N \ge 1.$$

Then the sufficient condition for boundedness in Proposition 3 holds for 3-D networks with $2N_\mathrm{a}\overline{\delta}$ being replaced by $3N_\mathrm{a}\overline{\delta}$.

3) Error Analysis: According to the proof of Proposition 6 in Appendix III, lower bounds on the expected error reduction in the form of (18) are needed to develop upper bounds on the time-averaged NLE and largest individual error. For 3-D networks, let $\mathbf{u}_i^{(n)}$ be the eigenvector of $\mathbf{Q}_{ii}^{(n)}$ corresponding to the largest eigenvalue. Suppose that there exist a $r > 0$ and a $\zeta_r > 0$ such that for all $n \ge 1$, we have

$$\mathbb{P}\big\{\big|\mathbf{u}_{\mathsf{i}_n^\star}^{(n)\mathrm{T}} \mathbf{u}_{\mathsf{i}_n^\star \mathsf{j}}^{(n)}\big| \ge r\big\} \ge \zeta_r \tag{65}$$

for a $\mathsf{j} \in \mathsf{N}_{\mathsf{b},\mathsf{i}_n^\star}^{(n)}$ ($\mathsf{i}_n^\star$ is given by (13)), i.e., with a positive probability the direction between agent $\mathsf{i}_n^\star$ and one of its neighboring anchor is not orthogonal to $\mathbf{u}_{\mathsf{i}_n^\star}^{(n)}$. Then, lower bounds on $\mathbb{E}\{\mathrm{tr}\{\boldsymbol{\Upsilon}_{\mathsf{i}_n\mathsf{j}_n}^{(n)}\} \,|\, \mathbf{Q}^{(n)}\}$ similar to (39) and (40) can be obtained for the opportunistic and random scheduling strategies, which together with the sufficient condition for boundedness in Proposition 3 lead to upper bounds on the time-averaged NLE. The derivations are similar to the proof of Proposition 6 and are therefore omitted. Following arguments similar to those in Section IV-C, the inequality (65) can be satisfied in 3-D networks, for example, if 1) the projections of anchors' locations onto the $x-y$ plane follow a homogeneous PPP or are deterministically placed on a grid, and 2) the heights of the anchors are set in a way that the neighboring anchors of an agent are not always on the same plane.

VIII. Numerical Results

This section provides simulation results to show the effects of the number of agents, multiplexing factor, and anchor density on the time-averaged NLE for situation-aware scheduling strategies. Due to the unified structure (8) of the error evolution for both the non-Bayesian and Bayesian estimations, the simulations focus on the non-Bayesian case, and the results in the Bayesian case are similar.

Consider a group of agents moving in a region $\mathcal{A}$ of $30\,\mathrm{m} \times 30\,\mathrm{m}$. The trajectory of each agent is drawn from a random walk reflected in $\mathcal{A}$,[19] which is characterized by the following dynamic model (take agent i for example)

$$\mathbf{p}_i^{(n+1)} = \boldsymbol{\gamma}\big(\mathbf{p}_i^{(n)} + \mathbf{w}_i^{(n+1)}\big)$$

where $\{\mathbf{w}_i^{(n+1)}\}_{n\ge1}$ are independent identically distributed 2×1 Gaussian random vectors, and $\boldsymbol{\gamma}(\cdot)$ reflects its argument within $\mathcal{A}$. The anchors' locations follow a homogeneous PPP with density μ_b restricted to $\mathcal{A}+\mathcal{B}$, where $\mathcal{B}$ is a circle centered at the origin with the radius being the communication range $R = 30\,\mathrm{m}$. A scenario with eight agents is illustrated in Fig. 3.

The inter-node measurement error in (58) is simulated using the channel model of IEEE 802.15.4a [82], and the error increase matrix due to the uncertainty in intra-node measurements is $\delta\,\boldsymbol{I}_{2N_\mathrm{a}}$ with $\delta = 0.1\,\mathrm{m}^2$. The total amount of the wireless resources is fixed, and the averaged received SNR is set to be 35 dB at 1 m when the multiplexing factor $L = 1$. The initial IFIM is $\boldsymbol{Q}^{(0)} = 5\,\boldsymbol{I}_{2N_\mathrm{a}}\,\mathrm{m}^2$. The time-averaged localization error per agent, defined as

$$q_{\mathrm{a},N} = \frac{1}{N_\mathrm{a}} q_N \tag{66}$$

is evaluated in the following simulation results for $N = 200$. Both dense and sparse anchor deployments with $\mu_\mathrm{b} = 5\times10^{-4}\,\mathrm{m}^{-2}$ and $\mu_\mathrm{b} = 5\times10^{-5}\,\mathrm{m}^{-2}$ are considered for evaluating the effects of the number of users N_a and the multiplexing factor L on the time-averaged NLE.[20] In the following figures, dense and sparse refer respectively to scenarios with dense and sparse anchor deployments.

[19]The trajectory of an agent is reflected when the agent reaches the boundary of $\mathcal{A}$ as shown in Fig. 3.

[20]The two anchor densities are chosen for the purpose of illustration. On average 1.4 and 0.14 anchors are within the communication range of an agent for dense and sparse anchor deployments, respectively.

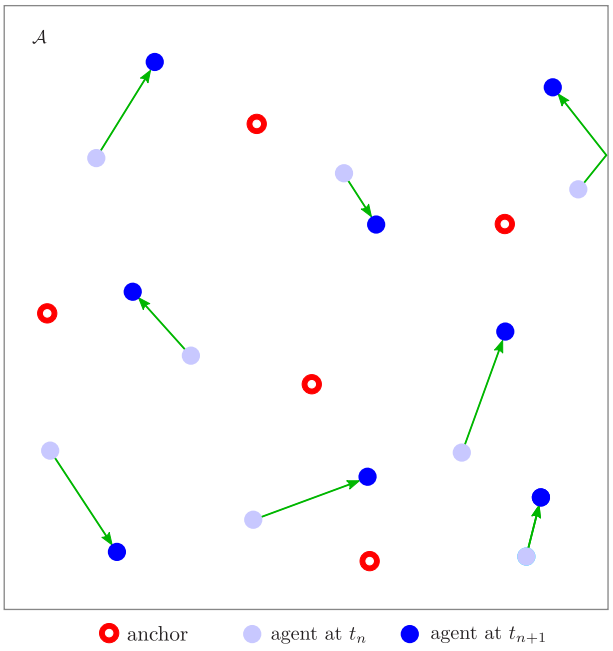

Fig. 3. An instantiation of the scenario with eight agents, where anchors' locations are drawn from a homogeneous PPP.

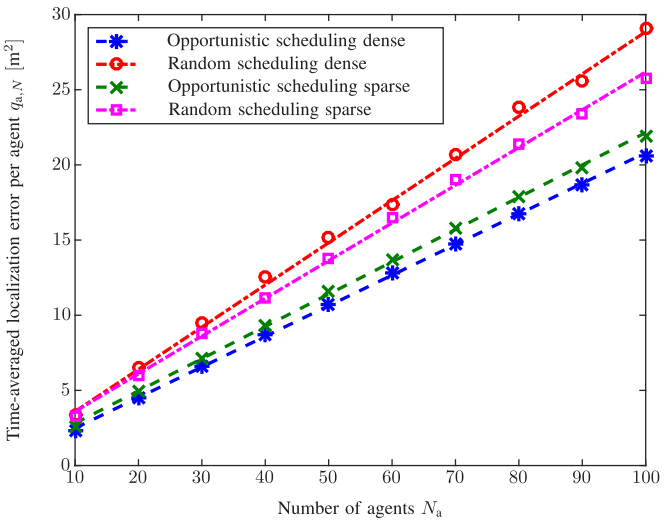

Fig. 4. Time-averaged localization error per agent as a function of N_a for $L = 1$.

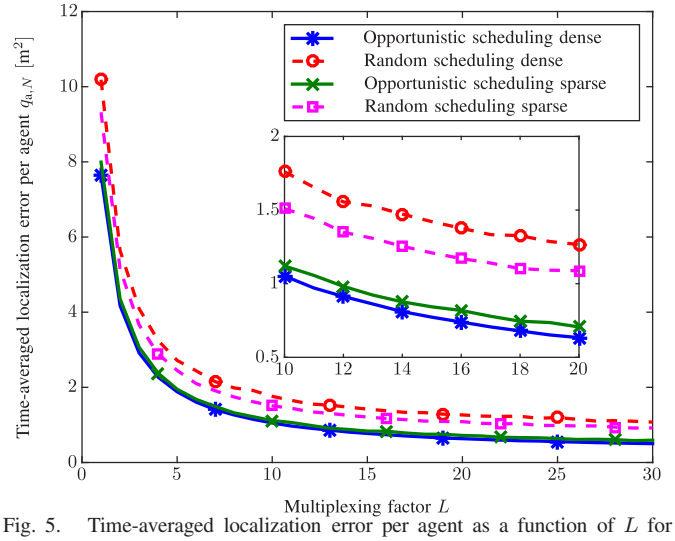

Fig. 5. Time-averaged localization error per agent as a function of L for $N_a = 30$. The curves are zoomed in from $L = 10$ to $L = 20$.

Fig. 4 shows the time-averaged localization error per agent as a function of the number of agents N_a with the multiplexing factor $L = 1$. The markers are the simulated time-averaged localization error per agent for the opportunistic and random scheduling strategies, respectively, and these simulation results are fitted with linear functions (i.e., the dashed lines). The results together with (66) validate the optimal scaling $\Theta(N_a^2)$ of the time-averaged NLE q_N in Section V-B and Section VI-C. While the error can be reduced by increasing the multiplexing factor L as will be shown in the following simulation results, the optimal error scaling $\Theta(N_a^2)$ holds for any fixed L as shown in Section VI-C. Fig. 4 also shows that the time-averaged localization error per agent for the opportunistic scheduling strategy is smaller than that for the random scheduling strategy. Therefore, measurement pair selections with the exploitation of the network states can reduce the time-averaged NLE.

Fig. 5 shows the time-averaged localization error per agent as a function of the multiplexing factor L with the number of agents $N_a = 30$, and the curves are zoomed in from $L = 10$ to $L = 20$. The resources are divided as in Section VI-D. It can be seen that, with the same amount of total resources, the time-averaged localization error per agent decreases as L increases. Thus, instead of allocating all the resources to one measurement pair, the localization accuracy can be improved by sharing the resources among multiple measurement pairs, which provides more freedom in resource allocation.

Fig. 6 shows the time-averaged localization error per agent as a function of the number of agents N_a with the multiplexing factor $L = N_a$. The squares and circles are simulated time-averaged localization errors per agent for the opportunistic and random scheduling strategies, respectively, and these simulation results are fitted with functions in the form of $f(x) = ax^b + c$ (i.e., the dashed curves) to quantify the error scaling. Since the error scaling is an asymptotic behavior, only the results for $N_a \geq 30$ are used for curve fitting, and the results for $N_a = 10$ may deviate from the curves. The exponential b is -0.02, 0.50, -0.46, and 0.77 respectively for the "Opportunistic scheduling dense", "Random scheduling dense", "Opportunistic scheduling sparse", and "Random scheduling sparse" curves. In contrast, the scaling of the time-averaged localization error per agent for fixed L is linear as shown in Fig. 4. This agrees with the result on the reduction of the error scaling by increasing the multiplexing factor L with the number of agents N_a in Section VI-D.

Fig. 7 shows the time-averaged localization error per agent as a function of the anchor density μ_b with the number of agents $N_a = 10$ and the multiplexing factor $L = 1$. The expected number of the candidate measurement pairs increases with μ_b (more candidate node pairs with an agent and an anchor). The benefit of such increase can be exploited

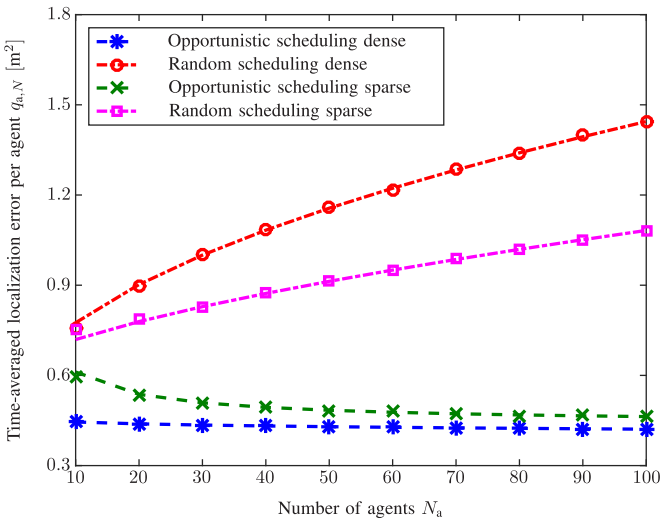

Fig. 6. Time-averaged localization error per agent as a function of N_a for $L = N_a$.

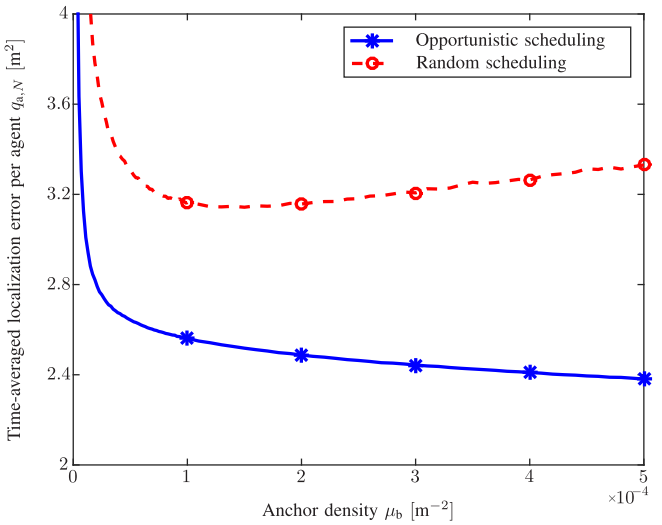

Fig. 7. Time-averaged localization error per agent as a function of μ_b for $N_a = 10$ and $L = 1$.

in the opportunistic scheduling strategy as shown by the decrease of the corresponding time-averaged localization error per agent with μ_b in Fig. 7. More specifically, the opportunistic scheduling strategy achieves a "diversity gain" provided by multiple candidate measurement pairs by selecting the ones providing the largest error reductions. This is similar to the multi-user diversity gain in opportunistic communication [83], where the links with the best channel qualities are selected for transmission. On the other hand, the random scheduling strategy cannot effectively achieve such "diversity gain" since it uniformly selects measurement pairs at random. Furthermore, for large anchor densities, agents perform inter-node measurements with anchors most of the time under the random scheduling strategy, while the error reduction from the inter-node measurements between two agents can be larger than that between an agent and an anchor for some network topologies. As a result, the random scheduling strategy loses the potential advantage of inter-node measurements between agents as the anchor density increases.

IX. Conclusion

This paper developed a framework to devise situation-aware scheduling strategies for network navigation and determine the localization error evolution for different scheduling strategies and network settings. Both sufficient and necessary conditions for the boundedness of the error evolution are provided, and bounds on the time-averaged NLEs for the proposed opportunistic and random scheduling strategies are derived. Furthermore, the optimal scaling of the time-averaged NLE with the number of agents is determined. We showed that the random scheduling strategy without exploiting the network states can achieve the optimal error scaling, and that the opportunistic scheduling strategy can further reduce the time-averaged NLE by exploiting the network states. Moreover, we showed the reduction of the error scaling by increasing the multiplexing factor under fixed total wireless resources. These results provide insights into the effects of scheduling strategies and network settings on the error evolution, leading to the design of techniques for efficient network operation.

Appendix I
Proofs of Results in Section II

A. Proof of Proposition 1

For $n \geq 2$, $\boldsymbol{J}^{(n)}$ can be decomposed as

$$\boldsymbol{J}^{(n)} = \boldsymbol{E}_{1,1}^{(n)} \otimes \boldsymbol{J}^{(1)} + \boldsymbol{F}^{(n)}. \tag{67}$$

The first term $\boldsymbol{E}_{1,1}^{(n)} \otimes \boldsymbol{J}^{(1)}$ in (67) is the FIM about $\boldsymbol{p}_a^{(1:n)}$ (non-Bayesian) and $\mathbf{p}_a^{(1:n)}$ (Bayesian) from the initial measurements (and from the prior knowledge about $\mathbf{p}_a^{(1)}$ for the Bayesian case), where $\boldsymbol{E}_{i,j}^{(n)}$ is an $n \times n$ matrix with all zeros except a 1 on the (i,j)th entry. The second term $\boldsymbol{F}^{(n)}$ in (67) is described in the following.

- In the non-Bayesian case, $\boldsymbol{F}^{(n)}$ is the FIM about $\boldsymbol{p}_a^{(1:n)}$ from the measurements in $\mathbf{z}^{(1:n-1)}$, given by
$$\boldsymbol{F}^{(n)} = \mathbb{E}\Big\{ \jmath_{\text{bm}}\big(\mathbf{z}^{(1:n-1)}, \boldsymbol{p}_a^{(1:n)}, \boldsymbol{p}_a^{(1:n)}\big) \Big\} \tag{68}$$
noting that $f\big(\boldsymbol{z}^{(1:n)}; \boldsymbol{p}_a^{(1:n)}\big)$ can be factorized as
$$f\big(\boldsymbol{z}^{(1:n-1)}; \boldsymbol{p}_a^{(1:n)}\big) = \prod_{k=1}^{n-1} f\big(\boldsymbol{z}_{i_k j_k}^{(k)}; d_{i_k j_k}^{(k)}\big) \times \prod_{k=2}^{n} \prod_{i \in \mathcal{N}_a} f\big(\boldsymbol{z}_{ii}^{(k)}; \boldsymbol{p}_i^{(k-1:k)}\big) \tag{69}$$
by the independence of the measurements.
- In the Bayesian case, $\boldsymbol{F}^{(n)}$ is the FIM about $\mathbf{p}_a^{(1:n)}$ from the measurements in $\mathbf{z}^{(1:n-1)}$ and the prior knowledge about $\mathbf{p}_a^{(2:n)}$, given by
$$\boldsymbol{F}^{(n)} = \mathbb{E}\Big\{ \jmath_{\text{bm}}\big(\mathbf{z}^{(1:n-1)}, \mathbf{p}_a^{(1:n)}, \mathbf{p}_a^{(1:n)}\big) \Big\} + \mathbb{E}\Big\{ \jmath_{\text{bp}}\big(\mathbf{p}_a^{(2:n)}, \mathbf{p}_a^{(1)}, \mathbf{p}_a^{(1:n)}\big) \Big\} \tag{70}$$
noting that $f\big(\boldsymbol{p}_a^{(2:n)} \,\big|\, \boldsymbol{p}_a^{(1)}\big)$ can be factorized as
$$f\big(\boldsymbol{p}_a^{(2:n)} \,\big|\, \boldsymbol{p}_a^{(1)}\big) = \prod_{k=2}^{n} f\big(\boldsymbol{p}_a^{(k)} \,\big|\, \boldsymbol{p}_a^{(k-1)}\big) \tag{71}$$

$$\boldsymbol{J}^{(n)}=\begin{bmatrix} \boldsymbol{J}^{(1)}+\boldsymbol{C}^{(1)}_{i_1j_1}+\boldsymbol{D}^{(2)} & -\boldsymbol{D}^{(2)} & \boldsymbol{O}_{2N_\mathrm{a}} & \cdots & \boldsymbol{O}_{2N_\mathrm{a}} & \boldsymbol{O}_{2N_\mathrm{a}} \\ -\boldsymbol{D}^{(2)} & \boldsymbol{D}^{(2)}+\boldsymbol{C}^{(2)}_{i_2j_2}+\boldsymbol{D}^{(3)} & -\boldsymbol{D}^{(3)} & \cdots & \boldsymbol{O}_{2N_\mathrm{a}} & \boldsymbol{O}_{2N_\mathrm{a}} \\ \boldsymbol{O}_{2N_\mathrm{a}} & -\boldsymbol{D}^{(3)} & \boldsymbol{D}^{(3)}+\boldsymbol{C}^{(3)}_{i_3j_3}+\boldsymbol{D}^{(4)} & \cdots & \boldsymbol{O}_{2N_\mathrm{a}} & \boldsymbol{O}_{2N_\mathrm{a}} \\ \vdots & \vdots & \vdots & \ddots & \vdots & \vdots \\ \boldsymbol{O}_{2N_\mathrm{a}} & \boldsymbol{O}_{2N_\mathrm{a}} & \boldsymbol{O}_{2N_\mathrm{a}} & \cdots & \boldsymbol{D}^{(n-1)}+\boldsymbol{C}^{(n-1)}_{i_{n-1}j_{n-1}}+\boldsymbol{D}^{(n)} & -\boldsymbol{D}^{(n)} \\ \boldsymbol{O}_{2N_\mathrm{a}} & \boldsymbol{O}_{2N_\mathrm{a}} & \boldsymbol{O}_{2N_\mathrm{a}} & \cdots & -\boldsymbol{D}^{(n)} & \boldsymbol{D}^{(n)} \end{bmatrix} \tag{72}$$

according to (1), and that $f\big(\boldsymbol{z}^{(1:n-1)}\,\big|\,\boldsymbol{p}_\mathrm{a}^{(1:n)}\big)$ can be factorized as in (69).

Following (67)–(71), the FIMs $\boldsymbol{J}^{(n)}$ for $n\geq 2$ in both the non-Bayesian and Bayesian cases have a diagonally-striped structure given by (72) at the top of this page, which can be written as (2). The matrices $\boldsymbol{C}_{ij}^{(k)}$ and $\boldsymbol{D}^{(k)}$ are explained in the following.

- In the non-Bayesian case, the matrix $\boldsymbol{C}_{ij}^{(k)}$ is given by
$$\boldsymbol{C}_{ij}^{(k)}=\mathbb{E}\Big\{\jmath_{\mathfrak{bm}}\big(\mathbf{z}_{ij}^{(k)},d_{ij}^{(k)},\boldsymbol{p}_\mathrm{a}^{(k)}\big)\Big\} \tag{73}$$
and (4a) is obtained using the chain rule, by first taking the second derivative of f in (73) with respect to $d_{ij}^{(k)}$ and then taking the derivative of $d_{ij}^{(k)}$ with respect to $\boldsymbol{p}_\mathrm{a}^{(k)}$.
The matrix $\boldsymbol{D}^{(k)}$ is given by
$$\boldsymbol{D}^{(k)}=\sum_{i\in\mathcal{N}_\mathrm{a}}\mathbb{E}\Big\{\jmath_{\mathfrak{bm}}\big(\mathbf{z}_{ii}^{(k)},\boldsymbol{p}_i^{(k)}-\boldsymbol{p}_i^{(k-1)},\boldsymbol{p}_\mathrm{a}^{(k)}\big)\Big\}. \tag{74}$$
- In the Bayesian case,
$$\begin{aligned}\boldsymbol{C}_{ij}^{(k)}&=\mathbb{E}\Big\{\jmath_{\mathrm{bm}}\big(\mathbf{z}_{ij}^{(k)},\mathsf{d}_{ij}^{(k)},\mathbf{p}_\mathrm{a}^{(k)}\big)\Big\}\\&=\mathbb{E}\Big\{\mathbb{E}\Big\{\jmath_{\mathrm{bm}}\big(\mathbf{z}_{ij}^{(k)},\mathsf{d}_{ij}^{(k)},\mathbf{p}_\mathrm{a}^{(k)}\big)\,\Big|\,\mathbf{p}_\mathrm{a}^{(k)}\Big\}\Big\}\end{aligned}$$
where the second equality is by the double expectation formula, leading to (7) using (73) and (4a).
The matrix $\boldsymbol{D}^{(k)}$ is given by
$$\begin{aligned}\boldsymbol{D}^{(k)}=&\sum_{i\in\mathcal{N}_\mathrm{a}}\mathbb{E}\Big\{\jmath_{\mathrm{bm}}\big(\mathbf{z}_{ii}^{(k)},\mathbf{p}_i^{(k)}-\mathbf{p}_i^{(k-1)},\mathbf{p}_\mathrm{a}^{(k)}\big)\Big\}\\&+\mathbb{E}\Big\{\jmath_{\mathrm{bp}}\big(\mathbf{p}_\mathrm{a}^{(k)},\mathbf{p}_\mathrm{a}^{(k-1)},\mathbf{p}_\mathrm{a}^{(k)}\big)\Big\}\end{aligned} \tag{75}$$
where the first term represents the contribution from intra-node measurements and the second term represents the contribution from prior knowledge.

B. A Toy Example

Consider the network with two agents and three anchors as illustrated in Fig. 1. In this case, we have $\mathcal{N}_\mathrm{a}=\{1,2\}$, $\mathcal{N}_\mathrm{b}=\{3,4,5\}$, and $\boldsymbol{p}_\mathrm{a}^{(k)}=\big[\,\boldsymbol{p}_1^{(k)\mathrm{T}}\;\boldsymbol{p}_2^{(k)\mathrm{T}}\,\big]^\mathrm{T}$.

- For $k=n$, agent 1 performs inter-node measurements with anchor 3. Following (73),
$$\begin{aligned}\boldsymbol{C}_{13}^{(k)}&=\frac{1}{\varepsilon_{13}^{(k)}}\begin{bmatrix}\boldsymbol{u}\big(\varphi_{13}^{(k)}\big)\boldsymbol{u}^\mathrm{T}\big(\varphi_{13}^{(k)}\big) & \boldsymbol{O}_2\\ \boldsymbol{O}_2 & \boldsymbol{O}_2\end{bmatrix}\\&=\frac{1}{\varepsilon_{13}^{(k)}}\begin{bmatrix}\boldsymbol{I}_2\\ \boldsymbol{O}_2\end{bmatrix}\boldsymbol{u}\big(\varphi_{13}^{(k)}\big)\boldsymbol{u}^\mathrm{T}\big(\varphi_{13}^{(k)}\big)\,\big[\,\boldsymbol{I}_2\;\boldsymbol{O}_2\,\big]\end{aligned}$$
which is in the form of (4a) by (4b) and (6).
- For $k=n+1$, agent 1 performs inter-node measurements with agent 2. Following (73),
$$\begin{aligned}\boldsymbol{C}_{12}^{(k)}&=\frac{1}{\varepsilon_{12}^{(k)}}\begin{bmatrix}\boldsymbol{u}\big(\varphi_{12}^{(k)}\big)\boldsymbol{u}^\mathrm{T}\big(\varphi_{12}^{(k)}\big) & -\boldsymbol{u}\big(\varphi_{12}^{(k)}\big)\boldsymbol{u}^\mathrm{T}\big(\varphi_{12}^{(k)}\big)\\ -\boldsymbol{u}\big(\varphi_{12}^{(k)}\big)\boldsymbol{u}^\mathrm{T}\big(\varphi_{12}^{(k)}\big) & \boldsymbol{u}\big(\varphi_{12}^{(k)}\big)\boldsymbol{u}^\mathrm{T}\big(\varphi_{12}^{(k)}\big)\end{bmatrix}\\&=\frac{1}{\varepsilon_{12}^{(k)}}\begin{bmatrix}\boldsymbol{I}_2\\ -\boldsymbol{I}_2\end{bmatrix}\boldsymbol{u}\big(\varphi_{12}^{(k)}\big)\boldsymbol{u}^\mathrm{T}\big(\varphi_{12}^{(k)}\big)\,\big[\,\boldsymbol{I}_2\;-\boldsymbol{I}_2\,\big]\end{aligned}$$
which is in the form of (4a) by (4b) and (6).

C. Proof of Proposition 2

The proof uses the following lemma.

Lemma 1: Suppose that an invertible matrix $\boldsymbol{F}\in\mathbb{R}^{n\times n}$ is in the form of
$$\boldsymbol{F}=\begin{bmatrix}\boldsymbol{A} & \boldsymbol{B}^\mathrm{T}\\ \boldsymbol{B} & \boldsymbol{C}\end{bmatrix}$$
where $\boldsymbol{C}\in\mathbb{R}^{m\times m}$ with $m<n$. Then the last $m\times m$ principal submatrix of $[\,\boldsymbol{F}\,]^{-1}$ is given by $(\boldsymbol{C}-\boldsymbol{B}\boldsymbol{A}^{-1}\boldsymbol{B}^\mathrm{T})^{-1}$.

Remark 10: The matrix $(\boldsymbol{C}-\boldsymbol{B}\boldsymbol{A}^{-1}\boldsymbol{B}^\mathrm{T})$ is the Schur complement of $\boldsymbol{A}$ [84].

We now prove Proposition 2. According to (72), the matrix $\boldsymbol{J}^{(n+1)}$ for $n\geq 1$ can be partitioned as
$$\boldsymbol{J}^{(n+1)}=\begin{bmatrix}\boldsymbol{A}^{(n)} & \boldsymbol{B}^{(n+1)\mathrm{T}}\\ \boldsymbol{B}^{(n+1)} & \boldsymbol{D}^{(n+1)}\end{bmatrix}$$
where $\boldsymbol{A}^{(n)}\in\mathbb{R}^{2nN_\mathrm{a}\times 2nN_\mathrm{a}}$ is in the form of
$$\boldsymbol{A}^{(n)}=\begin{bmatrix}\boldsymbol{G}^{(1)} & -\boldsymbol{D}^{(2)} & \boldsymbol{O}_{2N_\mathrm{a}} & \cdots & \boldsymbol{O}_{2N_\mathrm{a}} & \boldsymbol{O}_{2N_\mathrm{a}}\\ -\boldsymbol{D}^{(2)} & \boldsymbol{G}^{(2)} & -\boldsymbol{D}^{(3)} & \cdots & \boldsymbol{O}_{2N_\mathrm{a}} & \boldsymbol{O}_{2N_\mathrm{a}}\\ \boldsymbol{O}_{2N_\mathrm{a}} & -\boldsymbol{D}^{(3)} & \boldsymbol{G}^{(3)} & \cdots & \boldsymbol{O}_{2N_\mathrm{a}} & \boldsymbol{O}_{2N_\mathrm{a}}\\ \vdots & \vdots & \vdots & \ddots & \vdots & \vdots\\ \boldsymbol{O}_{2N_\mathrm{a}} & \boldsymbol{O}_{2N_\mathrm{a}} & \boldsymbol{O}_{2N_\mathrm{a}} & \cdots & \boldsymbol{G}^{(n-1)} & -\boldsymbol{D}^{(n)}\\ \boldsymbol{O}_{2N_\mathrm{a}} & \boldsymbol{O}_{2N_\mathrm{a}} & \boldsymbol{O}_{2N_\mathrm{a}} & \cdots & -\boldsymbol{D}^{(n)} & \boldsymbol{G}^{(n)}\end{bmatrix} \tag{76}$$
and $\boldsymbol{B}^{(n+1)}\in\mathbb{R}^{2N_\mathrm{a}\times 2nN_\mathrm{a}}$ is in the form of
$$\boldsymbol{B}^{(n+1)}=\big[\,\boldsymbol{O}_{2N_\mathrm{a}}\;\boldsymbol{O}_{2N_\mathrm{a}}\;\boldsymbol{O}_{2N_\mathrm{a}}\cdots\boldsymbol{O}_{2N_\mathrm{a}}\;\boldsymbol{D}^{(n+1)}\,\big]. \tag{77}$$
The IFIM $\boldsymbol{Q}^{(n+1)}$ is the $(n+1)$th $2N_\mathrm{a}\times 2N_\mathrm{a}$ principal submatrix of $[\,\boldsymbol{J}^{(n+1)}]^{-1}$. Then by Lemma 1, we have
$$\begin{aligned}\boldsymbol{Q}^{(n+1)}&=\big(\boldsymbol{D}^{(n+1)}-\boldsymbol{B}^{(n+1)}[\,\boldsymbol{A}^{(n)}]^{-1}\boldsymbol{B}^{(n+1)\mathrm{T}}\big)^{-1}\\&=\big(\boldsymbol{D}^{(n+1)}-\boldsymbol{D}^{(n+1)}\boldsymbol{\Psi}^{(n)}\boldsymbol{D}^{(n+1)\mathrm{T}}\big)^{-1}\end{aligned} \tag{78}$$
where $\boldsymbol{\Psi}^{(n)}$ is defined as the nth $2N_\mathrm{a}\times 2N_\mathrm{a}$ principal submatrix of $[\,\boldsymbol{A}^{(n)}]^{-1}$. The expression of $\boldsymbol{\Psi}^{(n)}$ is given as follows.

- For $n=1$, we have $\boldsymbol{A}^{(1)}=\boldsymbol{G}^{(1)}$, and

$$\begin{aligned}\boldsymbol{\Psi}^{(1)} &= [\,\boldsymbol{G}^{(1)}]^{-1}\\ &= \big([\,\boldsymbol{Q}^{(1)}]^{-1}+\boldsymbol{C}^{(1)}_{i_1j_1}+\boldsymbol{D}^{(2)}\big)^{-1} \qquad (79)\end{aligned}$$

  where (79) is by (76) and the definition of $\boldsymbol{\Psi}^{(n)}$; (79) is by (3) and the fact that $\boldsymbol{Q}^{(1)}=[\,\boldsymbol{J}^{(1)}]^{-1}$.
- For $n>1$, we have

$$\begin{aligned}\boldsymbol{\Psi}^{(n)} &= \big(\boldsymbol{G}^{(n)}-\boldsymbol{B}^{(n)}[\,\boldsymbol{A}^{(n-1)}]^{-1}\boldsymbol{B}^{(n)\mathrm{T}}\big)^{-1} \qquad (80a)\\ &= \big(\boldsymbol{D}^{(n)}-\boldsymbol{D}^{(n)}\boldsymbol{\Psi}^{(n-1)}\boldsymbol{D}^{(n)}+\boldsymbol{C}^{(n)}_{i_nj_n}+\boldsymbol{D}^{(n+1)}\big)^{-1} \qquad (80b)\\ &= \big([\,\boldsymbol{Q}^{(n)}]^{-1}+\boldsymbol{C}^{(n)}_{i_nj_n}+\boldsymbol{D}^{(n+1)}\big)^{-1} \qquad (80c)\end{aligned}$$

  where (80a) is by Lemma 1 noting that

$$\boldsymbol{A}^{(n)}=\begin{bmatrix}\boldsymbol{A}^{(n-1)} & \boldsymbol{B}^{(n)\mathrm{T}}\\ \boldsymbol{B}^{(n)} & \boldsymbol{G}^{(n)}\end{bmatrix}$$

  by (76) and (77); (80b) is by (3) and the definition of $\boldsymbol{\Psi}^{(n)}$; (80c) is by (78).

Therefore, (80c) holds for all $n\geq 1$. By substituting (80c) into (78), applying the matrix inversion lemma [85], and using $\boldsymbol{\Delta}^{(n)}=[\,\boldsymbol{D}^{(n)}]^{-1}$, we obtain

$$\boldsymbol{Q}^{(n+1)}=\big([\,\boldsymbol{Q}^{(n)}]^{-1}+\boldsymbol{C}^{(n)}_{i_nj_n}\big)^{-1}+\boldsymbol{\Delta}^{(n+1)} \qquad (81)$$

for all $n\geq 1$. Finally,

- for the non-Bayesian case, (8) and (9) are obtained by substituting (4a) into (81) and applying the matrix inversion lemma [85] on $([\,\boldsymbol{Q}^{(n)}]^{-1}+\boldsymbol{C}^{(n)}_{i_nj_n})^{-1}$;
- for the Bayesian case, (8) and (10) are obtained by substituting (7) into (81).

APPENDIX II
PROOFS OF RESULTS IN SECTION III

A. Proof of Proposition 3

By taking trace on both sides of (8) and reorganizing terms, we have

$$\mathrm{tr}\{\mathbf{Q}^{(n+1)}\}-\mathrm{tr}\{\mathbf{Q}^{(n)}\}=-\mathrm{tr}\{\boldsymbol{\Upsilon}^{(n)}_{\mathsf{i}_n\mathsf{j}_n}\}+\mathrm{tr}\{\boldsymbol{\Delta}^{(n+1)}\}$$

noting that the selected measurement pair $(\mathsf{i}_n,\mathsf{j}_n)$ is random. By taking the expectation on both sides of the equation above conditioned on $\mathbf{Q}^{(n)}$ and using (18), we have

$$\begin{aligned}&\mathbb{E}\big\{\mathrm{tr}\{\mathbf{Q}^{(n+1)}\}\,\big|\,\mathbf{Q}^{(n)}\big\}-\mathrm{tr}\{\mathbf{Q}^{(n)}\}\\ &\quad=-\,\mathbb{E}\big\{\mathrm{tr}\{\boldsymbol{\Upsilon}^{(n)}_{\mathsf{i}_n\mathsf{j}_n}\}\,\big|\,\mathbf{Q}^{(n)}\big\}+\mathrm{tr}\{\boldsymbol{\Delta}^{(n+1)}\}\\ &\quad\leq -g\big(\upsilon(\mathbf{Q}^{(n)})\big)+\mathrm{tr}\{\boldsymbol{\Delta}^{(n+1)}\}.\end{aligned}$$

By taking the expectation with respect to $\mathbf{Q}^{(n)}$ on both sides of the above inequality, we obtain

$$\begin{aligned}&\mathbb{E}\big\{\mathrm{tr}\{\mathbf{Q}^{(n+1)}\}\big\}-\mathbb{E}\big\{\mathrm{tr}\{\mathbf{Q}^{(n)}\}\big\}\\ &\qquad\leq -\,\mathbb{E}\big\{g\big(\upsilon(\mathbf{Q}^{(n)})\big)\big\}+\mathrm{tr}\{\boldsymbol{\Delta}^{(n+1)}\}. \qquad (82)\end{aligned}$$

Then by taking the arithmetic mean over the first N time intervals on both sides of the inequality above, using (15), and applying the Jensen's inequality on the convex function g, we have

$$\begin{aligned}&\frac{1}{N}\,\mathbb{E}\big\{\mathrm{tr}\{\mathbf{Q}^{(N+1)}\}\big\}-\frac{1}{N}\,\mathbb{E}\big\{\mathrm{tr}\{\mathbf{Q}^{(1)}\}\big\}\\ &\quad\leq -\frac{1}{N}\sum_{n=1}^{N}\mathbb{E}\big\{g\big(\upsilon(\mathbf{Q}^{(n)})\big)\big\}+2N_{\mathrm{a}}\overline{\delta}\\ &\quad\leq -g(\upsilon_N)+2N_{\mathrm{a}}\overline{\delta} \qquad (83)\end{aligned}$$

where

$$\upsilon_N\triangleq\frac{1}{N}\sum_{n=1}^{N}\mathbb{E}\big\{\upsilon(\mathbf{Q}^{(n)})\big\}. \qquad (84)$$

After reorganizing (83) and using the fact that $\mathbf{Q}^{(N+1)}\in\mathbb{S}_+^{2N_{\mathrm{a}}}$,

$$\begin{aligned}g(\upsilon_N)&\leq 2N_{\mathrm{a}}\overline{\delta}+\frac{1}{N}\,\mathbb{E}\big\{\mathrm{tr}\{\mathbf{Q}^{(1)}\}\big\}-\frac{1}{N}\,\mathbb{E}\big\{\mathrm{tr}\{\mathbf{Q}^{(N+1)}\}\big\}\\ &\leq 2N_{\mathrm{a}}\overline{\delta}+\frac{1}{N}\,\mathbb{E}\big\{\mathrm{tr}\{\mathbf{Q}^{(1)}\}\big\} \qquad (85)\end{aligned}$$

which together with (20) and (84) implies (19). Furthermore, since $\lim_{x\to\infty}g(x)=\infty$, there exists an $x_N<\infty$ such that

$$g(x)>2N_{\mathrm{a}}\overline{\delta}+\frac{1}{N}\,\mathbb{E}\big\{\mathrm{tr}\{\mathbf{Q}^{(1)}\}\big\}$$

for all $x\geq x_N$. Then by (20), we have $B_N\leq x_N<\infty$.

Finally, since $\mathbb{E}\{\mathrm{tr}\{\mathbf{Q}^{(1)}\}\}<\infty$, for any $N_1,N_2\geq 1$ with $N_1<N_2$, we have

$$2N_{\mathrm{a}}\overline{\delta}+\frac{1}{N_1}\,\mathbb{E}\big\{\mathrm{tr}\{\mathbf{Q}^{(1)}\}\big\}>2N_{\mathrm{a}}\overline{\delta}+\frac{1}{N_2}\,\mathbb{E}\big\{\mathrm{tr}\{\mathbf{Q}^{(1)}\}\big\}.$$

Thus,

$$\begin{aligned}&\Big\{x:g(x)\leq 2N_{\mathrm{a}}\overline{\delta}+\frac{1}{N_2}\,\mathbb{E}\big\{\mathrm{tr}\{\mathbf{Q}^{(1)}\}\big\}\Big\}\\ &\qquad\subseteq\Big\{x:g(x)\leq 2N_{\mathrm{a}}\overline{\delta}+\frac{1}{N_1}\,\mathbb{E}\big\{\mathrm{tr}\{\mathbf{Q}^{(1)}\}\big\}\Big\}\end{aligned}$$

which together with (20) implies $B_{N_2}\leq B_{N_1}$. Therefore, $\{B_N\}$ is non-increasing.

B. Proof of Corollary 1

The proof is similar to that in Appendix II-A. By taking the expectation on both sides of (8), applying (17), and using the fact that $\boldsymbol{\Upsilon}^{(k)}_{\mathsf{i}_k\mathsf{j}_k}\in\mathbb{S}_+^{2N_{\mathrm{a}}}$, we have

$$\mathbb{E}\big\{\mathrm{tr}\{\mathbf{Q}^{(k+1)}\}\big\}\leq\mathbb{E}\big\{\mathrm{tr}\{\mathbf{Q}^{(k)}\}\big\}+2N_{\mathrm{a}}\overline{\delta} \qquad (86)$$

for all $k\geq 1$. For any positive integer n_0 and $n>n_0$, by summing (86) from $k=n_0$ to $n-1$, we obtain

$$\mathbb{E}\big\{\mathrm{tr}\{\mathbf{Q}^{(n)}\}\big\}\leq\mathbb{E}\big\{\mathrm{tr}\{\mathbf{Q}^{(n_0)}\}\big\}+2(n-n_0)N_{\mathrm{a}}\overline{\delta}.$$

For $N\geq n_0$, by summing the above inequality from $n=n_0$ to N, we have

$$\begin{aligned}\sum_{n=n_0}^{N}\mathbb{E}\big\{\mathrm{tr}\{\mathbf{Q}^{(n)}\}\big\}&\leq(N-n_0+1)\,\mathbb{E}\big\{\mathrm{tr}\{\mathbf{Q}^{(n_0)}\}\big\}\\ &\quad+2(1+2+\cdots+N-n_0)N_{\mathrm{a}}\overline{\delta}\\ &=(N-n_0+1)\,\mathbb{E}\big\{\mathrm{tr}\{\mathbf{Q}^{(n_0)}\}\big\}\\ &\quad+(1+N-n_0)(N-n_0)N_{\mathrm{a}}\overline{\delta}. \qquad (87)\end{aligned}$$

By applying (82) with $\upsilon(\mathbf{Q}^{(n)}) = \mathrm{tr}\{\mathbf{Q}^{(n)}\}$ and using (17), we have

$$\mathbb{E}\{\mathrm{tr}\{\mathbf{Q}^{(n+1)}\}\} - \mathbb{E}\{\mathrm{tr}\{\mathbf{Q}^{(n)}\}\} \le -\mathbb{E}\big\{g\big(\mathrm{tr}\{\mathbf{Q}^{(n)}\}\big)\big\} + 2N_{\mathrm{a}}\overline{\delta} \tag{88}$$

for $n = kN_{\mathrm{r}}$ with $k \ge 1$; from (86), we have

$$\mathbb{E}\{\mathrm{tr}\{\mathbf{Q}^{(n+1)}\}\} - \mathbb{E}\{\mathrm{tr}\{\mathbf{Q}^{(n)}\}\} \le 2N_{\mathrm{a}}\overline{\delta} \tag{89}$$

for $n \ne kN_{\mathrm{r}}$ with $k \ge 1$. By summing (88) and (89) from $n = 1$ to KN_{r} with $K \ge 1$, dividing both sides by K, and applying the Jensen's inequality on g, we have

$$\begin{aligned}
&\frac{1}{K}\,\mathbb{E}\big\{\mathrm{tr}\{\mathbf{Q}^{(KN_{\mathrm{r}}+1)}\}\big\} - \frac{1}{K}\,\mathbb{E}\big\{\mathrm{tr}\{\mathbf{Q}^{(1)}\}\big\} \\
&\quad \le -\frac{1}{K}\sum_{k=1}^{K}\mathbb{E}\big\{g\big(\mathrm{tr}\{\mathbf{Q}^{(kN_{\mathrm{r}})}\}\big)\big\} + 2N_{\mathrm{r}}N_{\mathrm{a}}\overline{\delta} \\
&\quad \le -g\bigg(\frac{1}{K}\sum_{k=1}^{K}\mathbb{E}\big\{\mathrm{tr}\{\mathbf{Q}^{(kN_{\mathrm{r}})}\}\big\}\bigg) + 2N_{\mathrm{r}}N_{\mathrm{a}}\overline{\delta}
\end{aligned}$$

which together with the fact that $\mathbf{Q}^{(KN_{\mathrm{r}}+1)} \in \mathbb{S}_{+}^{2N_{\mathrm{a}}}$ implies

$$g\bigg(\frac{1}{K}\sum_{k=1}^{K}\mathbb{E}\big\{\mathrm{tr}\{\mathbf{Q}^{(kN_{\mathrm{r}})}\}\big\}\bigg) \le 2N_{\mathrm{r}}N_{\mathrm{a}}\overline{\delta} + \frac{1}{K}\,\mathbb{E}\big\{\mathrm{tr}\{\mathbf{Q}^{(1)}\}\big\}.$$

Thus, we have

$$\frac{1}{K}\sum_{k=1}^{K}\mathbb{E}\big\{\mathrm{tr}\{\mathbf{Q}^{(kN_{\mathrm{r}})}\}\big\} \le \breve{B}_K, \quad \forall\, K \ge 1 \tag{90}$$

where $\breve{B}_K$ is given by (24) and is non-increasing with K.

For $N \ge 1$, let $K_N = \lfloor N/N_{\mathrm{r}} \rfloor$. We have

$$\begin{aligned}
&\sum_{n=1}^{N}\mathbb{E}\{\mathrm{tr}\{\mathbf{Q}^{(n)}\}\} \\
&\quad \le \sum_{n=1}^{(K_N+1)N_{\mathrm{r}}-1}\mathbb{E}\{\mathrm{tr}\{\mathbf{Q}^{(n)}\}\} \\
&\quad = \sum_{n=1}^{N_{\mathrm{r}}-1}\mathbb{E}\{\mathrm{tr}\{\mathbf{Q}^{(n)}\}\} + \sum_{k=1}^{K_N}\sum_{n=kN_{\mathrm{r}}}^{(k+1)N_{\mathrm{r}}-1}\mathbb{E}\{\mathrm{tr}\{\mathbf{Q}^{(n)}\}\} \\
&\quad \le (N_{\mathrm{r}}-1)\,\mathbb{E}\{\mathrm{tr}\{\mathbf{Q}^{(1)}\}\} + (N_{\mathrm{r}}-1)(N_{\mathrm{r}}-2)N_{\mathrm{a}}\overline{\delta} \quad (91a) \\
&\qquad + \sum_{k=1}^{K_N}\big[\,N_{\mathrm{r}}\,\mathbb{E}\{\mathrm{tr}\{\mathbf{Q}^{(kN_{\mathrm{r}})}\}\} + N_{\mathrm{r}}(N_{\mathrm{r}}-1)N_{\mathrm{a}}\overline{\delta}\,\big] \quad (91b) \\
&\quad \le (N_{\mathrm{r}}-1)\,\mathbb{E}\{\mathrm{tr}\{\mathbf{Q}^{(1)}\}\} + (N_{\mathrm{r}}-1)(N_{\mathrm{r}}-2)N_{\mathrm{a}}\overline{\delta} \\
&\qquad + N_{\mathrm{r}}K_N\breve{B}_{K_N} + K_N N_{\mathrm{r}}(N_{\mathrm{r}}-1)N_{\mathrm{a}}\overline{\delta} \quad (91c) \\
&\quad \le (N_{\mathrm{r}}-1)\,\mathbb{E}\{\mathrm{tr}\{\mathbf{Q}^{(1)}\}\} + (N_{\mathrm{r}}-1)(N_{\mathrm{r}}-2)N_{\mathrm{a}}\overline{\delta} \\
&\qquad + N\breve{B}_{K_N} + N(N_{\mathrm{r}}-1)N_{\mathrm{a}}\overline{\delta} \quad (91d)
\end{aligned}$$

where (91a) uses the fact that $N \le (K_N+1)N_{\mathrm{r}} - 1$, (91b) is by (87), (91c) is by (90), and (91d) uses the fact that $N_{\mathrm{r}}K_N \le N$. Thus, we have $q_N \le B_N$ for all $N \ge 1$, where B_N is given by (23). Finally, since $\breve{B}_{K_N}$ is non-increasing with K_N and K_N is non-decreasing with N, $\breve{B}_{K_N}$ is non-increasing with N, which together with (23) implies that B_N is non-increasing with N.

C. Proof of Proposition 4

We first introduce the following lemma.

Lemma 2: If the nonnegative sequence $\{a_n\}_{n\ge1}$ satisfies

$$\limsup_{N\to\infty}\frac{1}{N}\sum_{n=1}^{N}a_n < \infty \tag{92}$$

then

$$\liminf_{N\to\infty}\frac{a_N}{N} = 0. \tag{93}$$

Proof: The proof is by contradiction. Suppose that

$$\liminf_{N\to\infty}\frac{a_N}{N} = a > 0.$$

Thus, there exists an N_1 such that $\frac{a_n}{n} \ge \frac{a}{2}$ for all $n \ge N_1$. Then for all $N > N_1$,

$$\begin{aligned}
\frac{1}{N}\sum_{n=1}^{N}a_n &\ge \frac{1}{N}\sum_{n=N_1}^{N}a_n = \frac{1}{N}\sum_{n=N_1}^{N}n\cdot\frac{a_n}{n} \\
&\ge \frac{a}{2N}\sum_{n=N_1}^{N}n = \frac{(N+N_1)(N-N_1+1)}{4N}a
\end{aligned}$$

which grows to infinity as $N \to \infty$. This contradicts (92). Therefore, we have (93). □

We now prove Proposition 4. By taking the trace, the arithmetic mean over N time intervals, and the expectation on both sides of (8), we obtain

$$\begin{aligned}
\frac{1}{N}\sum_{n=1}^{N}\mathbb{E}\big\{\mathrm{tr}\{\boldsymbol{\Upsilon}_{\mathrm{i}_n\mathrm{j}_n}^{(n)}\}\big\} &= \frac{1}{N}\sum_{n=1}^{N}\mathrm{tr}\{\boldsymbol{\Delta}^{(n+1)}\} + \frac{1}{N}\,\mathbb{E}\big\{\mathrm{tr}\{\mathbf{Q}^{(1)}\}\big\} \\
&\quad - \frac{1}{N}\,\mathbb{E}\big\{\mathrm{tr}\{\mathbf{Q}^{(N+1)}\}\big\}. \qquad (94)
\end{aligned}$$

Since $\mathbb{E}\big\{\mathrm{tr}\{\mathbf{Q}^{(1)}\}\big\} < \infty$ according to Condition 1, we have

$$\lim_{N\to\infty}\frac{1}{N}\,\mathbb{E}\big\{\mathrm{tr}\{\mathbf{Q}^{(1)}\}\big\} = 0. \tag{95}$$

Also, $\limsup_{N\to\infty} q_N < \infty$ since $q_N \le B$ for all $N \ge 1$. By (11) and Lemma 2, we have

$$\begin{aligned}
&\liminf_{N\to\infty}\frac{1}{N}\,\mathbb{E}\big\{\mathrm{tr}\{\mathbf{Q}^{(N+1)}\}\big\} \\
&\qquad = \liminf_{N\to\infty}\frac{N+1}{N}\frac{1}{N+1}\,\mathbb{E}\big\{\mathrm{tr}\{\mathbf{Q}^{(N+1)}\}\big\} = 0. \qquad (96)
\end{aligned}$$

Then by taking $\liminf_{N\to\infty}$ on both sides of (94) and using (26), (95), and (96), we obtain

$$\liminf_{N\to\infty}\frac{1}{N}\sum_{n=1}^{N}\mathbb{E}\big\{\mathrm{tr}\{\boldsymbol{\Upsilon}_{\mathrm{i}_n\mathrm{j}_n}^{(n)}\}\big\} = 2N_{\mathrm{a}}\delta.$$

Furthermore, by taking $\limsup_{N\to\infty}$ on both sides of (94), using the fact that $\mathbb{E}\{\mathrm{tr}\{\mathbf{Q}^{(N+1)}\}\} \ge 0$ (since $\mathbf{Q}^{(N+1)} \in \mathbb{S}_{++}^{2N_{\mathrm{a}}}$), and applying (26), we have

$$\limsup_{N\to\infty}\frac{1}{N}\sum_{n=1}^{N}\mathbb{E}\big\{\mathrm{tr}\{\boldsymbol{\Upsilon}_{\mathrm{i}_n\mathrm{j}_n}^{(n)}\}\big\} \le 2N_{\mathrm{a}}\delta.$$

Therefore, (27) holds.

D. Proof of Proposition 5

According to (8), we have

$$\boldsymbol{a}^{\mathrm{T}}\mathbf{Q}^{(n+1)}\boldsymbol{a} = \boldsymbol{a}^{\mathrm{T}}\mathbf{Q}^{(n)}\boldsymbol{a} - \boldsymbol{a}^{\mathrm{T}}\boldsymbol{\Upsilon}^{(n)}_{\mathrm{i}_n\mathrm{j}_n}\boldsymbol{a} + \boldsymbol{a}^{\mathrm{T}}\boldsymbol{\Delta}^{(n+1)}\boldsymbol{a} \quad (97)$$

for any $\boldsymbol{a} \in \mathbb{R}^{2N_{\mathrm{a}}}$. By taking the arithmetic mean over the first N time intervals and the expectation on both sides of (97), we obtain

$$\frac{1}{N}\sum_{n=1}^{N}\boldsymbol{a}^{\mathrm{T}}\mathbb{E}\{\boldsymbol{\Upsilon}^{(n)}_{\mathrm{i}_n\mathrm{j}_n}\}\boldsymbol{a} = \frac{1}{N}\sum_{n=1}^{N}\boldsymbol{a}^{\mathrm{T}}\boldsymbol{\Delta}^{(n+1)}\boldsymbol{a} + \frac{1}{N}\boldsymbol{a}^{\mathrm{T}}\mathbb{E}\{\mathbf{Q}^{(1)}\}\boldsymbol{a} - \frac{1}{N}\boldsymbol{a}^{\mathrm{T}}\mathbb{E}\{\mathbf{Q}^{(N+1)}\}\boldsymbol{a}. \quad (98)$$

Equation (28) implies

$$\lim_{N\to\infty}\frac{1}{N}\sum_{n=1}^{N}\boldsymbol{a}^{\mathrm{T}}\boldsymbol{\Delta}^{(n+1)}\boldsymbol{a} = \boldsymbol{a}^{\mathrm{T}}\boldsymbol{\Delta}\boldsymbol{a}.$$

Since $\mathbf{Q}^{(1)}$ and $\mathbf{Q}^{(N)}$ are positive definite, (95) and (96) imply

$$\lim_{N\to\infty}\frac{1}{N}\boldsymbol{a}^{\mathrm{T}}\mathbb{E}\{\mathbf{Q}^{(1)}\}\boldsymbol{a} = 0$$
$$\liminf_{N\to\infty}\frac{1}{N}\boldsymbol{a}^{\mathrm{T}}\mathbb{E}\{\mathbf{Q}^{(N+1)}\}\boldsymbol{a} = 0$$

respectively. Thus, by taking $\liminf_{N\to\infty}$ on both sides of (98), we have

$$\liminf_{N\to\infty}\frac{1}{N}\sum_{n=1}^{N}\boldsymbol{a}^{\mathrm{T}}\mathbb{E}\{\boldsymbol{\Upsilon}^{(n)}_{\mathrm{i}_n\mathrm{j}_n}\}\boldsymbol{a} = \boldsymbol{a}^{\mathrm{T}}\boldsymbol{\Delta}\boldsymbol{a}. \quad (99)$$

Furthermore, by taking $\limsup_{N\to\infty}$ on both sides of (98) and using the fact that $\boldsymbol{a}^{\mathrm{T}}\mathbb{E}\{\mathbf{Q}^{(N+1)}\}\boldsymbol{a} \geq 0$ (since $\mathbf{Q}^{(N+1)} \in \mathbb{S}^{2N_{\mathrm{a}}}_{++}$), we have

$$\limsup_{N\to\infty}\frac{1}{N}\sum_{n=1}^{N}\boldsymbol{a}^{\mathrm{T}}\mathbb{E}\{\boldsymbol{\Upsilon}^{(n)}_{\mathrm{i}_n\mathrm{j}_n}\}\boldsymbol{a} \leq \boldsymbol{a}^{\mathrm{T}}\boldsymbol{\Delta}\boldsymbol{a}. \quad (100)$$

From (99) and (100), and using the linearity of expectation, we have

$$\lim_{N\to\infty}\frac{1}{N}\sum_{n=1}^{N}\mathbb{E}\{\boldsymbol{a}^{\mathrm{T}}\boldsymbol{\Upsilon}^{(n)}_{\mathrm{i}_n\mathrm{j}_n}\boldsymbol{a}\} = \boldsymbol{a}^{\mathrm{T}}\boldsymbol{\Delta}\boldsymbol{a}. \quad (101)$$

Thus, for all $\boldsymbol{b} \in \mathbb{R}^{2N_{\mathrm{a}}}$ and $\boldsymbol{c} = \boldsymbol{a} + \boldsymbol{b}$, we have

$$\lim_{N\to\infty}\frac{1}{N}\sum_{n=1}^{N}\mathbb{E}\{\boldsymbol{b}^{\mathrm{T}}\boldsymbol{\Upsilon}^{(n)}_{\mathrm{i}_n\mathrm{j}_n}\boldsymbol{b}\} = \boldsymbol{b}^{\mathrm{T}}\boldsymbol{\Delta}\boldsymbol{b} \quad (102)$$

$$\lim_{N\to\infty}\frac{1}{N}\sum_{n=1}^{N}\mathbb{E}\{\boldsymbol{c}^{\mathrm{T}}\boldsymbol{\Upsilon}^{(n)}_{\mathrm{i}_n\mathrm{j}_n}\boldsymbol{c}\} = \boldsymbol{c}^{\mathrm{T}}\boldsymbol{\Delta}\boldsymbol{c}. \quad (103)$$

By subtracting (101) and (102) from (103), we have

$$\lim_{N\to\infty}\frac{1}{N}\sum_{n=1}^{N}\mathbb{E}\{\boldsymbol{a}^{\mathrm{T}}\boldsymbol{\Upsilon}^{(n)}_{\mathrm{i}_n\mathrm{j}_n}\boldsymbol{b}\} + \frac{1}{N}\sum_{n=1}^{N}\mathbb{E}\{\boldsymbol{b}^{\mathrm{T}}\boldsymbol{\Upsilon}^{(n)\mathrm{T}}_{\mathrm{i}_n\mathrm{j}_n}\boldsymbol{a}\} = \boldsymbol{a}^{\mathrm{T}}\boldsymbol{\Delta}\boldsymbol{b} + \boldsymbol{b}^{\mathrm{T}}\boldsymbol{\Delta}^{\mathrm{T}}\boldsymbol{a}. \quad (104)$$

The matrix $\boldsymbol{\Upsilon}^{(n)}_{\mathrm{i}_n\mathrm{j}_n}$ is symmetric by (9) and (10), and the matrix $\boldsymbol{\Delta}$ is symmetric since it is the limit of a sequence of symmetric matrices as in (26). Thus, (104) implies

$$\lim_{N\to\infty}\frac{1}{N}\sum_{n=1}^{N}\mathbb{E}\{\boldsymbol{a}^{\mathrm{T}}\boldsymbol{\Upsilon}^{(n)}_{\mathrm{i}_n\mathrm{j}_n}\boldsymbol{b}\} = \boldsymbol{a}^{\mathrm{T}}\boldsymbol{\Delta}\boldsymbol{b}.$$

Finally, we obtain (29) by choosing $\boldsymbol{a}$ and $\boldsymbol{b}$ as vectors with all zeros except a 1 on the ith and jth entry, respectively, for all $i, j = 1, 2, \ldots, 2N_{\mathrm{a}}$.

E. Proof of Corollary 3

The proof is by contradiction. Suppose there exists a $B < \infty$ such that $q_N < B$ for all $N \geq 1$. Then by taking $\liminf_{N\to\infty}$ on both sides of (94) and using (96), we have

$$\liminf_{N\to\infty}\frac{1}{N}\sum_{n=1}^{N}\mathbb{E}\big\{\mathrm{tr}\{\boldsymbol{\Upsilon}^{(n)}_{\mathrm{i}_n\mathrm{j}_n}\}\big\} = \liminf_{N\to\infty}\frac{1}{N}\sum_{n=1}^{N}\mathrm{tr}\{\boldsymbol{\Delta}^{(n+1)}\}$$

which contradicts (30).

Appendix III
Proof of Proposition 6

The main idea of the proof is to obtain a lower bound on the expected error reduction $\mathbb{E}\big\{\mathrm{tr}\{\boldsymbol{\Upsilon}^{(n)}_{\mathrm{i}_n\mathrm{j}_n}\}\,\big|\,\mathbf{Q}^{(n)}\big\}$ and apply the sufficient condition for boundedness in Proposition 3. The following lemma will be used.

Lemma 3: Let $\boldsymbol{H}$ be a 2×2 positive definite symmetric matrix. If φ follows the uniform distribution on $[\,0, 2\pi)$, then

$$\mathbb{E}\left\{\frac{\boldsymbol{u}(\varphi)\,\boldsymbol{u}^{\mathrm{T}}(\varphi)}{\boldsymbol{u}^{\mathrm{T}}(\varphi)\,\boldsymbol{H}\,\boldsymbol{u}(\varphi)}\right\} = \frac{\boldsymbol{H}^{-\frac{1}{2}}}{\mathrm{tr}\{\boldsymbol{H}^{\frac{1}{2}}\}}. \quad (105)$$

Proof: The SEDs of $\boldsymbol{H}$ and $\boldsymbol{H}^{\frac{1}{2}}$ are given by

$$\boldsymbol{H} = \sum_{l=1}^{2}\lambda_l\boldsymbol{u}(\psi_l)\boldsymbol{u}^{\mathrm{T}}(\psi_l) \quad (106a)$$

$$\boldsymbol{H}^{\frac{1}{2}} = \sum_{l=1}^{2}\sqrt{\lambda_l}\boldsymbol{u}(\psi_l)\boldsymbol{u}^{\mathrm{T}}(\psi_l) \quad (106b)$$

where $\psi_l = \psi_l(\boldsymbol{H})$ and $\lambda_l = \lambda_l(\boldsymbol{H})$ for $l = 1, 2$. For unitary matrix $\boldsymbol{U} = [\,\boldsymbol{u}(\psi_1)\ \boldsymbol{u}(\psi_2)\,]$, we have

$$\boldsymbol{U}^{\mathrm{T}}\,\boldsymbol{u}(\varphi) = \boldsymbol{u}(\alpha) \quad (107a)$$

$$\boldsymbol{u}(\varphi) = \boldsymbol{U}\,\boldsymbol{u}(\alpha) \quad (107b)$$

where $\alpha = \varphi - \psi_1$.

Substituting (106a) and (107) into the left-hand side of (105) gives

$$\mathbb{E}\left\{\frac{\boldsymbol{u}(\varphi)\,\boldsymbol{u}^{\mathrm{T}}(\varphi)}{\boldsymbol{u}^{\mathrm{T}}(\varphi)\,\boldsymbol{H}\,\boldsymbol{u}(\varphi)}\right\} = \mathbb{E}\left\{\frac{\boldsymbol{U}\boldsymbol{u}(\alpha)\boldsymbol{u}^{\mathrm{T}}(\alpha)\boldsymbol{U}^{\mathrm{T}}}{\lambda_1\cos^2(\alpha) + \lambda_2\sin^2(\alpha)}\right\} \quad (108)$$

where the expectation is with respect to α, which follows the uniform distribution on $\big[-\psi_1,\, 2\pi - \psi_1\big)$, and

$$\boldsymbol{u}(\alpha)\boldsymbol{u}^{\mathrm{T}}(\alpha) = \begin{bmatrix}\cos^2(\alpha) & \cos(\alpha)\sin(\alpha)\\ \cos(\alpha)\sin(\alpha) & \sin^2(\alpha)\end{bmatrix}.$$

The expectation on the right-hand side of (108) involves the following identities

$$\int_{-\psi_1}^{2\pi-\psi_1} \frac{1}{2\pi} \frac{\cos^2(\alpha)}{\lambda_1 \cos^2(\alpha) + \lambda_2 \sin^2(\alpha)} d\alpha = \frac{1}{\sqrt{\lambda_1}(\sqrt{\lambda_1}+\sqrt{\lambda_2})}$$
$$\int_{-\psi_1}^{2\pi-\psi_1} \frac{1}{2\pi} \frac{\sin^2(\alpha)}{\lambda_1 \cos^2(\alpha) + \lambda_2 \sin^2(\alpha)} d\alpha = \frac{1}{\sqrt{\lambda_2}(\sqrt{\lambda_1}+\sqrt{\lambda_2})}$$
$$\int_{-\psi_1}^{2\pi-\psi_1} \frac{1}{2\pi} \frac{\cos(\alpha)\sin(\alpha)}{\lambda_1 \cos^2(\alpha) + \lambda_2 \sin^2(\alpha)} d\alpha = 0.$$

Using them together with (106) and (108) proves the lemma. □

Now we begin to prove Proposition 6 for both the non-Bayesian and Bayesian cases. Since the following steps are applied for the nth time interval, the superscript (n) is omitted in the proof for notational convenience.

A. Non-Bayesian Case

We first provide the following result. Recall that $\mathsf{N}_{\mathrm{b},i}$ is the index set of anchors within the communication range of agent i.

Lemma 4: For $i \in \mathcal{N}_{\mathrm{a}}$ and j being randomly selected from $\mathsf{N}_{\mathrm{b},i}$, we have

$$\mathbb{E}\{\mathrm{tr}\{\boldsymbol{\Upsilon}_{ij}\} \,|\, \mathbf{Q}\} \geq \frac{\zeta_{\mathrm{b}}(\mathrm{tr}\{\mathbf{Q}_{ii}\})^2}{2(\mathrm{tr}\{\mathbf{Q}_{ii}\} + 2\overline{\varepsilon})} \tag{109}$$

where ζ_{b} is given by (33).

Proof: Since $|\mathsf{N}_{\mathrm{b},i}|$ is independent of $\mathbf{Q}$, we have

$$\mathbb{E}\{\mathrm{tr}\{\boldsymbol{\Upsilon}_{ij}\} \,|\, \mathbf{Q}\} = \sum_{K=1}^{\infty} \mathbb{P}\{|\mathsf{N}_{\mathrm{b},i}| = K\}\ \mathbb{E}\{\,\mathrm{tr}\{\boldsymbol{\Upsilon}_{ij}\} \,|\, \mathbf{Q},\, |\mathsf{N}_{\mathrm{b},i}| = K\,\} \tag{110}$$

where the expectation is with respect to $\mathbf{p}_{\mathrm{b}}$. Let $\mathbf{B}_{ij} = \mathbf{Q}\,\boldsymbol{A}_{ij}$. We have

$$\mathbb{E}\big\{\,\mathrm{tr}\{\boldsymbol{\Upsilon}_{ij}\} \,\big|\, \mathbf{Q},\, |\mathsf{N}_{\mathrm{b},i}| = K\big\} = \mathbb{E}\left\{ \frac{\mathrm{tr}\{\mathbf{B}_{ij}\, \boldsymbol{u}(\varphi_{ij})\, \boldsymbol{u}^{\mathrm{T}}(\varphi_{ij})\, \mathbf{B}_{ij}^{\mathrm{T}}\}}{\boldsymbol{u}^{\mathrm{T}}(\varphi_{ij})(\varepsilon_{ij}\boldsymbol{I}_2 + \mathbf{Q}_{ii})\boldsymbol{u}(\varphi_{ij})} \,\middle|\, \mathbf{Q},\, |\mathsf{N}_{\mathrm{b},i}| = K \right\} \tag{111a}$$

$$\geq \mathbb{E}\left\{ \frac{\mathrm{tr}\{\mathbf{B}_{ij}\, \boldsymbol{u}(\varphi_{ij})\, \boldsymbol{u}^{\mathrm{T}}(\varphi_{ij})\, \mathbf{B}_{ij}^{\mathrm{T}}\}}{\boldsymbol{u}^{\mathrm{T}}(\varphi_{ij})(\overline{\varepsilon}\,\boldsymbol{I}_2 + \mathbf{Q}_{ii})\boldsymbol{u}(\varphi_{ij})} \,\middle|\, \mathbf{Q},\, |\mathsf{N}_{\mathrm{b},i}| = K \right\} \tag{111b}$$

$$= \frac{\mathrm{tr}\{\mathbf{B}_{ij}\, (\overline{\varepsilon}\,\boldsymbol{I}_2 + \mathbf{Q}_{ii})^{-\frac{1}{2}}\, \mathbf{B}_{ij}^{\mathrm{T}}\}}{\mathrm{tr}\{(\overline{\varepsilon}\,\boldsymbol{I}_2 + \mathbf{Q}_{ii})^{\frac{1}{2}}\}}. \tag{111c}$$

The equality in (111a) follows (9). The inequality in (111b) is obtained by recognizing that

$$\frac{\mathrm{tr}\{\mathbf{B}_{ij}\, \boldsymbol{u}(\varphi_{ij})\, \boldsymbol{u}^{\mathrm{T}}(\varphi_{ij})\, \mathbf{B}_{ij}^{\mathrm{T}}\}}{\boldsymbol{u}^{\mathrm{T}}(\varphi_{ij})(\varepsilon_{ij}\boldsymbol{I}_2 + \mathbf{Q}_{ii})\boldsymbol{u}(\varphi_{ij})} \tag{112}$$

is a convex function of ε_{ij}, and by taking the expectation in (111a) first with respect to φ_{ij} and then with respect to ε_{ij}. Finally, by moving the inner expectation inside over ε_{ij} in the denominator of (112), applying the Jensen's inequality, and using (14), we have (111b). The equality in (111c) is by first exchanging the order of expectation and trace, and then applying Lemma 3 using the fact that φ_{ij} given $\{|\mathsf{N}_{\mathrm{b},i}| = K,\, \mathbf{Q}\}$ follows uniform distribution on $[\,0, 2\pi)$.[21]

By substituting $\mathbf{B}_{ij} = \mathbf{Q}\,\boldsymbol{A}_{ij}$ into (111c) and using (6), we obtain

$$\mathbb{E}\big\{\,\mathrm{tr}\{\boldsymbol{\Upsilon}_{ij}\} \,\big|\, \mathbf{Q},\, |\mathsf{N}_{\mathrm{b},i}| = K\big\} \geq \sum_{m=1}^{N_{\mathrm{a}}} \frac{\mathrm{tr}\big\{\mathbf{Q}_{mi}\,(\overline{\varepsilon}\,\boldsymbol{I}_2 + \mathbf{Q}_{ii})^{-\frac{1}{2}}\,\mathbf{Q}_{mi}^{\mathrm{T}}\big\}}{\mathrm{tr}\big\{(\overline{\varepsilon}\,\boldsymbol{I}_2 + \mathbf{Q}_{ii})^{\frac{1}{2}}\big\}}$$
$$\geq \frac{\mathrm{tr}\big\{\mathbf{Q}_{ii}\,(\overline{\varepsilon}\,\boldsymbol{I}_2 + \mathbf{Q}_{ii})^{-\frac{1}{2}}\,\mathbf{Q}_{ii}^{\mathrm{T}}\big\}}{\mathrm{tr}\big\{(\overline{\varepsilon}\,\boldsymbol{I}_2 + \mathbf{Q}_{ii})^{\frac{1}{2}}\big\}} \tag{113a}$$
$$= \sum_{l=1}^{2} \frac{\lambda_l^2(\mathbf{Q}_{ii})}{\lambda_l(\mathbf{Q}_{ii}) + \overline{\varepsilon} + \sqrt{(\lambda_1(\mathbf{Q}_{ii}) + \overline{\varepsilon})(\lambda_2(\mathbf{Q}_{ii}) + \overline{\varepsilon})}} \tag{113b}$$
$$\geq \sum_{l=1}^{2} \frac{\lambda_l^2(\mathbf{Q}_{ii})}{\lambda_l(\mathbf{Q}_{ii}) + 2\overline{\varepsilon} + \mathrm{tr}\{\mathbf{Q}_{ii}\}/2} \tag{113c}$$
$$= 2 \times \frac{1}{2} \sum_{l=1}^{2} \frac{\lambda_l^2(\mathbf{Q}_{ii})}{\lambda_l(\mathbf{Q}_{ii}) + 2\overline{\varepsilon} + \mathrm{tr}\{\mathbf{Q}_{ii}\}/2} \tag{113d}$$
$$\geq \frac{\big(\mathrm{tr}\{\mathbf{Q}_{ii}\}\big)^2}{2\big(\mathrm{tr}\{\mathbf{Q}_{ii}\} + 2\overline{\varepsilon}\big)}. \tag{113e}$$

The equality in (113b) is obtained by substituting the SED

$$\mathbf{Q}_{ii} = \sum_{l=1}^{2} \lambda_l(\mathbf{Q}_{ii}) \boldsymbol{u}(\psi_l(\mathbf{Q}_{ii})) \boldsymbol{u}^{\mathrm{T}}(\psi_l(\mathbf{Q}_{ii}))$$

and the SED

$$\overline{\varepsilon}\,\boldsymbol{I}_2 + \mathbf{Q}_{ii} = \sum_{l=1}^{2} (\overline{\varepsilon} + \lambda_l(\mathbf{Q}_{ii})) \boldsymbol{u}(\psi_l(\mathbf{Q}_{ii})) \boldsymbol{u}^{\mathrm{T}}(\psi_l(\mathbf{Q}_{ii}))$$

into (113a). The inequality in (113c) is due to the fact that

$$x_1 x_2 \leq \left(\frac{x_1 + x_2}{2}\right)^2, \quad \forall\, x_1, x_2 \geq 0.$$

The inequality in (113e) is obtained by applying the Jensen's inequality on (113d) using the fact that $ax^2/(x+b)$ with $a > 0$ and $b \geq 0$ is a convex function of x.

By substituting (113e) into (110), we have

$$\mathbb{E}\{\mathrm{tr}\{\boldsymbol{\Upsilon}_{ij}\} \,|\, \mathbf{Q}\} \geq \frac{\zeta_{\mathrm{b}}(\mathrm{tr}\{\mathbf{Q}_{ii}\})^2}{2(\mathrm{tr}\{\mathbf{Q}_{ii}\} + 2\overline{\varepsilon})}$$

where $\zeta_{\mathrm{b}} = \sum_{K=1}^{\infty} \mathbb{P}\{|\mathsf{N}_{\mathrm{b},i}| = K\}$. Since $\mathsf{N}_{\mathrm{b},i}$ is the set of anchors within a circle centered at $\boldsymbol{p}_i$ with radius R, and the anchors' locations in $\mathbf{p}_{\mathrm{b}}$ follow a homogeneous PPP with density μ_{b}, $|\mathsf{N}_{\mathrm{b},i}|$ follows a Poisson distribution with parameter $\pi R^2 \mu_{\mathrm{b}}$. Thus,

$$\zeta_{\mathrm{b}} = 1 - \mathbb{P}\{|\mathsf{N}_{\mathrm{b},i}| = 0\} = 1 - e^{-\pi R^2 \mu_{\mathrm{b}}}$$

which agrees with (33). □

[21] Note that φ_{ij} is a function of $\boldsymbol{p}_i$ (which is part of $\boldsymbol{p}_{\mathrm{a}}$) and $\mathbf{p}_{\mathsf{j}}$ (which is part of $\mathbf{p}_{\mathrm{b}}$). Since $\mathbf{p}_{\mathrm{b}}$ follows a homogeneous PPP that is independent of $\mathbf{Q}$, and anchor j is randomly selected from $\mathsf{N}_{\mathrm{b},i}$, φ_{ij} given $\{|\mathsf{N}_{\mathrm{b},i}| = K,\, \mathbf{Q}\}$ is uniformly distributed on $[\,0, 2\pi)$.

1) Opportunistic Scheduling Strategy: Let $(\mathsf{i}_n, \mathsf{j}_n)$ be the measurement pair selected by the opportunistic scheduling strategy, and let j be the index of an anchor randomly selected from $\mathcal{N}_{\mathrm{b},\mathsf{i}_n^\star}$ with $\mathsf{i}_n^\star$ given in (13). We have

$$\mathbb{E}\{\mathrm{tr}\{\boldsymbol{\Upsilon}_{\mathsf{i}_n\mathsf{j}_n}\}\,|\,\mathbf{Q}\} \geq \mathbb{E}\{\mathrm{tr}\{\boldsymbol{\Upsilon}_{\mathsf{i}_n^\star\mathsf{j}}\}\,|\,\mathbf{Q}\} \tag{114a}$$

$$\geq \frac{\zeta_{\mathrm{b}}(\mathrm{tr}\{\mathbf{Q}_{\mathsf{i}_n^\star\mathsf{i}_n^\star}\})^2}{2(\mathrm{tr}\{\mathbf{Q}_{\mathsf{i}_n^\star\mathsf{i}_n^\star}\}+2\overline{\varepsilon})} \tag{114b}$$

where (114a) follows the policy of the opportunistic scheduling strategy and (114b) is by Lemma 4. Since

$$g_1(x) \triangleq \frac{\zeta_{\mathrm{b}}x^2}{2(x+2\overline{\varepsilon})} \tag{115}$$

is convex and strictly increasing in $\mathbb{R}_{\geq 0}$ (which implies $\lim_{x\to\infty} g_1(x)=\infty$), the condition in Proposition 3 is satisfied with $\upsilon(\mathbf{Q})=\mathrm{tr}\{\mathbf{Q}_{\mathsf{i}_n^\star\mathsf{i}_n^\star}\}$ and $g=g_1$. Thus, (19) holds with B_N given by (21). Then by solving for g_1^{-1} from (115), we obtain (35). Finally, (32) holds since $\mathrm{tr}\{\mathbf{Q}\}\leq N_{\mathrm{a}}\,\mathrm{tr}\{\mathbf{Q}_{\mathsf{i}_n^\star\mathsf{i}_n^\star}\}$.

2) Random Scheduling Strategy: Let $(\mathsf{i}_n, \mathsf{j}_n)$ be the measurement pair selected by the random scheduling strategy, and let j_i be the index of an anchor randomly selected from $\mathsf{N}_{\mathrm{b},i}$. We have

$$\mathbb{E}\{\mathrm{tr}\{\boldsymbol{\Upsilon}_{\mathsf{i}_n\mathsf{j}_n}\}\,|\,\mathbf{Q}\} \geq \frac{1}{N_{\mathrm{a}}}\sum_{i=1}^{N_{\mathrm{a}}}\mathbb{E}\{\mathrm{tr}\{\boldsymbol{\Upsilon}_{ij_i}\}\,|\,\mathbf{Q}\} \tag{116a}$$

$$\geq \frac{\zeta_{\mathrm{b}}}{2N_{\mathrm{a}}}\sum_{i=1}^{N_{\mathrm{a}}}\frac{(\mathrm{tr}\{\mathbf{Q}_{ii}\})^2}{\mathrm{tr}\{\mathbf{Q}_{ii}\}+2\overline{\varepsilon}} \tag{116b}$$

$$\geq \frac{\zeta_{\mathrm{b}}(\mathrm{tr}\{\mathbf{Q}\})^2}{2N_{\mathrm{a}}(\mathrm{tr}\{\mathbf{Q}\}+2N_{\mathrm{a}}\overline{\varepsilon})} \tag{116c}$$

where the inequality in (116a) follows the policy of the random scheduling strategy without considering the cases of inter-node measurements between two agents (only the inter-node measurements between an agent and an anchor are taken into account), (116b) follows Lemma 4, and (116c) uses the Jensen's inequality by moving the average over i in (116b) inside a convex function. Since

$$g_2(x) \triangleq \frac{\zeta_{\mathrm{b}}x^2}{2N_{\mathrm{a}}(x+2\overline{\varepsilon})} \tag{117}$$

is convex and strictly increasing in $\mathbb{R}_{\geq 0}$ (which implies $\lim_{x\to\infty} g_2(x)=\infty$), the condition in Proposition 3 is satisfied with $\upsilon(\mathbf{Q}^{(n)})=\mathrm{tr}\{\mathbf{Q}^{(n)}\}$ and $g=g_2$. Thus, (19) holds with B_N given by (21). Then by solving for g_2^{-1} from (117), we obtain (32).

B. Bayesian Case

For the Bayesian case, we first derive the following lower bound on the error reduction matrix $\boldsymbol{\Upsilon}_{ij}$.

Lemma 5: For every $i\in\mathcal{N}_{\mathrm{a}}$ and $j\in\mathcal{N}_{\mathrm{a}}\cup\mathcal{N}_{\mathrm{b}}\setminus\{i\}$,

$$\boldsymbol{\Upsilon}_{ij} \succcurlyeq \underline{\boldsymbol{\Upsilon}}_{ij} = \mathbb{E}_{\mathbf{p}_{\mathrm{a}}}\left\{\frac{\mathbf{Q}\,\boldsymbol{A}_{ij}\boldsymbol{u}(\varphi_{ij})\boldsymbol{u}^{\mathrm{T}}(\varphi_{ij})\boldsymbol{A}_{ij}^{\mathrm{T}}\mathbf{Q}}{\boldsymbol{u}^{\mathrm{T}}(\varphi_{ij})(\varepsilon_{ij}\boldsymbol{I}_2+\boldsymbol{A}_{ij}^{\mathrm{T}}\mathbf{Q}\,\boldsymbol{A}_{ij})\boldsymbol{u}(\varphi_{ij})}\right\}. \tag{118}$$

Proof: From (10), we have

$$\boldsymbol{\Upsilon}_{ij} = \mathbf{Q}-\left([\,\mathbf{Q}\,]^{-1}+\mathbb{E}_{\mathbf{p}_{\mathrm{a}}}\{\boldsymbol{\Xi}_{ij}(\varphi_{ij},\varepsilon_{ij})\}\right)^{-1}$$

$$\succcurlyeq \mathbf{Q}-\mathbb{E}_{\mathbf{p}_{\mathrm{a}}}\left\{\left([\,\mathbf{Q}\,]^{-1}+\boldsymbol{\Xi}_{ij}(\varphi_{ij},\varepsilon_{ij})\right)^{-1}\right\} \tag{119a}$$

$$= \mathbb{E}_{\mathbf{p}_{\mathrm{a}}}\left\{\mathbf{Q}-\left([\,\mathbf{Q}\,]^{-1}+\boldsymbol{\Xi}_{ij}(\varphi_{ij},\varepsilon_{ij})\right)^{-1}\right\}=\underline{\boldsymbol{\Upsilon}}_{ij} \tag{119b}$$

where (119a) is by the convexity of matrix inverse in the set of positive definite matrices [86], and (119b) is by applying the matrix inversion lemma [85] on $\left([\,\mathbf{Q}\,]^{-1}+\boldsymbol{\Xi}_{ij}(\varphi_{ij},\varepsilon_{ij})\right)^{-1}$. □

Now we start the proof for the Bayesian case. For $i\in\mathcal{N}_{\mathrm{a}}$ and $K>0$, let j be the index of a randomly selected anchor from $\mathsf{N}_{\mathrm{b},i}$. We have

$$\mathbb{E}\{\mathrm{tr}\{\underline{\boldsymbol{\Upsilon}}_{ij}\}\,|\,\mathbf{Q}\}$$

$$= \mathbb{E}_{\mathbf{p}_{\mathrm{a}}}\left\{\mathbb{E}_{\mathbf{p}_{\mathrm{b}}}\left\{\frac{\mathbf{Q}\boldsymbol{A}_{ij}\boldsymbol{u}(\varphi_{ij})\boldsymbol{u}^{\mathrm{T}}(\varphi_{ij})\boldsymbol{A}_{ij}^{\mathrm{T}}\mathbf{Q}}{\boldsymbol{u}^{\mathrm{T}}(\varphi_{ij})(\varepsilon_{ij}\boldsymbol{I}_2+\mathbf{Q}_{ii})\boldsymbol{u}(\varphi_{ij})}\,\middle|\,\mathbf{Q}\right\}\,\middle|\,\mathbf{Q}\right\} \tag{120a}$$

$$\geq \mathbb{E}_{\mathbf{p}_{\mathrm{a}}}\left\{\frac{\zeta_{\mathrm{b}}(\mathrm{tr}\{\mathbf{Q}_{ii}\})^2}{2(\mathrm{tr}\{\mathbf{Q}_{ii}\}+2\overline{\varepsilon})}\,\middle|\,\mathbf{Q}\right\}=\frac{\zeta_{\mathrm{b}}(\mathrm{tr}\{\mathbf{Q}_{ii}\})^2}{2(\mathrm{tr}\{\mathbf{Q}_{ii}\}+2\overline{\varepsilon})} \tag{120b}$$

where (120a) follows (118) by exchanging the order of expectations with respect to $\mathbf{p}_{\mathrm{b}}$ and $\mathbf{p}_{\mathrm{a}}$; (120b) follows Lemma 4 noting that the expression inside the inner expectation of (120a) is in the form of the non-Bayesian error reduction matrix (9) and that the expectation in (109) is with respect to $\mathbf{p}_{\mathrm{b}}$.

1) Opportunistic Scheduling Strategy: Let $(\mathsf{i}_n, \mathsf{j}_n)$ be the measurement pair selected by the opportunistic scheduling strategy, and let j be the index of an anchor randomly selected from $\mathcal{N}_{\mathrm{b},\mathsf{i}_n^\star}$ with $\mathsf{i}_n^\star$ given in (13). We have

$$\mathbb{E}\{\mathrm{tr}\{\boldsymbol{\Upsilon}_{\mathsf{i}_n\mathsf{j}_n}\}\,|\,\mathbf{Q}\} \geq \mathbb{E}\{\mathrm{tr}\{\boldsymbol{\Upsilon}_{\mathsf{i}_n^\star\mathsf{j}}\}\,|\,\mathbf{Q}\} \tag{121a}$$

$$\geq \mathbb{E}\{\mathrm{tr}\{\underline{\boldsymbol{\Upsilon}}_{\mathsf{i}_n^\star\mathsf{j}}\}\,|\,\mathbf{Q}\} \tag{121b}$$

$$\geq \frac{\zeta_{\mathrm{b}}\left(\mathrm{tr}\{\mathbf{Q}_{\mathsf{i}_n^\star\mathsf{i}_n^\star}\}\right)^2}{2\left(\mathrm{tr}\{\mathbf{Q}_{\mathsf{i}_n^\star\mathsf{i}_n^\star}\}+2\overline{\varepsilon}\right)} = g_1\left(\mathrm{tr}\{\mathbf{Q}_{\mathsf{i}_n^\star\mathsf{i}_n^\star}\}\right) \tag{121c}$$

where (121a) follows the policy of the opportunistic scheduling strategy, (121b) is by Lemma 5, (121c) is by (33) and (120b), and $g_1(x)$ is given by (115). Therefore, the condition in Proposition 3 is satisfied with $\upsilon(\mathbf{Q}^{(n)})=\mathrm{tr}\{\mathbf{Q}^{(n)}_{\mathsf{i}_n^\star\mathsf{i}_n^\star}\}$ and $g=g_1$. Thus, (19) holds with B_N given by (21). Then by solving for g_1^{-1} from (115), we obtain (35). Finally, (32) holds since $\mathrm{tr}\{\mathbf{Q}^{(n)}\}\leq N_{\mathrm{a}}\,\mathrm{tr}\{\mathbf{Q}^{(n)}_{\mathsf{i}_n^\star\mathsf{i}_n^\star}\}$.

2) Random Scheduling Strategy: Let $(\mathsf{i}_n, \mathsf{j}_n)$ be the measurement pair selected by the random scheduling, and let j_i be the index of a randomly selected anchor from $\mathsf{N}_{\mathrm{b},i}$. We have

$$\mathbb{E}\{\mathrm{tr}\{\boldsymbol{\Upsilon}_{\mathsf{i}_n\mathsf{j}_n}\}\,|\,\mathbf{Q}\} \geq \mathbb{E}\{\mathrm{tr}\{\underline{\boldsymbol{\Upsilon}}_{\mathsf{i}_n\mathsf{j}_n}\}\,|\,\mathbf{Q}\} \tag{122a}$$

$$\geq \frac{1}{N_{\mathrm{a}}}\sum_{i=1}^{N_{\mathrm{a}}}\mathbb{E}\{\mathrm{tr}\{\underline{\boldsymbol{\Upsilon}}_{ij_i}\}\,|\,\mathbf{Q}\} \tag{122b}$$

$$\geq \frac{\zeta_{\mathrm{b}}}{2N_{\mathrm{a}}}\sum_{i=1}^{N_{\mathrm{a}}}\frac{\left(\mathrm{tr}\{\mathbf{Q}_{ii}\}\right)^2}{\mathrm{tr}\{\mathbf{Q}_{ii}\}+2\overline{\varepsilon}} \tag{122c}$$

$$\geq \frac{\zeta_{\mathrm{b}}\left(\mathrm{tr}\{\mathbf{Q}\}\right)^2}{2N_{\mathrm{a}}\left(\mathrm{tr}\{\mathbf{Q}\}+2N_{\mathrm{a}}\overline{\varepsilon}\right)} = g_2(\mathrm{tr}\{\mathbf{Q}\}) \tag{122d}$$

where (122a) is by Lemma 5, the inequality in (122b) follows the policy of random scheduling strategy by removing the cases of inter-node measurements between two agents, (122c) is by (33) and (120b), (122d) is by the Jensen's inequality, and $g_2(x)$ is given by (117). Therefore, the condition in Proposition 3 is satisfied with $\upsilon(\mathbf{Q}^{(n)}) = \mathrm{tr}\{\mathbf{Q}^{(n)}\}$ and $g = g_2$. Thus, (19) holds with B_N given by (21). Then by solving for g_2^{-1} from (117), we obtain (32).

APPENDIX IV
PROOF OF PROPOSITION 7

The main idea of the proof is to construct a converging matrix evolution that provides a lower bound for the error evolution (8). We first introduce a *reference evolution* $\{\boldsymbol{\Gamma}^{(n)}\}_{n\geq 1}$ with $\boldsymbol{\Gamma}^{(2)} = \underline{\delta}\,\boldsymbol{I}_{2N_\mathrm{a}}$, and let $\boldsymbol{\Gamma}_{ij}^{(n)}$ be the (i,j)th 2×2 block of $\boldsymbol{\Gamma}^{(n)}$. Recall that (i_n, j_n) is the selected measurement pair in $[t_n, t_{n+1})$. The reference evolution is described in the following. For $n \geq 2$,

- if $i_n, j_n \in \mathcal{N}_\mathrm{a}$, then $\boldsymbol{\Gamma}_{i_n i_n}^{(n+1)} = \boldsymbol{\Gamma}_{j_n j_n}^{(n+1)} = \underline{\delta}\,\boldsymbol{I}_2$, $\boldsymbol{\Gamma}_{i_n j_n}^{(n+1)} = \boldsymbol{\Gamma}_{j_n i_n}^{(n+1)} = \boldsymbol{O}_2$, and $\boldsymbol{\Gamma}_{ii}^{(n+1)} = \boldsymbol{\Gamma}_{ii}^{(n)} + \underline{\delta}\,\boldsymbol{I}_2$, $\forall\, i \neq i_n, j_n$;
- if $i_n \in \mathcal{N}_\mathrm{a}$ and $j_n \in \mathcal{N}_\mathrm{b}$, then $\boldsymbol{\Gamma}_{i_n i_n}^{(n+1)} = \underline{\delta}\,\boldsymbol{I}_2$ and $\boldsymbol{\Gamma}_{ii}^{(n+1)} = \boldsymbol{\Gamma}_{ii}^{(n)} + \underline{\delta}\,\boldsymbol{I}_2$, $\forall\, i \neq i_n$.

In the reference evolution, we have $\boldsymbol{\Gamma}^{(n)} = \mathrm{diag}\big\{\boldsymbol{\Gamma}_{11}^{(n)}, \boldsymbol{\Gamma}_{22}^{(n)}, \ldots, \boldsymbol{\Gamma}_{N_\mathrm{a}N_\mathrm{a}}^{(n)}\big\}$ for all $n \geq 2$. Also, the principal submatrices $\big\{\boldsymbol{\Gamma}_{ii}^{(n)}\big\}_{i=1}^{N_\mathrm{a}}$ can be ordered by $\succcurlyeq$ since they are multiples of $\underline{\delta}\,\boldsymbol{I}_2$.

Next, based on the reference evolution, we introduce the *one-step optimal scheduling* as follows. If $N_\mathrm{a} > 1$, then i_n and j_n are selected as the indices of two most positive semidefinite 2×2 principal submatrices of $\boldsymbol{\Gamma}^{(n)}$ (by $\boldsymbol{A}$ being more positive semidefinite than $\boldsymbol{B}$ we mean $\boldsymbol{A} \succcurlyeq \boldsymbol{B}$). If $N_\mathrm{a} = 1$, then $i_n = 1$ and j_n is randomly selected from $\mathcal{N}_\mathrm{b}$. Let $\{\underline{\boldsymbol{\Gamma}}^{(n)}\}_{n\geq 1}$ be the reference evolution for the one-step optimal scheduling. Note that if $N_\mathrm{a} = 1$, then $\underline{\boldsymbol{\Gamma}}^{(n)} = \boldsymbol{\Gamma}^{(n)}$ for all $n \geq 2$.

We now introduce a lemma that will be used in the proof.

Lemma 6: Let $\{\boldsymbol{Q}_\mathrm{I}^{(n)}\}$ and $\{\boldsymbol{Q}_\mathrm{II}^{(n)}\}$ be two error evolutions satisfying (8) with error increase matrices $\boldsymbol{\Delta}_\mathrm{I}^{(n+1)}$ and $\boldsymbol{\Delta}_\mathrm{II}^{(n+1)}$, respectively. For the same (i_n, j_n) and $\boldsymbol{p}_\mathrm{b}^{(n)}$ for all $n \geq 1$, if $\boldsymbol{Q}_\mathrm{I}^{(n_0)} \succcurlyeq \boldsymbol{Q}_\mathrm{II}^{(n_0)}$ for an $n_0 \geq 1$ and $\boldsymbol{\Delta}_\mathrm{I}^{(n+1)} \succcurlyeq \boldsymbol{\Delta}_\mathrm{II}^{(n+1)}$ for $n \geq n_0$, then $\boldsymbol{Q}_\mathrm{I}^{(n)} \succcurlyeq \boldsymbol{Q}_\mathrm{II}^{(n)}$ for all $n \geq n_0$.

Proof: Note that the recursive equation (8) can be equivalently expressed as (81). Suppose that $\boldsymbol{Q}_\mathrm{I}^{(n)} \succcurlyeq \boldsymbol{Q}_\mathrm{II}^{(n)}$ for an $n \geq n_0$. Then by (81) and the fact that $\boldsymbol{\Delta}_\mathrm{I}^{(n+1)} \succcurlyeq \boldsymbol{\Delta}_\mathrm{II}^{(n+1)}$, we have

$$\begin{aligned}\boldsymbol{Q}_\mathrm{I}^{(n+1)} &= \big([\boldsymbol{Q}_\mathrm{I}^{(n)}]^{-1} + \boldsymbol{C}_{i_n j_n}^{(n)}\big)^{-1} + \boldsymbol{\Delta}_\mathrm{I}^{(n+1)} \\ &\succcurlyeq \big([\boldsymbol{Q}_\mathrm{II}^{(n)}]^{-1} + \boldsymbol{C}_{i_n j_n}^{(n)}\big)^{-1} + \boldsymbol{\Delta}_\mathrm{II}^{(n+1)} = \boldsymbol{Q}_\mathrm{II}^{(n+1)}.\end{aligned}$$

Also, $\boldsymbol{Q}_\mathrm{I}^{(n_0)} \succcurlyeq \boldsymbol{Q}_\mathrm{II}^{(n_0)}$. By induction, $\boldsymbol{Q}_\mathrm{I}^{(n)} \succcurlyeq \boldsymbol{Q}_\mathrm{II}^{(n)}$ for all $n \geq n_0$. □

Now we begin to prove Proposition 7 via four steps:

1) prove that $\{\boldsymbol{\Gamma}^{(n)}\}$ provides a lower bound for $\{\boldsymbol{Q}^{(n)}\}$;
2) prove that $\{\underline{\boldsymbol{\Gamma}}^{(n)}\}$ provides a lower bound for $\{\boldsymbol{\Gamma}^{(n)}\}$;
3) prove the convergence of $\{\underline{\boldsymbol{\Gamma}}^{(n)}\}$; and
4) derive universal lower bound on NLE based on $\{\underline{\boldsymbol{\Gamma}}^{(n)}\}$.

A. $\{\boldsymbol{\Gamma}^{(n)}\}$ Provides Lower Bound for $\{\boldsymbol{Q}^{(n)}\}$

We start by proving the following lemma.

Lemma 7: Consider the error evolution $\{\boldsymbol{Q}^{(n)}\}_{n\geq 1}$ satisfying (8) and the reference evolution $\{\boldsymbol{\Gamma}^{(n)}\}_{n\geq 1}$. For the same sequence of selected measurement pairs $\{(i_n, j_n)\}_{n\geq 1}$, $\boldsymbol{Q}^{(n)} \succcurlyeq \boldsymbol{\Gamma}^{(n)}$ for all $n \geq 2$.

Proof: Suppose $\boldsymbol{Q}^{(n)} \succcurlyeq \boldsymbol{\Gamma}^{(n)}$ for an $n \geq 2$. Let

$$\widetilde{\boldsymbol{Q}}^{(n+1)} = \big([\boldsymbol{\Gamma}^{(n)}]^{-1} + \boldsymbol{C}_{i_n j_n}^{(n)}\big)^{-1} + \underline{\delta}\,\boldsymbol{I}_{2N_\mathrm{a}}.$$

Then by Lemma 6 with $\boldsymbol{\Delta}_\mathrm{I}^{(n+1)} = \boldsymbol{\Delta}_\mathrm{II}^{(n+1)} = \underline{\delta}\,\boldsymbol{I}_{2N_\mathrm{a}}$, we have

$$\boldsymbol{Q}^{(n+1)} = \big([\boldsymbol{Q}^{(n)}]^{-1} + \boldsymbol{C}_{i_n j_n}^{(n)}\big)^{-1} + \underline{\delta}\,\boldsymbol{I}_{2N_\mathrm{a}} \succcurlyeq \widetilde{\boldsymbol{Q}}^{(n+1)}.$$

Consider that $i_n, j_n \in \mathcal{N}_\mathrm{a}$. Then following the reference evolution, $\widetilde{\boldsymbol{Q}}^{(n+1)} - \boldsymbol{\Gamma}^{(n+1)}$ is a matrix with the same (i_n, i_n)th, (i_n, j_n)th, (j_n, i_n)th, and (j_n, j_n)th blocks as those of the matrix $\big([\boldsymbol{\Gamma}^{(n)}]^{-1} + \boldsymbol{C}_{i_n j_n}^{(n)}\big)^{-1}$, and zero blocks elsewhere. Since $\big([\boldsymbol{\Gamma}^{(n)}]^{-1} + \boldsymbol{C}_{i_n j_n}^{(n)}\big)^{-1}$ is positive definite, $\widetilde{\boldsymbol{Q}}^{(n+1)} - \boldsymbol{\Gamma}^{(n+1)}$ is positive semidefinite, i.e., $\widetilde{\boldsymbol{Q}}^{(n+1)} \succcurlyeq \boldsymbol{\Gamma}^{(n+1)}$. Thus, we have

$$\boldsymbol{Q}^{(n+1)} \succcurlyeq \widetilde{\boldsymbol{Q}}^{(n+1)} \succcurlyeq \boldsymbol{\Gamma}^{(n+1)}.$$

Following a similar argument, the above relationship also holds for $i_n \in \mathcal{N}_\mathrm{a}$ and $j_n \in \mathcal{N}_\mathrm{b}$. Moreover, we have $\boldsymbol{Q}^{(2)} \succcurlyeq \boldsymbol{\Delta}^{(2)} \succcurlyeq \underline{\delta}\,\boldsymbol{I}_{2N_\mathrm{a}} = \boldsymbol{\Gamma}^{(2)}$ according to (81). By induction, we have $\boldsymbol{Q}^{(n)} \succcurlyeq \boldsymbol{\Gamma}^{(n)}$ for all $n \geq 2$. □

B. $\{\underline{\boldsymbol{\Gamma}}^{(n)}\}$ Provides Lower Bound for $\{\boldsymbol{\Gamma}^{(n)}\}$

Let $\boldsymbol{\Gamma}_{(1)}^{(n)} \succcurlyeq \boldsymbol{\Gamma}_{(2)}^{(n)} \succcurlyeq \cdots \succcurlyeq \boldsymbol{\Gamma}_{(N_\mathrm{a})}^{(n)}$ and $\underline{\boldsymbol{\Gamma}}_{(1)}^{(n)} \succcurlyeq \underline{\boldsymbol{\Gamma}}_{(2)}^{(n)} \succcurlyeq \cdots \succcurlyeq \underline{\boldsymbol{\Gamma}}_{(N_\mathrm{a})}^{(n)}$ be the *ordered* 2×2 principal submatrices of $\boldsymbol{\Gamma}^{(n)}$ and $\underline{\boldsymbol{\Gamma}}^{(n)}$, respectively. Then we have the following result.

Lemma 8: For any sequence of selected measurement pairs $\{(i_n, j_n)\}_{n\geq 1}$, the reference evolution $\{\boldsymbol{\Gamma}^{(n)}\}_{n\geq 1}$ satisfies $\boldsymbol{\Gamma}_{(i)}^{(n)} \succcurlyeq \underline{\boldsymbol{\Gamma}}_{(i)}^{(n)}$ for all $i \in \mathcal{N}_\mathrm{a}$ and $n \geq 2$.

Proof: Suppose $\boldsymbol{\Gamma}_{(i)}^{(n)} \succcurlyeq \underline{\boldsymbol{\Gamma}}_{(i)}^{(n)}$ for all $i \in \mathcal{N}_\mathrm{a}$ and an $n \geq 2$. Starting from the matrix $\underline{\boldsymbol{\Gamma}}^{(n)}$, follow the reference evolution for one time interval with the selected measurement pair (i_n, j_n), and let $\widetilde{\boldsymbol{\Gamma}}$ be the resulting matrix with ordered 2×2 principal submatrices $\widetilde{\boldsymbol{\Gamma}}_{(1)} \succcurlyeq \widetilde{\boldsymbol{\Gamma}}_{(2)} \succcurlyeq \cdots \succcurlyeq \widetilde{\boldsymbol{\Gamma}}_{(N_\mathrm{a})}$.

Then, by following the update rules in the reference evolution and using the hypothesis $\boldsymbol{\Gamma}_{(i)}^{(n)} \succcurlyeq \underline{\boldsymbol{\Gamma}}_{(i)}^{(n)}$ for all $i \in \mathcal{N}_\mathrm{a}$, we have $\boldsymbol{\Gamma}_{(i)}^{(n+1)} \succcurlyeq \widetilde{\boldsymbol{\Gamma}}_{(i)}$ for all $i \in \mathcal{N}_\mathrm{a}$. Furthermore, following the policy of the one-step optimal scheduling, we have $\widetilde{\boldsymbol{\Gamma}}_{(i)} \succcurlyeq \underline{\boldsymbol{\Gamma}}_{(i)}^{(n+1)}$ for all $i \in \mathcal{N}_\mathrm{a}$. Thus, $\boldsymbol{\Gamma}_{(i)}^{(n+1)} \succcurlyeq \widetilde{\boldsymbol{\Gamma}}_{(i)} \succcurlyeq \underline{\boldsymbol{\Gamma}}_{(i)}^{(n+1)}$ for all $i \in \mathcal{N}_\mathrm{a}$. We also have $\boldsymbol{\Gamma}_{(i)}^{(2)} = \underline{\boldsymbol{\Gamma}}_{(i)}^{(2)} = \underline{\delta}\,\boldsymbol{I}_2$ for all $i \in \mathcal{N}_\mathrm{a}$. Then by induction, we have $\boldsymbol{\Gamma}_{(i)}^{(n)} \succcurlyeq \underline{\boldsymbol{\Gamma}}_{(i)}^{(n)}$ for all $i \in \mathcal{N}_\mathrm{a}$ and $n \geq 2$. □

C. Convergence of $\{\underline{\boldsymbol{\Gamma}}^{(n)}\}$

Following the reference evolution for the one-step optimal scheduling,

- if N_a is even, then for $n \geq N_\mathrm{a}/2+1$, the ordered principal submatrices of $\underline{\boldsymbol{\Gamma}}^{(n)}$ are

$$\frac{N_\mathrm{a}\underline{\delta}}{2}\boldsymbol{I}_2,\ \frac{N_\mathrm{a}\underline{\delta}}{2}\boldsymbol{I}_2,\ \frac{(N_\mathrm{a}-2)\underline{\delta}}{2}\boldsymbol{I}_2,\ \frac{(N_\mathrm{a}-2)\underline{\delta}}{2}\boldsymbol{I}_2,\ \ldots,\ \underline{\delta}\,\boldsymbol{I}_2,\ \underline{\delta}\,\boldsymbol{I}_2 \quad (123)$$

- if $N_{\rm a}$ is odd, then for $n \geq (N_{\rm a}+1)/2+1$, the ordered principal submatrices of $\underline{\boldsymbol{\Gamma}}^{(n)}$ are

$$\frac{(N_{\rm a}+1)\underline{\delta}}{2}\boldsymbol{I}_2,\ \frac{(N_{\rm a}-1)\underline{\delta}}{2}\boldsymbol{I}_2,\ \frac{(N_{\rm a}-1)\underline{\delta}}{2}\boldsymbol{I}_2,\ \frac{(N_{\rm a}-3)\underline{\delta}}{2}\boldsymbol{I}_2,\ \frac{(N_{\rm a}-3)\underline{\delta}}{2}\boldsymbol{I}_2,\ \ldots,\ \underline{\delta}\,\boldsymbol{I}_2,\ \underline{\delta}\,\boldsymbol{I}_2. \tag{124}$$

From (123) and (124), we have

$$\mathrm{tr}\{\underline{\boldsymbol{\Gamma}}^{(n)}\} = \begin{cases} \left(\frac{N_{\rm a}^2}{2}+N_{\rm a}\right)\underline{\delta}\,, & \forall\, n \geq \frac{N_{\rm a}}{2}+1,\ N_{\rm a} \text{ is even} \\ \frac{1}{2}(N_{\rm a}+1)^2\underline{\delta}\,, & \forall\, n \geq \frac{N_{\rm a}+1}{2}+1,\ N_{\rm a} \text{ is odd.} \end{cases}$$

Thus,

$$\mathrm{tr}\{\underline{\boldsymbol{\Gamma}}^{(n)}\} \geq \left(\frac{N_{\rm a}^2}{2}+N_{\rm a}\right)\underline{\delta}\,, \quad \forall\, n \geq \left\lceil \frac{N_{\rm a}}{2} \right\rceil + 1. \tag{125}$$

D. Universal Lower Bound on NLE

For any sequence of selected measurement pairs $\{(i_n, j_n)\}$, we have $\mathrm{tr}\{\boldsymbol{Q}^{(n)}\} \geq \mathrm{tr}\{\boldsymbol{\Gamma}^{(n)}\}$ for all $n \geq 2$ by Lemma 7, and $\mathrm{tr}\{\boldsymbol{\Gamma}^{(n)}\} \geq \mathrm{tr}\{\underline{\boldsymbol{\Gamma}}^{(n)}\}$ for all $n \geq 2$ by Lemma 8. These results imply that $\mathrm{tr}\{\boldsymbol{Q}^{(n)}\} \geq \mathrm{tr}\{\underline{\boldsymbol{\Gamma}}^{(n)}\}$ for all $n \geq 2$, which together with (125) leads to (41).

APPENDIX V
PROOFS OF RESULTS IN SECTION VI

A. Proof of Proposition 9

Following (44), we have

$$\breve{\boldsymbol{Q}}^{(2)} = \breve{\boldsymbol{Q}}^{(1)} - \breve{\boldsymbol{\Upsilon}}^{(1)}_{i_1 j_1} + \breve{\boldsymbol{\Delta}}^{(2)}. \tag{126}$$

By (46), (47), (4a), and (7), following the definitions of $\breve{\varphi}^{(m)}_{i_m j_m}$, $\breve{\varepsilon}^{(m)}_{i_m j_m}$, and $\breve{\boldsymbol{\Delta}}^{(m)}$, and by applying the matrix inversion lemma [85] (for the non-Bayesian case), we have

$$\breve{\boldsymbol{Q}}^{(2)} = \left([\breve{\boldsymbol{Q}}^{(1)}]^{-1} + \boldsymbol{C}^{(1)}_{i_{1,1} j_{1,1}}\right)^{-1}.$$

Similarly, we have

$$\begin{aligned}\breve{\boldsymbol{Q}}^{(3)} &= \left([\breve{\boldsymbol{Q}}^{(2)}]^{-1} + \boldsymbol{C}^{(1)}_{i_{1,2} j_{1,2}}\right)^{-1} \\ &= \left([\breve{\boldsymbol{Q}}^{(1)}]^{-1} + \boldsymbol{C}^{(1)}_{i_{1,1} j_{1,1}} + \boldsymbol{C}^{(1)}_{i_{1,2} j_{1,2}}\right)^{-1}.\end{aligned}$$

Following this procedure and using (45), we have

$$\breve{\boldsymbol{Q}}^{(L+1)} = \left([\breve{\boldsymbol{Q}}^{(1)}]^{-1} + \sum\nolimits_{l=1}^{L} \boldsymbol{C}^{(1)}_{i_{1,l} j_{1,l}}\right)^{-1} + \boldsymbol{\Delta}^{(2)}. \tag{127}$$

Since $\breve{\boldsymbol{Q}}^{(1)} = \boldsymbol{Q}^{(1)}$, we have $\breve{\boldsymbol{Q}}^{(L+1)} = \boldsymbol{Q}^{(2)}$ by (127) and (43). Following similar argument as above, we have $\breve{\boldsymbol{Q}}^{(m)} = \boldsymbol{Q}^{(n)}$ for $m = (n-1)L+1$ and $n \geq 1$.

B. Proof of Proposition 11

Following derivations similar to those in Appendix III and using (48), we can show that the expected error reduction can be lower bounded as

$$\mathbb{E}\{\mathrm{tr}\{\breve{\boldsymbol{\Upsilon}}_{\mathsf{i}_m \mathsf{j}_m}\} \,|\, \breve{\mathbf{Q}}\} \geq \frac{\zeta_{\rm b}\left(\mathrm{tr}\{\breve{\mathbf{Q}}_{\mathsf{i}^\star_m \mathsf{i}^\star_m}\}\right)^2}{2\left(\mathrm{tr}\{\breve{\mathbf{Q}}_{\mathsf{i}^\star_m \mathsf{i}^\star_m}\} + 2\overline{\varepsilon}_L\right)}$$

for the opportunistic scheduling strategy and

$$\mathbb{E}\{\mathrm{tr}\{\breve{\boldsymbol{\Upsilon}}_{\mathsf{i}_m \mathsf{j}_m}\} \,|\, \breve{\mathbf{Q}}\} \geq \frac{\zeta_{\rm b}(\mathrm{tr}\{\breve{\mathbf{Q}}\})^2}{2N_{\rm a}(\mathrm{tr}\{\breve{\mathbf{Q}}\} + 2N_{\rm a}\overline{\varepsilon}_L)}$$

TABLE II
ORDERED 2×2 PRINCIPAL SUBMATRICES OF $\{\underline{\boldsymbol{\Gamma}}^{(m)}\}$

$m=1$	$m=2$	$m=3$	$m=4$	$m=5$	$m=6$	$\cdots$
$\boldsymbol{O}_2$	$\boldsymbol{O}_2$	$\underline{\delta}\,\boldsymbol{I}_2$	$\underline{\delta}\,\boldsymbol{I}_2$	$\underline{\delta}\,\boldsymbol{I}_2$	$\underline{\delta}\,\boldsymbol{I}_2$	$\cdots$
$\boldsymbol{O}_2$	$\boldsymbol{O}_2$	$\underline{\delta}\,\boldsymbol{I}_2$	$\underline{\delta}\,\boldsymbol{I}_2$	$\underline{\delta}\,\boldsymbol{I}_2$	$\underline{\delta}\,\boldsymbol{I}_2$	$\cdots$
$\boldsymbol{O}_2$	$\boldsymbol{O}_2$	$\underline{\delta}\,\boldsymbol{I}_2$	$\boldsymbol{O}_2$	$\underline{\delta}\,\boldsymbol{I}_2$	$\boldsymbol{O}_2$	$\cdots$
$\boldsymbol{O}_2$	$\boldsymbol{O}_2$	$\underline{\delta}\,\boldsymbol{I}_2$	$\boldsymbol{O}_2$	$\underline{\delta}\,\boldsymbol{I}_2$	$\boldsymbol{O}_2$	$\cdots$

for the random scheduling strategy, which together with Proposition 10 with $\upsilon(\breve{\mathbf{Q}}^{(m)}) = \mathrm{tr}\{\breve{\mathbf{Q}}^{(m)}_{\mathsf{i}^\star_n \mathsf{i}^\star_n}\}$ and $\upsilon(\breve{\mathbf{Q}}^{(m)}) = \mathrm{tr}\{\breve{\mathbf{Q}}^{(m)}\}$ lead to (54) and (53), respectively.

C. Proof of Proposition 12

The proof is similar to that in Appendix IV, and a sketch is provided here. We first modify the reference evolution provided in Appendix IV as follows. Let $\boldsymbol{\Gamma}^{(1)} = \boldsymbol{O}_{2N_{\rm a}}$. For $m = kL$ with $k \geq 1$,

- if $i_m, j_m \in \mathcal{N}_{\rm a}$, then $\boldsymbol{\Gamma}^{(m+1)}_{i_m i_m} = \boldsymbol{\Gamma}^{(m+1)}_{j_m j_m} = \underline{\delta}\,\boldsymbol{I}_2$, $\boldsymbol{\Gamma}^{(m+1)}_{i_m j_m} = \boldsymbol{\Gamma}^{(m+1)}_{j_m i_m} = \boldsymbol{O}_2$, and $\boldsymbol{\Gamma}^{(m+1)}_{ii} = \boldsymbol{\Gamma}^{(m)}_{ii} + \underline{\delta}\,\boldsymbol{I}_2$, $\forall\, i \neq i_m, j_m$;
- if $i_m \in \mathcal{N}_{\rm a}$ and $j_m \in \mathcal{N}_{\rm b}$, then $\boldsymbol{\Gamma}^{(m+1)}_{i_m i_m} = \underline{\delta}\,\boldsymbol{I}_2$ and $\boldsymbol{\Gamma}^{(m+1)}_{ii} = \boldsymbol{\Gamma}^{(m)}_{ii} + \underline{\delta}\,\boldsymbol{I}_2$, $\forall\, i \neq i_m$.

For other $m \geq 1$,

- if $i_m, j_m \in \mathcal{N}_{\rm a}$, then $\boldsymbol{\Gamma}^{(m+1)}_{i_m i_m} = \boldsymbol{\Gamma}^{(m+1)}_{j_m j_m} = \boldsymbol{\Gamma}^{(m+1)}_{i_m j_m} = \boldsymbol{\Gamma}^{(m+1)}_{j_m i_m} = \boldsymbol{O}_2$, and $\boldsymbol{\Gamma}^{(m+1)}_{ii} = \boldsymbol{\Gamma}^{(m)}_{ii}$, $\forall\, i \neq i_m, j_m$;
- if $i_m \in \mathcal{N}_{\rm a}$ and $j_m \in \mathcal{N}_{\rm b}$, then $\boldsymbol{\Gamma}^{(m+1)}_{i_m i_m} = \boldsymbol{O}_2$ and $\boldsymbol{\Gamma}^{(m+1)}_{ii} = \boldsymbol{\Gamma}^{(m)}_{ii}$, $\forall\, i \neq i_m$.

Next, let $\{\underline{\boldsymbol{\Gamma}}^{(m)}\}_{m\geq 1}$ be the reference evolution for the one-step optimal scheduling introduced in Appendix IV. Following arguments similar to those in Appendix IV, we have $\mathrm{tr}\{\underline{\boldsymbol{\Gamma}}^{(m)}\} \leq \mathrm{tr}\{\boldsymbol{\Gamma}^{(m)}\} \leq \mathrm{tr}\{\breve{\boldsymbol{Q}}^{(m)}\}$ for all $m \geq 2$ and all sequences of selected measurement pairs $\{i_m, j_m\}_{m\geq 1}$. Furthermore, following the update rules in the reference evolution and the policy of the one-step optimal scheduling, $\{\mathrm{tr}\{\underline{\boldsymbol{\Gamma}}^{(m)}\}\}_{m\geq 1}$ becomes a periodic sequence with period L after finite number of steps, which leads to the lower bound in Proposition 12.

The reason that $\{\mathrm{tr}\{\underline{\boldsymbol{\Gamma}}^{(m)}\}\}_{m\geq 1}$ converges to a periodic sequence with period L is that the update rule in the above reference evolution for $m = kL$ with $k \geq 1$ is different from that for other $m \geq 1$. For example, the ordered 2×2 principal submatrices of $\{\underline{\boldsymbol{\Gamma}}^{(m)}\}_{m\geq 1}$ for $N_{\rm a} = 4$ and $L = 2$ are shown in Table II. Starting from $m = 3$, the sequence of the ordered 2×2 principal submatrices become periodic with period 2. Thus, $\{\mathrm{tr}\{\underline{\boldsymbol{\Gamma}}^{(m)}\}\}_{m\geq 1}$ converges to a periodic sequence with period 2.

ACKNOWLEDGMENT

The authors wish to thank W. Dai, G. C. Ferrante, Z. Liu, M. Mohammadkarimi, N. Tadayon, S. Bartoletti, and L. Ruan for their helpful suggestions and careful reading of the manuscript.

REFERENCES

[1] M. Z. Win *et al.*, "Network localization and navigation via cooperation," *IEEE Commun. Mag.*, vol. 49, no. 5, pp. 56–62, May 2011.

[2] K. Pahlavan, X. Li, and J.-P. Makela, "Indoor geolocation science and technology," *IEEE Commun. Mag.*, vol. 40, no. 2, pp. 112–118, Feb. 2002.

[3] S. Gezici *et al.*, "Localization via ultra-wideband radios: A look at positioning aspects for future sensor networks," *IEEE Signal Process. Mag.*, vol. 22, no. 4, pp. 70–84, Jul. 2005.

[4] Y. Shen, S. Mazuelas, and M. Z. Win, "Network navigation: Theory and interpretation," *IEEE J. Sel. Areas Commun.*, vol. 30, no. 9, pp. 1823–1834, Oct. 2012.

[5] R. Niu and P. K. Varshney, "Target location estimation in sensor networks with quantized data," *IEEE Trans. Signal Process.*, vol. 54, no. 12, pp. 4519–4528, Dec. 2006.

[6] R. Niu, R. S. Blum, P. K. Varshney, and A. L. Drozd, "Target localization and tracking in noncoherent multiple-input multiple-output radar systems," *IEEE Trans. Aerosp. Electron. Syst.*, vol. 48, no. 2, pp. 1466–1489, Apr. 2012.

[7] N. Patwari, J. N. Ash, S. Kyperountas, A. O. Hero, R. L. Moses, and N. S. Correal, "Locating the nodes: Cooperative localization in wireless sensor networks," *IEEE Signal Process. Mag.*, vol. 22, no. 4, pp. 54–69, Jul. 2005.

[8] N. Atanasov, R. Tron, V. M. Preciado, and G. J. Pappas, "Joint estimation and localization in sensor networks," in *Proc. IEEE Conf. Decision Control*, Los Angeles, CA, USA, Dec. 2014, pp. 6875–6882.

[9] M. W. M. G. Dissanayake, P. Newman, S. Clark, H. F. Durrant-Whyte, and M. Csorba, "A solution to the simultaneous localization and map building (SLAM) problem," *IEEE Trans. Robot. Autom.*, vol. 17, no. 3, pp. 229–241, Jun. 2001.

[10] G. Cardone *et al.*, "Fostering participAction in smart cities: A geo-social crowdsensing platform," *IEEE Commun. Mag.*, vol. 51, no. 6, pp. 112–119, Jun. 2013.

[11] X. Wang, S. Yuan, R. Laur, and W. Lang, "Dynamic localization based on spatial reasoning with RSSI in wireless sensor networks for transport logistics," *Sens. Actuators A, Phys.*, vol. 171, no. 2, pp. 421–428, Nov. 2011.

[12] S. M. George *et al.*, "Distressnet: A wireless ad hoc and sensor network architecture for situation management in disaster response," *IEEE Commun. Mag.*, vol. 48, no. 3, pp. 128–136, Mar. 2010.

[13] F. Zabini and A. Conti, "Inhomogeneous Poisson sampling of finite-energy signals with uncertainties in $\mathbb{R}^d$," *IEEE Trans. Signal Process.*, vol. 64, no. 18, pp. 4679–4694, Sep. 2016.

[14] L. Evans, "Maps as deep: Reading the code of location-based social networks," *IEEE Technol. Soc. Mag.*, vol. 33, no. 1, pp. 73–80, Mar. 2014.

[15] J. Ko, T. Gao, R. Rothman, and A. Terzis, "Wireless sensing systems in clinical environments: Improving the efficiency of the patient monitoring process," *IEEE Eng. Med. Biol. Mag.*, vol. 29, no. 2, pp. 103–109, Mar./Apr. 2010.

[16] D. Dardari, A. Conti, C. Buratti, and R. Verdone, "Mathematical evaluation of environmental monitoring estimation error through energy-efficient wireless sensor networks," *IEEE Trans. Mobile Comput.*, vol. 6, no. 7, pp. 790–802, Jul. 2007.

[17] J. A. Costa, N. Patwari, and A. O. Hero, III, "Distributed weighted-multidimensional scaling for node localization in sensor networks," *ACM Trans. Sensor Netw.*, vol. 2, no. 1, pp. 39–64, Feb. 2006.

[18] B. Song and A. K. Roy-Chowdhury, "Robust tracking in a camera network: A multi-objective optimization framework," *IEEE J. Sel. Topics Signal Process.*, vol. 2, no. 4, pp. 582–596, Aug. 2008.

[19] R. Verdone, D. Dardari, G. Mazzini, and A. Conti, *Wireless Sensor and Actuator Networks: Technologies, Analysis and Design*. Amsterdam, The Netherlands: Elsevier, 2008.

[20] H. Wymeersch, J. Lien, and M. Z. Win, "Cooperative localization in wireless networks," *Proc. IEEE*, vol. 97, no. 2, pp. 427–450, Feb. 2009.

[21] S. Kumar, C. Micheloni, C. Piciarelli, and G. L. Foresti, "Stereo localization based on network's uncalibrated camera pairs," in *Proc. IEEE Int. Conf. Adv. Video Signal Based Surveill.*, Genoa, Italy, Sep. 2009, pp. 502–507.

[22] S. Bi, A. T. Kamal, C. Soto, C. Ding, J. A. Farrell, and A. K. Roy-Chowdhury, "Tracking and activity recognition through consensus in distributed camera networks," *IEEE Trans. Image Process.*, vol. 19, no. 10, pp. 2564–2579, Oct. 2010.

[23] Y. Shen and M. Z. Win, "Fundamental limits of wideband localization—Part I: A general framework," *IEEE Trans. Inf. Theory*, vol. 56, no. 10, pp. 4956–4980, Oct. 2010.

[24] T. Ali, A. Z. Sadeque, M. Saquib, and M. Ali, "MIMO radar for target detection and localization in sensor networks," *IEEE Syst. J.*, vol. 8, no. 1, pp. 75–82, Mar. 2014.

[25] T. Wang, Y. Shen, S. Mazuelas, H. Shin, and M. Z. Win, "On OFDM ranging accuracy in multipath channels," *IEEE Syst. J.*, vol. 8, no. 1, pp. 104–114, Mar. 2014.

[26] L. Lu, H. Zhang, and H.-C. Wu, "Novel energy-based localization technique for multiple sources," *IEEE Syst. J.*, vol. 8, no. 1, pp. 142–150, Mar. 2014.

[27] K. Yan, H.-C. Wu, and S. S. Iyengar, "Robustness analysis and new hybrid algorithm of wideband source localization for acoustic sensor networks," *IEEE Trans. Wireless Commun.*, vol. 9, no. 6, pp. 2033–2043, Jun. 2010.

[28] L. Lu and H.-C. Wu, "Novel robust direction-of-arrival-based source localization algorithm for wideband signals," *IEEE Trans. Wireless Commun.*, vol. 11, no. 11, pp. 3850–3859, Nov. 2012.

[29] Y. Luo and C. L. Law, "Indoor positioning using UWB-IR signals in the presence of dense multipath with path overlapping," *IEEE Trans. Wireless Commun.*, vol. 11, no. 10, pp. 3734–3743, Oct. 2012.

[30] J. Xu, M. Ma, and C. L. Law, "Performance of time-difference-of-arrival ultra wideband indoor localisation," *IET Sci., Meas. Technol.*, vol. 5, no. 2, pp. 46–53, Mar. 2011.

[31] S. Bartoletti, W. Dai, A. Conti, and M. Z. Win, "A mathematical model for wideband ranging," *IEEE J. Sel. Topics Signal Process.*, vol. 9, no. 2, pp. 216–228, Mar. 2015.

[32] S. Mazuelas, R. M. Lorenzo, A. Bahillo, P. Fernandez, J. Prieto, and E. J. Abril, "Topology assessment provided by weighted barycentric parameters in harsh environment wireless location systems," *IEEE Trans. Signal Process.*, vol. 58, no. 7, pp. 3842–3857, Jul. 2010.

[33] B. Sinopoli, L. Schenato, M. Franceschetti, K. Poolla, M. I. Jordan, and S. S. Sastry, "Kalman filtering with intermittent observations," *IEEE Trans. Autom. Control*, vol. 49, no. 9, pp. 1453–1464, Sep. 2004.

[34] V. Gupta, T. H. Chung, B. Hassibi, and R. M. Murray, "On a stochastic sensor selection algorithm with applications in sensor scheduling and sensor coverage," *Automatica*, vol. 42, no. 2, pp. 251–260, 2006.

[35] L. Shi, M. Epstein, B. Sinopoli, and R. M. Murray, "Effective sensor scheduling schemes in a sensor network by employing feedback in the communication loop," in *Proc. IEEE Int. Conf. Control Appl.*, Singapore, Oct. 2007, pp. 1006–1011.

[36] D. Dardari, A. Conti, U. Ferner, A. Giorgetti, and M. Z. Win, "Ranging with ultrawide bandwidth signals in multipath environments," *Proc. IEEE*, vol. 97, no. 2, pp. 404–426, Feb. 2009.

[37] A. Rabbachin, I. Oppermann, and B. Denis, "GML ToA estimation based on low complexity UWB energy detection," in *Proc. PIMRC*, Helsinki, Finland, Sep. 2006, pp. 1–5.

[38] K. Yu, J.-P. Montillet, A. Rabbachin, P. Cheong, and I. Oppermann, "UWB location and tracking for wireless embedded networks," *Signal Process.*, vol. 86, no. 9, pp. 2153–2171, Sep. 2006.

[39] L. Mailaender, "On the geolocation bounds for round-trip time-of-arrival and all non-line-of-sight channels," *EURASIP J. Adv. Signal Process.*, vol. 2008, pp. 1–10, Jan. 2008.

[40] A. I. Mourikis and S. I. Roumeliotis, "Performance analysis of multirobot cooperative localization," *IEEE Trans. Robot.*, vol. 22, no. 4, pp. 666–681, Aug. 2006.

[41] S. Bartoletti, A. Giorgetti, M. Z. Win, and A. Conti, "Blind selection of representative observations for sensor radar networks," *IEEE Trans. Veh. Technol.*, vol. 64, no. 4, pp. 1388–1400, Apr. 2015.

[42] E. Masazade, R. Niu, and P. K. Varshney, "Dynamic bit allocation for object tracking in wireless sensor networks," *IEEE Trans. Signal Process.*, vol. 60, no. 10, pp. 5048–5063, Oct. 2012.

[43] A. Conti, M. Guerra, D. Dardari, N. Decarli, and M. Z. Win, "Network experimentation for cooperative localization," *IEEE J. Sel. Areas Commun.*, vol. 30, no. 2, pp. 467–475, Feb. 2012.

[44] X. Shen and P. K. Varshney, "Sensor selection based on generalized information gain for target tracking in large sensor networks," *IEEE Trans. Signal Process.*, vol. 62, no. 2, pp. 363–375, Jan. 2014.

[45] T. Wang, Y. Shen, S. Mazuelas, and M. Z. Win, "Distributed scheduling for cooperative localization based on information evolution," in *Proc. IEEE Int. Conf. Commun.*, Ottawa, ON, Canada, Jun. 2012, pp. 576–580.

[46] M. J. D. Rendas and J. M. F. Moura, "Cramér–Rao bound for location systems in multipath environments," *IEEE Trans. Signal Process.*, vol. 39, no. 12, pp. 2593–2610, Dec. 1991.

[47] U. A. Khan, S. Kar, and J. M. F. Moura, "Distributed sensor localization in random environments using minimal number of anchor nodes," *IEEE Trans. Signal Process.*, vol. 57, no. 5, pp. 2000–2016, May 2009.

[48] U. A. Khan, S. Kar, and J. M. F. Moura, "DILAND: An algorithm for distributed sensor localization with noisy distance measurements," *IEEE Trans. Signal Process.*, vol. 58, no. 3, pp. 1940–1947, Mar. 2010.
[49] J. Chen, W. Dai, Y. Shen, V. K. Lau, and M. Z. Win, "Resource management games for distributed network localization," *IEEE J. Sel. Areas Commun.*, vol. 35, no. 2, pp. 317–329, Feb. 2017.
[50] W. Dai, Y. Shen, and M. Z. Win, "A computational geometry framework for efficient network localization," *IEEE Trans. Inf. Theory*, to be published.
[51] K. You and L. Xie, "Kalman filtering with scheduled measurements," *IEEE Trans. Signal Process.*, vol. 61, no. 6, pp. 1520–1530, Mar. 2013.
[52] C. Soto, B. Song, and A. K. Roy-Chowdhury, "Distributed multi-target tracking in a self-configuring camera network," in *Proc. IEEE Conf. Comput. Vis. Pattern Recognit.*, Miami, FL, USA, Jun. 2009, pp. 1486–1493.
[53] G. E. Garcia, L. S. Muppirisetty, and H. Wymeersch, "On the trade-off between accuracy and delay in cooperative UWB navigation," in *Proc. IEEE Wireless Commun. Netw. Conf.*, Shanghai, China, Apr. 2013, pp. 1603–1608.
[54] S. Dwivedi, D. Zachariah, A. De Angelis, and P. Handel, "Cooperative decentralized localization using scheduled wireless transmissions," *IEEE Commun. Lett.*, vol. 17, no. 6, pp. 1240–1243, Jun. 2013.
[55] J. Gribben, A. Boukerche, and R. W. N. Pazzi, "Scheduling for scalable energy-efficient localization in mobile ad hoc networks," in *Proc. IEEE Conf. Sensor Mesh Ad Hoc Commun. Netw.*, Boston, MA, USA, Jun. 2010, pp. 1–9.
[56] Z. Zhao, R. Zhang, X. Cheng, L. Yang, and B. Jiao, "Network formation games for the link selection of cooperative localization in wireless networks," in *Proc. IEEE Int. Conf. Commun.*, Sydney, NSW, Australia, Jun. 2014, pp. 4577–4582.
[57] L. Tassiulas and A. Ephremides, "Stability properties of constrained queueing systems and scheduling policies for maximum throughput in multihop radio networks," *IEEE Trans. Autom. Control*, vol. 37, no. 12, pp. 1936–1948, Dec. 1992.
[58] L. Georgiadis, M. J. Neely, and L. Tassiulas, *Resource Allocation and Cross-Layer Control in Wireless Networks*. Hanover, MA, USA: NOW, 2006.
[59] M. J. Neely, "Order optimal delay for opportunistic scheduling in multi-user wireless uplinks and downlinks," *IEEE/ACM Trans. Netw.*, vol. 16, no. 5, pp. 1188–1199, Oct. 2008.
[60] H. L. Van Trees, *Detection, Estimation and Modulation Theory, Part 1*. New York, NY, USA: Wiley, 1968.
[61] A. Catovic and Z. Sahinoglu, "The Cramér–Rao bounds of hybrid TOA/RSS and TDOA/RSS location estimaion schemes," *IEEE Commun. Lett.*, vol. 8, no. 10, pp. 626–628, Oct. 2004.
[62] C. Chang and A. Sahai, "Cramér–Rao-type bounds for localization," *EURASIP J. Appl. Signal Process.*, vol. 2006, pp. 1–13, 2006.
[63] A. N. D'Andrea, U. Mengali, and R. Reggiannini, "The modified Cramér–Rao bound and its application to synchronization problems," *IEEE Trans. Commun.*, vol. 42, no. 234, pp. 1391–1399, Feb./Apr. 1994.
[64] P. Tichavsky, C. H. Muravchik, and A. Nehorai, "Posterior Cramér–Rao bounds for discrete-time nonlinear filtering," *IEEE Trans. Signal Process.*, vol. 46, no. 5, pp. 1386–1396, May 1998.
[65] A. Conti, M. Z. Win, M. Chiani, and J. H. Winters, "Bit error outage for diversity reception in shadowing environment," *IEEE Commun. Lett.*, vol. 7, no. 1, pp. 15–17, Jan. 2003.
[66] P. Mary, M. Dohler, J.-M. Gorce, G. Villemaud, and M. Arndt, "BPSK bit error outage over Nakagami-m fading channels in lognormal shadowing environments," *IEEE Commun. Lett.*, vol. 11, no. 7, pp. 565–567, Jul. 2007.
[67] A. Conti, W. M. Gifford, M. Z. Win, and M. Chiani, "Optimized simple bounds for diversity systems," *IEEE Trans. Commun.*, vol. 57, no. 9, pp. 2674–2685, Sep. 2009.
[68] *P410 RCM Product Brochure*, Time Domain Corp., Huntsville, AL, USA. [Online]. Available: http://www.timedomain.com/datasheets/TD_DS_P410_RCM_FA.pdf
[69] R. E. Kalman, "A new approach to linear filtering and prediction problems," *Trans. ASME J. Basic Eng.*, vol. 82, no. 1, pp. 34–45, 1960.
[70] T. Kailath, "A view of three decades of linear filtering theory," *IEEE Trans. Inf. Theory*, vol. 20, no. 2, pp. 146–181, Mar. 1974.
[71] R. E. Kalman, P. L. Falb, and M. A. Arbib, *Topics in Mathematical System Theory*. New York, NY, USA: McGraw-Hill, 1969.
[72] T. Kailath, *Lectures on Wiener and Kalman Filtering*. New York, NY, USA: Springer-Verlag, 1981.
[73] T. Kailath, A. H. Sayed, and B. Hassibi, *Linear Estimation* (Information and System Sciences Series). Upper Saddle River, NJ, USA: Prentice-Hall, 2000.
[74] D. P. Bertsekas, *Dynamic Programming and Optimal Control*, vol. 1. Belmont, MA, USA: Athena Scientific, 2001.
[75] J. F. Kingman, *Poisson Processes*. London, U.K.: Oxford Univ. Press, 1993.
[76] F. Baccelli and B. Błaszczyszyn, *Stochastic Geometry and Wireless Networks, Theory* (Foundations and Trends in Networking), vol. 1. Norwell, MA, USA: NOW, 2009.
[77] M. Z. Win, P. C. Pinto, and L. A. Shepp, "A mathematical theory of network interference and its applications," *Proc. IEEE*, vol. 97, no. 2, pp. 205–230, Feb. 2009.
[78] A. Rabbachin, T. Q. S. Quek, H. Shin, and M. Z. Win, "Cognitive network interference," *IEEE J. Sel. Areas Commun.*, vol. 29, no. 2, pp. 480–493, Feb. 2011.
[79] H. Takagi and L. Kleinrock, "Optimal transmission ranges for randomly distributed packet radio terminals," *IEEE Trans. Commun.*, vol. 32, no. 3, pp. 246–257, May 1984.
[80] E. S. Sousa, "Performance of a spread spectrum packet radio network link in a Poisson field of interferers," *IEEE Trans. Inf. Theory*, vol. 38, no. 6, pp. 1743–1754, Nov. 1992.
[81] A. Rabbachin, A. Conti, and M. Z. Win, "Wireless network intrinsic secrecy," *IEEE/ACM Trans. Netw.*, vol. 23, no. 1, pp. 56–69, Feb. 2015.
[82] A. F. Molisch *et al.*, "A comprehensive standardized model for ultrawideband propagation channels," *IEEE Trans. Antennas Propag.*, vol. 54, no. 11, pp. 3151–3166, Nov. 2006.
[83] D. Tse and P. Viswanath, *Fundamentals of Wireless Communication*. Cambridge, U.K.: Cambridge Univ. Press, 2005.
[84] R. A. Horn and C. R. Johnson, *Matrix Analysis*. New York, NY, USA: Cambridge Univ. Press, 1999.
[85] H. V. Henderson and S. R. Searle, "On deriving the inverse of a sum of matrices," *SIAM Rev.*, vol. 23, no. 1, pp. 53–60, Jan. 1981.
[86] T. Groves and T. Rothenberg, "A note on the expected value of an inverse matrix," *Biometrika*, vol. 56, no. 3, pp. 690–691, Dec. 1969.

Tianheng Wang (S'07) received his B.E. degree in 2007 and M.S. degree in 2010, both in electrical engineering from Tsinghua University, China.

Since August 2010, he has been with theWireless Information and Network Sciences Laboratory at the Massachusetts Institute of Technology (MIT), where he is now a PhD candidate. His research interests include wireless communication and localization, network scheduling, statistical inference, and machine learning. Currently he is working on the performance analysis and strategy design for wireless localization and navigation systems.

Mr. Wang served as a reviewer for IEEE TRANSACTIONS ON WIRELESS COMMUNICATIONS, IEEE TRANSACTIONS ON AUTOMATIC CONTROL, and IEEE COMMUNICATIONS LETTERS. He received the School of Engineering Fellowship from MIT in 2010. He also received the scholarship for academic excellence from 2004 to 2006 and the Outstanding Thesis Award in 2007 from Tsinghua University.

Yuan Shen (S'05–M'14) received the Ph.D. degree and the S.M. degree in electrical engineering and computer science from the Massachusetts Institute of Technology (MIT), Cambridge, MA, USA, in 2014 and 2008, respectively, and the B.E. degree (with highest honor) in electronic engineering from Tsinghua University, Beijing, China, in 2005.

He is an Associate Professor with the Department of Electronic Engineering at Tsinghua University. Prior to that, he was a Research Assistant and then Postdoctoral Associate with the Wireless Information and Network Sciences Laboratory at MIT in 2005-2014. He was with the Hewlett-Packard Labs in winter 2009 and the Corporate R&D at Qualcomm Inc. in summer 2008. His research interests include statistical inference, network science, communication theory, information theory, and optimization. His current research focuses on network localization and navigation, inference techniques, resource allocation, and intrinsic wireless secrecy.

Professor Shen was a recipient of the Qiu Shi Outstanding Young Scholar Award (2015), the China's Youth 1000-Talent Program (2014), the Marconi Society Paul Baran Young Scholar Award (2010), and the MIT Walter A. Rosenblith Presidential Fellowship (2005). His papers received the IEEE Communications Society Fred W. Ellersick Prize (2012) and three Best Paper Awards from the IEEE Globecom (2011), ICUWB (2011), and WCNC (2007). He is elected Vice Chair (2017-2018) and Secretary (2015-2016) for the IEEE ComSoc Radio Communications Committee. He serves as TPC symposium Co-Chair for the IEEE Globecom (2016), the European Signal Processing Conference (EUSIPCO) (2016), and the IEEE ICC Advanced Network Localization and Navigation (ANLN) Workshop (2016 and 2017). He also serves as Editor for the IEEE COMMUNICATIONS LETTERS since 2015 and Guest-Editor for the *International Journal of Distributed Sensor Networks* (2015).

Andrea Conti (S'99–M'01–SM'11) received the Laurea *(summa cum laude)* in telecommunications engineering and the Ph.D. in electronic engineering and computer science from the University of Bologna, Italy, in 1997 and 2001, respectively.

He is an Associate Professor at the University of Ferrara, Italy. Prior to joining the University of Ferrara, he was with the Consorzio Nazionale Interuniversitario per le Telecomunicazioni and with the IEIIT-Consiglio Nazionale delle Ricerche, Bologna. In Summer 2001, he was with the Wireless Systems Research Department at AT&T Research Laboratories. Since 2003, he has been a frequent visitor to the Wireless Information and Network Sciences Laboratory at the Massachusetts Institute of Technology, where he presently holds the Research Affiliate appointment. His research interests involve theory and experimentation of wireless systems and networks including network localization, distributed sensing, adaptive diversity communications, and network secrecy. He is recipient of the HTE Puskás Tivadar Medal and co-recipient of the IEEE Communications Society's Stephen O. Rice Prize in the field of Communications Theory and of the IEEE Communications Society's Fred W. Ellersick Prize.

Dr. Conti has served as editor for IEEE journals, as well as chaired international conferences. He has been elected Chair of the IEEE Communications Society's Radio Communications Technical Committee. He is a co-founder and elected Secretary of the IEEE Quantum Communications & Information Technology Emerging Technical Subcommittee. He is an elected Fellow of the IET and has been selected as an IEEE Distinguished Lecturer.

Moe Z. Win (S'85–M'87–SM'97–F'04) is a professor at the Massachusetts Institute of Technology (MIT) and the founding director of the Wireless Information and Network Sciences Laboratory. Prior to joining MIT, he was with AT&T Research Laboratories and NASA Jet Propulsion Laboratory.

His research encompasses fundamental theories, algorithm design, and network experimentation for a broad range of real-world problems. His current research topics include network localization and navigation, network interference exploitation, and quantum information science. He has served the IEEE Communications Society as an elected Member-at-Large on the Board of Governors, as elected Chair of the Radio Communications Committee, and as an IEEE Distinguished Lecturer. Over the last two decades, he held various Editorial posts for IEEE journals and organized numerous international conferences. Currently, he is serving on the SIAM Diversity Advisory Committee.

Dr. Win is an elected Fellow of the AAAS, the IEEE, and the IET. He was honored with two IEEE Technical Field Awards: the IEEE Kiyo Tomiyasu Award (2011) and the IEEE Eric E. Sumner Award (2006, jointly with R. A. Scholtz). Together with students and colleagues, his papers have received numerous awards. Other recognitions include the IEEE Communications Society Edwin H. Armstrong Achievement Award (2016), the International Prize for Communications Cristoforo Colombo (2013), the Copernicus Fellowship (2011) and the *Laurea Honoris Causa* (2008) from the University of Ferrara, and the U.S. Presidential Early Career Award for Scientists and Engineers (2004). He is an ISI Highly Cited Researcher.